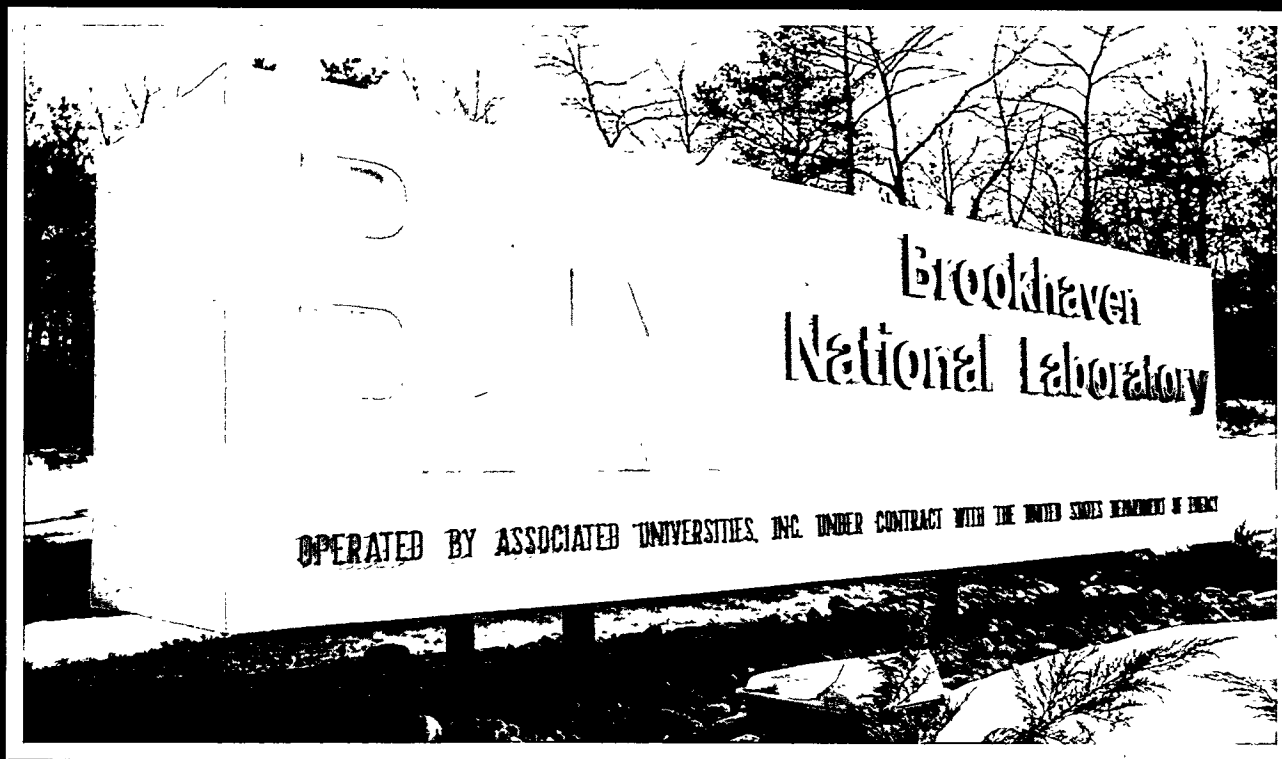


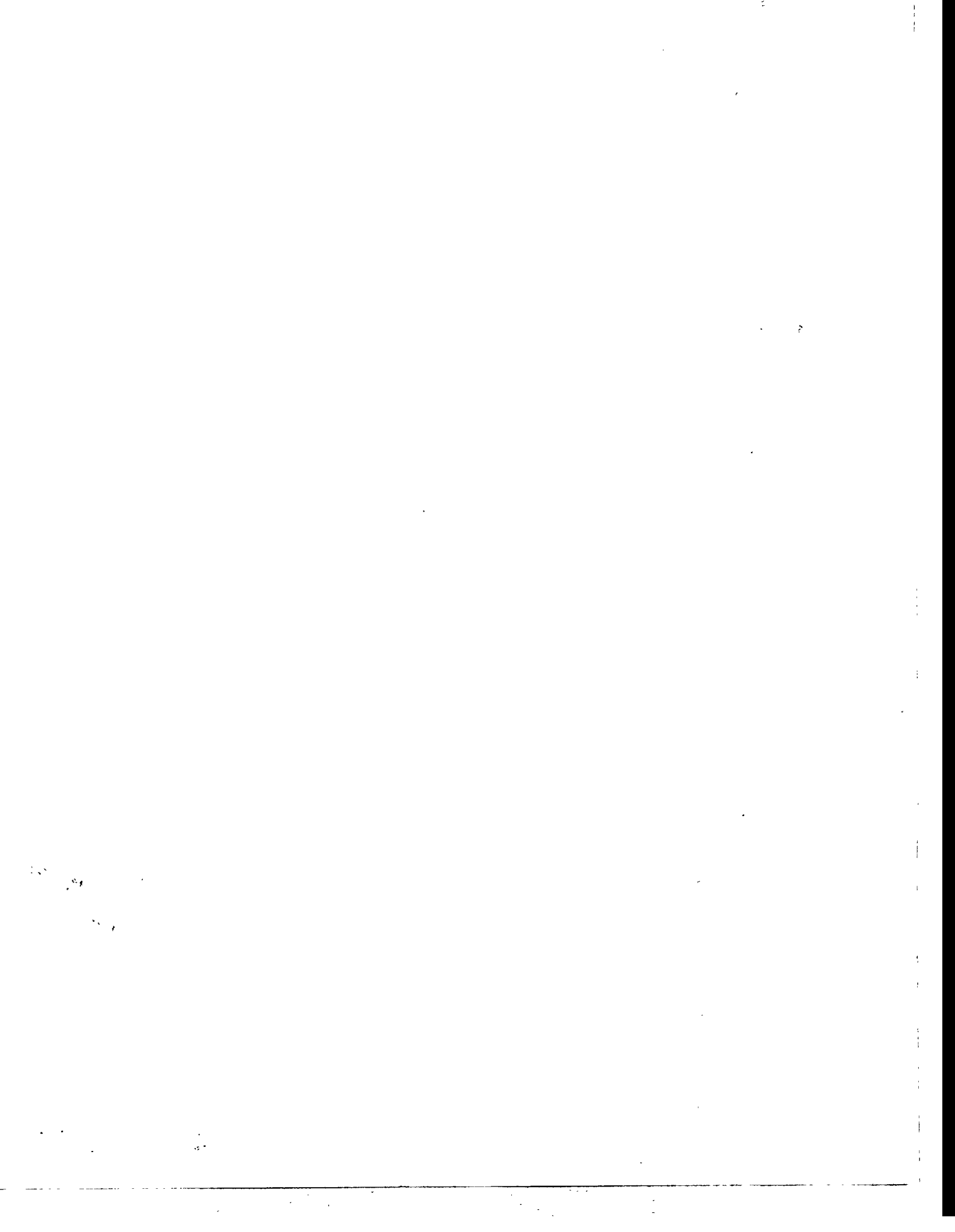
BNL-52351
(Rev. 12/95)

Laboratory Directed Research & Development

Annual Report to the Department of Energy
December 1995

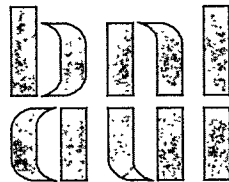


Brookhaven National Laboratory • Associated Universities, Inc.
Upton, New York 11973-5000
Under Contract No. DE-AC02-76CH00016 with the
United States Department of Energy



Laboratory Directed Research & Development Program

**Annual Report to the Department of Energy
December 1995**



**Gregory J. Ogeka and Anthony J. Romano
Special Assistants to the
Associate Director for Administration**

**BROOKHAVEN NATIONAL LABORATORY
ASSOCIATED UNIVERSITIES, INC.
UPTON, NEW YORK 11973-5000**

UNDER CONTRACT NO. DE-AC02-76CH00016

UNITED STATES DEPARTMENT OF ENERGY

DISTRIBUTION OF THIS DOCUMENT IS UNLIMITED

dic

MASTER

DISCLAIMER

This report was prepared as an account of work sponsored by an agency of the United States Government. Neither the United States Government nor any agency thereof, nor any of their employees, nor any of their contractors, subcontractors, or their employees, makes any warranty, express or implied, or assumes any legal liability or responsibility for the accuracy, completeness, or usefulness of any information, apparatus, product, or process disclosed, or represents that its use would not infringe privately owned rights. Reference herein to any specific commercial product, process, or service by trade name, trademark, manufacturer, or otherwise, does not necessarily constitute or imply its endorsement, recommendation, or favoring by the United States Government or any agency, contractor or subcontractor thereof. The views and opinions of authors expressed herein do not necessarily state or reflect those of the United States Government or any agency, contractor or subcontractor thereof.

Printed in the United States of America
Available from
National Technical Information Service
U.S. Department of Commerce
5285 Port Royal Road
Springfield, VA 22161

NTIS price codes:
Printed Copy: A06; Microfiche Copy: A01

Acknowledgments

The Laboratory Directed Research and Development (LDRD) Program is directed by Martin Blume, Deputy Director and is administered by Henry Grahn, Associate Director for Administration (ADA). Preparation of the FY 1995 report was coordinated and edited by Gregory Ogeka and Anthony Romano, Special Assistants to the ADA who wish to thank Regina Paquette for her assistance in organizing and typing the document. A special thank you is also extended to D.J. Greco and Susan Cuevas for their help in proof-reading sections of the report and to the Photography and Graphic Arts Division for their help in publishing. Of course, a very special acknowledgement is extended to all of the authors of the project annual reports, and to their secretaries.

Additions to this Report

This report contains two additional sections. The first is a discussion of the Laboratory's accomplishments as they relate to several success indicators. The second provides the reader with a summary of new projects funded for FY 1996.

Table of Contents

Introduction	1
Management Process	7
Summary of FY 1995 LDRD Program	15

Project Program Summaries

Investigation of the Utility of Max-Entropy Methods for the Analysis of Powder Diffraction Data	21
Analysis of Structures and Interactions of Nucleic Acids and Proteins by Small Angle X-Ray Diffraction	26
Relaxographic MRI and Functional MRI	29
Very Low Temperature Infra-Red Laser Absorption as a Potential Analytical Tool	34
State-Resolved Measurements of H ₂ Photodesorption: Development of Laser Probes of H ₂ for In-Situ Accelerator Measurements	38
Siberian Snake Prototype Development for RHIC	41
Synthesis and Characterization of Novel Microporous Solids	43
Ozone Depletion, Chemistry and Physics of Stratospheric Aerosols	46
Understanding the Molecular Basis for the Synthesis of Plant Fatty Acids Possessing Unusual Double Bond Positions	49
Structure Determination of Outer Surface Proteins of the Lyme Disease Spirochete	52
Low Mass, Low-Cost Multi-Wire Proportional Chambers for Muon Systems of Collider Experiments	55
Theory of Self-Organized Criticality	58
Development of the PCR-SSCP Technique for the Detection, at the Single Cell Level, of Specific Genetic Changes	59

Table of Contents

Feasibility of SPECT in Imaging of F-18 FDG Accumulation in Tumors	62
Visible Free Electron Laser Oscillator Experiment	65
Study of Possible 2 + 2 TeV Muon-Muon Collider	68
Ultraviolet FEL R&D	70
Precision Machining Using Hard X-Rays	72
New Directions in In-Vivo Enzyme Mapping: Catechol-O-Methyltransferase	77
Proposal to Develop a High Rate Muon Polarimeter	82
Development of Intense, Tunable 20-Femtosecond Laser Systems	85
Use of Extreme Thermophilic Bacterium <i>Thermatoga Maritima</i> as a Source of Ribosomal Components and Translation Factors for Structural Studies	89
Biochemical and Structural Studies of Chaperon Proteins from Thermophilic Bacteria	91
Magnetic Mapping of Rebars and Piping in Infrastructure Systems	93
Low Dose Gamma Imaging Facility for In-Vivo Molecular Medicine	96
Atmospheric Degradation of Halogenated Compounds	99
Extraction and Destruction of Hazardous and Toxic Chemical Pollutants During Soil/Sludge Remediation Using Innovative Technologies	101
Study of High Power Density Compact Target Design Associated Moderators, Beam Ports and Shielding for a Mw Pulsed Spallation Neutron Source	105
LDRD - 1996 Proposed Program	109

Introduction

Background: Brookhaven National Laboratory (BNL) was established in 1947 on the site of the former Army Camp Upton. Brookhaven is a multidisciplinary laboratory that carries out basic and applied research in the physical, biomedical and environmental sciences, and in selected energy technologies. The Laboratory is managed by Associated Universities, Inc., under contract with the U. S. Department of Energy. BNL's annual budget has averaged about \$380 million, and its facilities are valued at over \$2.2 billion. There are about 3,300 employees, and another 4,000 guest scientists and students who come each year to use the Laboratory's facilities and work with the staff. BNL's Relativistic Heavy Ion Collider (RHIC), presently under construction, will be the world's foremost facility for nuclear physics research. RHIC will create the hot, dense plasma of quarks and gluons from which particles condensed after the "Big Bang" of the early universe.

Mission and Core Competencies: Brookhaven National Laboratory's mission is to support the basic Department of Energy (DOE) activities through its research and technology development, educational efforts, and industrial involvement. Brookhaven was founded as a laboratory which would provide specialized research facilities that could not be designed, built and operated at a university or industrial complex, and this still remains a basic mission of the Laboratory. Brookhaven National Laboratory has four core competencies.

Brookhaven's four core competencies, Research Facilities, Scientific Research, Technology Development, and Knowledge Transfer are not independent isolated competencies. They are interrelated in a

complex manner.

MAJOR CORE COMPETENCIES
<p><u>RESEARCH FACILITIES</u> Expertise to conceive, design, build and operate complex leading-edge, user-oriented research facilities in a safe and environmentally responsible manner.</p>
<p><u>SCIENTIFIC RESEARCH</u> Expertise to carry out basic and applied scientific research in long-term, high-risk programs. This is an essential capability needed to keep our research facilities at the leading edge. These programs lead to new insights and technological advances which provide the underlying scientific base for the DOE missions and generate long-term benefit to the nation.</p>
<p><u>TECHNOLOGY DEVELOPMENT</u> Expertise to develop advanced technologies that address national needs, support and strengthen the ability of DOE to carry out its missions, support other federal and state agencies, and enable industry to benefit from the multidisciplinary research and development at the Laboratory.</p>
<p><u>KNOWLEDGE TRANSFER</u> Expertise and mechanisms for disseminating scientific and technical knowledge to educate new generations of scientists and engineers to produce a technically trained workforce, to enhance scientific literacy of the general public, and to improve the competitiveness of U. S. industry.</p>

Research Facilities and Scientific Research have a synergistic relationship. To maintain and constantly improve a research facility, and to keep it at the cutting edge, it is essential that the Laboratory have a significant research staff of excellent stature. The staff will drive the performance of the facility. Having the several complementary facilities at one location, such as the National Synchrotron Light Source and the High Flux Beam Reactor, allows a unique research capability, such as in material science and biological structure determination. The other two core competencies, Technology Development and Knowledge Transfer, bridges all of the research facilities and research programs.

Brookhaven's core competencies support and cut across the five central activities of the Department of Energy, as defined in its Strategic Plan.

DOE Strategic Plan Activities	
SCI	Science and Technology
ENV	Environmental Quality
IND	Industrial Competitiveness
ENER	Energy Resources
SEC	National Security

BNL plays a major role in the Science and Technology, the Environmental Quality, the Industrial Competitiveness and the Energy Resources sectors, with a smaller, but special role in the National Security arena. In order to better see the connection between the various Brookhaven activities that form the core competencies and the Department of Energy Strategic Plan activities, each BNL activity/competency is followed with the letter code describing the match in the Table 1, "Major Activity Clusters."

Summary: New ideas and opportunities, fostering the advancement of technology, are occurring at an every increasing rate. It, there-

fore, seems appropriate that a vehicle be available which fosters the development of new ideas and technologies, promotes the early exploration and exploitation of creative and innovative concepts, and develops new "fundable" R&D projects and programs if BNL is to carry out its primary mission and support the basic Department of Energy activities. At Brookhaven National Laboratory, one such method is through its Laboratory Directed Research and Development Program. This discretionary research and development tool is critical in maintaining the scientific excellence and vitality of the Laboratory. Additionally, it is a means to stimulate the scientific community, fostering new science and technology ideas, which is the major factor in achieving and maintaining staff excellence, and a means to address national needs, within the overall mission of the DOE and the BNL.

The Project Summaries, with their accomplishments described in this report, reflect the above. Aside from leading to new fundable or promising programs and producing especially noteworthy research, they have resulted in numerous publications in various professional and scientific journals, and presentations at meetings and forums.

TABLE 1: MAJOR ACTIVITY CLUSTERS

LARGE RESEARCH FACILITIES

ALTERNATING GRADIENT SYNCHROTRON (SCI)

- Research in Particle and Nuclear Physics
- High-Intensity Frontier of Particle Physics
- World's Only High Energy Polarized Proton Source
- At Present, Nation's Only High Energy, Heavy Ion Synchrotron
- Over 800 Users

RELATIVISTIC HEAVY ION COLLIDER

(under construction)

(SCI)

- High-Temperature Frontier of Nuclear Matter
- Large and Unique High Energy Physics Potential (e.g. spin physics)
- 600 Users in First Round Experiments

HIGH FLUX BEAM REACTOR

(SCI, ENER, ENV, IND)

- Instruments for Research in Condensed-Matter Physics, Biology, Chemistry, Applied Sciences and Industrial Applications
- 270 Users

NATIONAL SYNCHROTRON LIGHT SOURCE

(SCI, ENV, ENER, IND)

- Two Storage Rings Providing Intense UV and X-ray Photon Sources
- Instruments for Research in Materials Science, Biology, Chemistry, Medical and Industrial Applications
- Over 3300 Users, Including 400 Industrial Users

BIOMEDICAL FACILITIES

PET-CYCLOTRON CENTER

(SCI, IND)

- Medical Imaging for Basic Neuroscience and Substance Abuse, Radiotracer Synthesis

BROOKHAVEN LINEAR ISOTOPE PRODUCTION FACILITY

(SCI, IND)

- Production of Isotopes for Medical Purposes
- Approximately 200 Isotopes Produced for Commercial and/or Research Use

MEDICAL RADIATION FACILITY

(SCI, IND)

- Cancer Patient Treatment: 250 patients annually

BROOKHAVEN MEDICAL RESEARCH REACTOR

(SCI, IND)

- Structural Biology, Molecular Masses
- Over 75 Users

PROTEIN DATA BANK

(SCI, IND)

- World-Wide Repository for Three-Dimensional Structures of Biological Macromolecules

GENOME SEQUENCING CENTER

(under development)

(SCI, IND)

- Large-Scale DNA Sequencing

PROTON RADIATION THERAPY FACILITY (under development)

(SCI, IND)

- Utilizes Existing 200 MeV Linac
- Will Consist of Horizontal and Vertical Beam Treatment Rooms
- Capability of 900 Cancer Patients Per Year

OTHER FACILITIES

TANDEM VAN DE GRAAFF FACILITY

(SCI, SEC, ENV, ENER, IND)

- Microchip Radiation Testing Facility
- Film Irradiation Plant for Track Etching Filter Membranes
- 250 Industrial Users from 45 Institutions

ACCELERATOR TEST FACILITY

(SCI, IND, SEC)

- Advanced Acceleration Concepts

10-MEV ELECTRON PULSE RADIOLYSIS FACILITY (under construction)

(SCI, ENER, ENV.)

- Study of Rapid Chemical Reactions: Catalysis, Energy Conversion and Storage

NUCLEAR DATA COMPILATION AND EVALUATION CENTER

(SCI, SEC, IND)

- Nuclear Cross-Section and Structure Data
- 1100 Users

SCIENTIFIC RESEARCH

HIGH ENERGY PARTICLE AND NUCLEAR PHYSICS

(SCI)

- Beyond the Standard Model
 - Rare Kaon Decays
 - Muon Anomalous Magnetic Moment
 - Exotics and Glueball Spectroscopy
 - Neutrino Oscillation
 - Strange Matter
 - Solar Neutrinos
- Relativistic Heavy Ions
 - High-Temperature Nuclear Matter
 - Quark-Gluon Plasma

ADVANCED ACCELERATOR CONCEPTS

(SCI, IND, SEC)

- Short Wavelength Accelerating Structures
- Production of Coherent Radiation Free Electron Laser

MATERIALS SCIENCES

(SCI, ENER, IND, ENV)

- Materials Characterization with Neutron and X-ray Scattering, Magnetism and Superconductivity, Surface Studies, Corrosion, Adhesion, Catalysis, Metallic Alloys, Polymers

CHEMICAL SCIENCES

(SCI, ENER, IND, ENV)

- Molecular Dynamics, Reactive Transient Species, Thermal and Photo-Induced Charge Transfer, Structure and Reactivity

ENVIRONMENTAL SCIENCES

(SCI, ENV, IND)

- Global Change, Atmospheric Chemistry, Oceanography, Soil Chemistry, Cycling of Pollutants, Environmental Remediation

MEDICAL SCIENCE

(SCI, IND)

- Medical Imaging: PET, SPECT, MRI, Coronary Angiography
- Nuclear Medicine
- Radionuclides, Radiopharmaceuticals, Synthesis and Applications
- Advanced Cancer Therapies: Neutron Capture, Microbeam Radiation, Proton Radiation
- Mechanisms of Oncogenesis

MOLECULAR BIOLOGY AND BIOTECHNOLOGY

(SCI, IND)

- Genome Structure, Gene Expression
- DNA Damage and Repair
- Molecular Genetics
- Plant Science
- Bio-Structure Determination by X-ray and Neutron Scattering
- Enzyme Kinetics by Laue Crystallography
- Mass Measurements by Electron Microscopy

ADVANCED SCIENTIFIC COMPUTING AND SYSTEMS ANALYSIS

(SCI, IND, ENV, ENER)

- Risk Assessment
- Energy Modeling
- Groundwater Modeling

TECHNOLOGY DEVELOPMENT

PHYSICAL, CHEMICAL AND MATERIALS SCIENCE

(SCI, ENER, IND)

- State-of-the-Art Instrumentation and Devices for Precision Electronics, Optics and Microelectronics
- Superconducting Materials
- X-ray Lithography
- Micromachining
- Battery Technology
- Permanent Magnets
- Smart Polymers

ACCELERATOR TECHNOLOGY

(SCI, IND, SEC)

- High-Field, High-Quality Superconducting Magnets
- High-Power Radio Frequency Systems
- Ultrahigh Vacuum Systems
- Advanced Accelerator Designs
 - High-Gradient Acceleration
 - High-Beam Current Acceleration

ENVIRONMENTAL AND CONSERVATION TECHNOLOGIES

(SCI, ENV, ENER, IND, SEC)

- Environmental Remediation and Mitigation
- Energy-Efficiency Technologies
- Waste Treatment
- Disposal of Nuclear Materials
- Radiation Protection
- Infrastructure Modernization
- Transportation: Intelligent Vehicle Highway System, MAGLEV

MEDICAL TECHNOLOGIES

(SCI, IND)

- Biomedical Applications of Nuclear Technology
- Production of Radionuclides and Radiopharmaceuticals
- Development of Particle Radiation Therapies for Cancer
- Medical Imaging
- X-ray Microbeam Therapy

BIOTECHNOLOGY

(SEC, SCI, ENV, ENER)

- Neutron and Synchrotron X-ray Scattering
- Large-Scale Genome Sequencing
- High-Resolution Scanning and Cryo Electron Microscopy
- Cloning, Expressing and Engineering Genes
- Metal Cluster Compounds for Electron Microscope Labels
- Phage Displays for Probing Specific Interactions

SAFETY AND RISK ASSESSMENT

(SEC, SCI, ENV, ENER)

- Safeguards, Nonproliferation and Arms Control
- Safety Analysis of Complex Systems
- Probabilistic Risk Assessment

KNOWLEDGE TRANSFER

EDUCATING FUTURE GENERATIONS OF SCIENTISTS AND ENGINEERS

(SCI, ENV, IND, ENER, SEC)

- Lecturing, Conference Participation
- Visiting Scientist Program
- Accelerator Fellowship Program
- Postdoctoral Research Associates
- Engineering Intern Program
- Graduate Student Thesis Projects
- Adjunct Teaching Appointments at Local Colleges

- Office of Educational Program
 - Precollege and College Programs for Students and Teachers

EDUCATING THE GENERAL PUBLIC

(SCI, ENV, IND, ENER, SEC)

- Science Museum and Laboratory Tours (20,000 people/year)
- Speakers Bureau
- BNL Videos
- Laboratory Lectures for the Public
- Community Outreach Programs
- Information Storage and Transfer

TECHNOLOGY TRANSFER TO INDUSTRY

(SCI, ENV, IND, ENER, SEC)

- Industrial Users at the Research Facilities
- Consulting by Scientific Staff
- Technology Transfer Office
 - Patenting and Licensing Office
 - Technical Assistance for Industry
 - CRADAs
 - Visiting Scientist Program with Industry
 - Research Partnerships with Industry
 - Industry-Sponsored Proprietary Research and Development Long Island Research Institute (LIRI) (founding member)
 - Promotes Laboratory-Industry Interaction
 - ARPA-Funded BNL/LIRI Defense Conversion Project
 - NY State-Funded Biotechnology Initiative

INFORMATION TRANSFER

(SCI, ENV, IND, ENER, SEC)

- INFORM - Electronic Information Source
- Networking - "Information Superhighway"
- Technical and Scientific Publishing
- National Nuclear Data Center
- Protein Data Bank

Management Process

PROGRAM DESCRIPTION:

Introduction: The Department of Energy's (DOE) Laboratory Directed Research & Development (LDRD) Program at Brookhaven National Laboratory (BNL) was originally established as the "Exploratory Research Program" under the guidelines set forth in DOE Order 5000.1 in May 1984. From inception through September 1996, a period spanning twelve fiscal years, the Laboratory has authorized \$25.7 million in Exploratory R&D, consisting of 163 separate projects.

BNL LDRD PROGRAM HISTORY 1985-1996

FISCAL YEAR	AUTH K\$	COSTED K\$	NO. REC'D	NEW STARTS
1985	1,842	1,819	39	13
1986	2,552	2,515	22	15
1987	1,451	1,443	29	8
1988	1,545	1,510	46	14
1989	2,676	2,666	42	21
1990	2,008	1,941	47	9
1991	1,353	1,321	23	14
1992	1,892	1,865	30	14
1993	2,073	2,006	35	14
1994	2,334	2,323	44	15
1995	2,486	2,478	46	13
1996	3,500	—	47	12*
TOTALS	25,712	21,887	450	162

*Additional projects may be funded in FY 1996, pending the availability of funds.

Historical Perspective: Brookhaven National Laboratory was established in 1946. Throughout its history, certain projects of an

exploratory nature, sometimes referred to in the past as "seed money projects," were supported with overhead funding. In 1979, as a result of a Review Audit in that year, the seed money accounting procedures were formalized, and oversight by the then DOE Brookhaven Area Office Manager was first established. This seed money program operated at a variable level of funding, which averaged about 0.1 percent of the Laboratory's operating budget over the period 1979 to 1984.

In May 1984, the program was expanded. The expanded program embraced the new Exploratory R&D guidelines of DOE Order 5000.1. The new program, called the Exploratory Research Program, was put into effect for FY 1985 funding. The current Laboratory Directed Research & Development Program reflects the operating styles and many of the procedures of the earlier programs, which have evolved somewhat informally over the years. It also encompasses the requirements of the current DOE Order 5000.4A.

Goals and Objectives: The goals and objectives of BNL's LDRD Program can be inferred from the Program's stated purposes. These are to (1) encourage and support the development of new ideas and technology, (2) promote the early exploration and exploitation of creative and innovative concepts, and (3) develop new "fundable" R&D projects and programs. The emphasis is clearly articulated by BNL to be on supporting exploratory research "which could lead to new programs, projects, and directions" for the Laboratory.

General Characteristics of the LDRD Program: Projects or studies that are appropriate candidates for the Laboratory's LDRD Program include, but are not limited to, (1) projects, normally relatively small, in the

forefront areas of basic and applied science and technology for the primary purpose of enriching laboratory capabilities, (2) advanced study of new hypotheses, new concepts, or innovative approaches to scientific or technical problems, (3) experiments and analyses directed toward "proof of principle" or early determination of the utility of new scientific ideas, and (4) conception and preliminary technical analysis of experimental facilities or devices.

PROGRAM ADMINISTRATION:

Overall Coordination: Overall responsibility for coordination, oversight, and administration of BNL's LDRD Program resides with the Laboratory's Deputy Director. The Deputy Director is assisted in the administration of the program by the Office of the Associate Director for Administration, which administers the program budget, establishes the project accounts, maintains summary reports, and reports Program activities to the DOE through the Brookhaven Group Manager.

Responsibility for the allocation of resources and the orchestration, review and selection of proposals, lies with a management-level group, called the Laboratory Directed Research & Development Committee.

LDRD PROGRAM COMMITTEE

Martin Blume	Chairperson and for Applied Programs
Henry C. Grahn	Administration
Thomas Kirk	High Energy & Nuclear Physics
Denis B. McWhan	Basic Energy Sciences
Mark Sakitt	Planning & Policy
Richard B. Setlow	Life Sciences

The Committee is made up of six members. The Laboratory's Deputy Director is the chairperson of the Committee. The other members are the Associate and Assistant Directors of the Laboratory.

Allocating Funds: There are two types of decisions to be made each year concerning the allocation of funds for the LDRD Program. These are (1) how much money should be budgeted overall for the Program; and (2) of this, how much, if any, should go to each competing project or proposal. Both of these decisions are made by high-level management.

Concerning the overall budget, for each upcoming fiscal year the Laboratory Director, in consultation with the Deputy Director and the Associate Director for Administration, develops an overall level of funding for the LDRD Program. The budget amount is then incorporated into the Laboratory's LDRD Plan which formally requests authorization from the DOE to expend funds for the LDRD Program up to this ceiling amount.

The majority of projects are authorized for funding at the start of the fiscal year. However, projects can be authorized throughout the fiscal year, as long as the approved ceiling for the LDRD Program is not exceeded.

The actual level of funding available for LDRD, however, may turn out to be much less than this ceiling. The actual level is determined during the course of the year and is affected by several considerations, including: the specific merits of the various project proposals, as determined by Laboratory management and the members of the LDRD Program Committee; the overall financial health of the Laboratory; and a number of budgetary tradeoffs between LDRD and other overhead expenses.

LDRD COSTS VS. TOTAL LABORATORY COSTS

operating \$ in millions

FISCAL YEAR	DOE FUNDS	WFO FUNDS	TOTAL FUNDS	LDRD FUNDS	% OF TOTAL
1985	153.0	40.4	193.1	1.82	0.9
1986	156.5	45.1	201.6	2.52	1.2
1987	161.7	45.6	207.3	1.44	0.7
1988	176.7	45.9	222.6	1.51	0.7
1989	193.6	46.7	240.3	2.67	1.1
1990	203.8	45.2	249.0	1.94	0.8
1991	220.9	50.3	271.2	1.32	0.5
1992	234.3	47.2	281.5	1.87	0.7
1993	231.4	47.3	278.7	2.01	0.7
1994	237.0	47.9	284.9	2.32	0.8
1995	243.0	53.7	296.7	2.48	0.8

Concerning the allocation of resources to specific topic areas or to individual project proposals, such issues are addressed on a case-by-case basis by the LDRD Program Committee, once specific proposals have been received. The Committee meets periodically to review and recommend project proposals, and to determine the amount of funding to be made available to the LDRD Program. The requirements of DOE Order 5000.4A are carefully considered during the selection process to ensure that proposals are consistent with DOE's criteria.

Request for Proposals: The availability of special funds for research under the LDRD Program is well publicized throughout the Laboratory. This is done using two methods, one occurring at yearly intervals, the other occurring irregularly. Each year in May a memo is sent by the Laboratory Director to all scientific staff, issuing a "call for proposals." This memo is accompanied by an attached document, entitled "Guidelines and Procedures for Developing Proposals via the Laboratory Directed Research and Development (LDRD) Program." The other method is by announcement in the Brookhaven Bulletin, the Laboratory's weekly newspaper; but the nature

of the announcements varies and they appear at irregular intervals. In some years the Bulletin prints an article that amounts to a separate call for proposals. In other years the Bulletin publishes articles on specific research projects which, in effect, help advertise the LDRD Program.

The "Guidelines and Procedures" document specifies the requirements necessary for participation in the program. It states the program's purpose, general characteristics, procedures for applying, and restrictions. An application for funding, that is, a project proposal, takes the form of a completed "Proposal Questionnaire." An application must be approved up the chain-of-command, by the initiator's Department Chairperson or Division Head, and by the cognizant Associate Director. Plans to ensure the satisfactory continuation of the principal investigator's regularly funded programs must also be approved. The applications are then forwarded to the Chairperson of the LDRD Program Committee for further review and consideration for funding.

The process which solicits and encourages the development of proposals has evolved into two modes of operation. Specifically, the ideas for proposal development may originate among the scientific staff in response to the general call for proposals. Alternatively, they may be initiated by top-level Laboratory management. Eventually, both follow the standard procedure for proposal approval, up the chain-of-command to the same decision makers. The fact that all proposals must be approved up the chain-of-command permits BNL managers to consider all ideas together when designing the mix of projects for the LDRD Program.

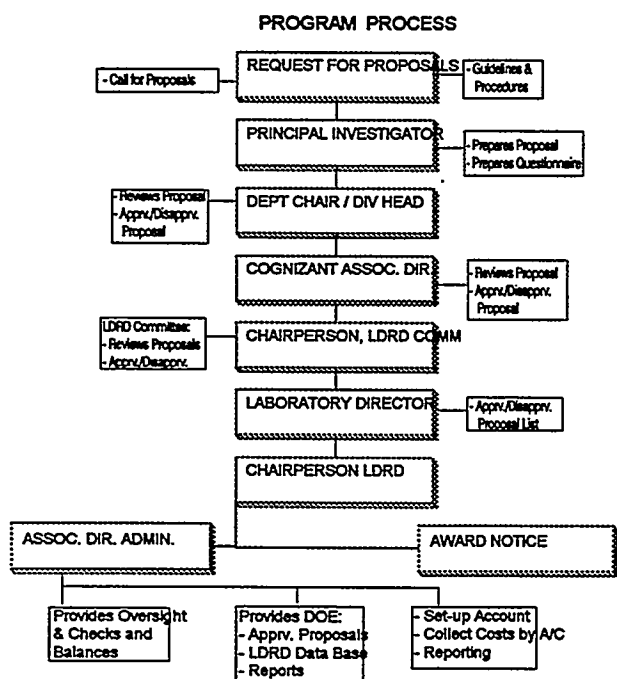
An initiative from management typically takes the form of a general topic area or item of special interest. It is not a directive, nor is it included in the call for proposals, but the idea is communicated to a group of

scientific staff, which is known to be in a position capable of pursuing and developing the idea in the form of a more formal proposal.

written comments by experts outside the normal lines of supervision, are not usually performed. The members of the Committee are considered to have sufficient technical knowledge so that peer reviews are seldom required.

At the next Committee meeting, the Committee member responsible for the review of the proposal presents the proposal to the other members of the Committee. This is done without the member necessarily becoming an advocate for the proposed project.

Selection Criteria: Before proposals can be considered by the Committee, they must be screened to ensure that they meet a set of minimum requirements concerning the Department's LDRD policies and the Laboratory's own guidelines.



Proposal Review: Once a proposal is approved by the cognizant line managers, all proposals are forwarded to the Chairperson of the Committee who transmits a copy of all proposals received to the Committee for review. The Committee considers all proposals that have met certain minimum requirements pertaining to the Department's and BNL's LDRD policies.

Lead responsibility for the review of a proposal is then assigned to that member of the Committee who last approved it in the chain-of-command, that is, the member who oversees and directs the technical area from which the proposal originated. All members have several weeks to review the proposal and prepare for the next Committee meeting. During this time, additional reviews, if desired, may be arranged.

Formal peer reviews, consisting of

Minimum requirements of each proposal are: (1) consistency with program purpose; (2) consistency with missions of BNL, DOE, and NRC; (3) approval by Department Chairperson and/or Division Head, and cognizant Associate Director; (4) assurance of satisfactory continuation of principal investigator's regularly funded programs; (5) modest size and limited duration; (6) will not substitute for, supplement, or extend funding for tasks normally funded by DOE, NRC, or other users of the Laboratory; (7) will not require the acquisition of permanent staff; (8) will not create a commitment of future multi-year funding to reach a useful stage of completion; and (9) will not fund construction line-item projects, facility maintenance, or general purpose capital equipment.

The selection criteria used to evaluate and rank individual proposals are not formally stated or published. While the "Guidelines and Procedures" document clearly states that "awards will be made on a competitive basis," the factors or selection criteria to be considered in this competition are not listed.

Nevertheless, selection is based on (1) scientific merit, (2) compliance with minimum requirements, (3) proposal cost as compared to the amount of available funding, (4) innovativeness, and (5) its potential for follow-on funding. The requirements of DOE Order 5000.4A are also carefully considered during the selection process to ensure that proposals are consistent with DOE criteria.

Project Approval: After all presentations are heard, the Committee attempts to arrive at a consensus concerning the highest priority proposals. Differences, if any, are resolved by the Chairperson. Also, a balance is struck between the prevailing financial needs of the Laboratory, which may vary over the course of the year, and the priorities of the projects considered. Some funding is held in reserve during the earlier meetings of the fiscal year so that funds remain available for proposals submitted at later dates. The funding amount requested in any one specific proposal may be changed or adjusted during the approval process. The Committee's recommendation is then submitted to the Director for his approval.

The Associate Director for Administration is then notified, so that a separate Laboratory overhead account can be established to budget and collect the costs for the project. Statistics on the number of projects approved, compared to those rejected, show an overall approval rate of about 36 percent for new starts. From inception of the program through September 1995, 450 project proposals were considered and 163 were approved. Seven scientific departments, the RHIC Project, and the Safety and Environmental Protection Division were represented in the FY 1995 LDRD Program.

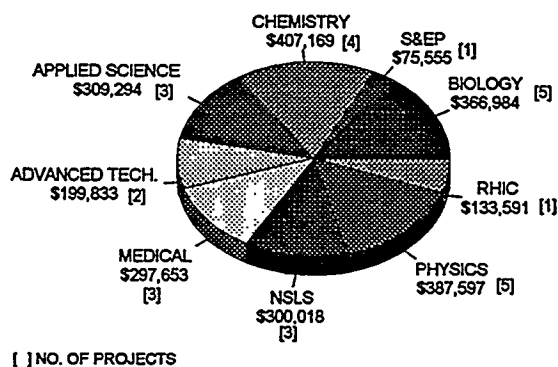
Project Supervision: Supervision over the actual performance of LDRD projects is carried out in the same way as other research projects at the Laboratory. Each principal investigator is assigned to an organizational

unit (Department, Division), which is supervised by a manager.

Each manager is responsible for seeing that the obligations of the principal investigator are satisfactorily fulfilled and that the research itself is carried out according to standard expectations of professionalism and scientific method. The manager is kept informed of the project's status, schedule, and progress.

The manager ensures that the work is completed in a timely manner and that annual status reports are submitted to the Deputy

FY 1995 FUNDING BY ORGANIZATION



Director. In addition, LDRD Program activity is reported to the DOE Brookhaven Group Manager, including copies of all funded proposals, a LDRD Program data base, and a project funding and schedule summary report.

Project Reporting: Routine documentation of each project funded under the LDRD Program consists of a file containing: (1) a copy of the written proposal; (2) all interim status reports; (3) notifications of changes in research direction, if any; and (4) reports on cost incurred. Also, a formal Annual Report on the LDRD Program is submitted to BNL management and the DOE, summarizing work progress, accomplishments, and project status on all projects.

Documentation for the overall Program consists of (1) various program history files; (2) a running list of all proposals with their acceptance/rejection status, (3) funding schedule and summary reports for all approved projects, (4) permanent records on cost accounting, and a data base containing information on each funded project (description, funding by fiscal year, status and accomplishments, follow-on funding, publications, etc.).

Some of the projects involve animals or humans. Those projects have received approval from the Laboratory's appropriate review committees. The projects which involve animals or humans are identified in this report as follows:

Note: Those projects which involve animal vertebrates or human subjects have been so identified in the text.

BROAD TECHNICAL AND SCIENTIFIC CATEGORIES:

Over the past several years, BNL has been categorizing its LDRD programs into six broad technical and scientific areas, including one miscellaneous area. The programs targeted for funding by BNL's LDRD Program fall into the following broad technical and scientific categories:

New Directions for Energy Technologies: In the course of basic research efforts there are occasionally discoveries which hold promise for utilization in energy technologies. Such research is of significance, both for the Laboratory and for the DOE.

Global Change: BNL has had several programs in atmospheric, oceanographic, and mathematical sciences, which produce results of relevance to questions of global climate change, pollution, and acid precipitation. LDRD proposals in these areas, which move in new avenues, are given priority as the Lab tries to make contributions to solutions of these

problems.

Radiation Therapies and Imaging: Applications of the Laboratory's facilities to the treatment of cancer and in imaging of the human body for diagnostic purposes, including such techniques as functional MRI, microplaner x-ray therapy, neutron capture therapy and the use of other imaging techniques, are a significant part of the LDRD effort.

Genetic Studies: This area of research at the Laboratory has produced many new ideas and applications which are too important to remain undeveloped. LDRD funded projects in this area are varied in subject matter covering many bio-medical topics.

New Directions for the Development and Utilization of BNL Facilities: High priority is assigned to ideas for more efficient utilization and for new directions for our major facilities. Ideas for more useful sources of x-rays at the synchrotron light source, for the utilization of new electron sources in the chemical study of pulse radiolysis, and new laser systems are all areas which are given priority for support.

Other Miscellaneous: Finally, the Program is open to significant and original ideas which do not necessarily fall within the bounds of the aforementioned priority areas. These usually involve small individual programs and projects that are judged to have high scientific/technical merit. Typically, materials development, electrochemical studies, advanced nuclear concepts and new bio-chemistry technologies fall into this category.

Brookhaven National Laboratory's FY 1995 LDRD Program covered the following Scientific and Technical Areas.

Programs/Projects	Funding \$000
New Directions for Energy	
Technologies	\$100
Global Change	274
Radiation Therapies and Imaging	627
Genetic Studies	407
New Directions for the Development and Utilization of BNL Facilities	896
Other - Miscellaneous	<u>174</u>
TOTAL	\$ 2,478

SUCCESS INDICATORS:

Overall the BNL LDRD Program has been very successful. Some of the more common indicators/measures of success are: (1) the amount of follow-on funding received, (2) the number of proposals anticipating future funding, (3) the number of full-length papers published, (4) the number of post-doctoral students supported, (5) the number of scientists/guests hired, and (6) the number of copyrights, invention disclosures and patents applied for or granted.

Although it is difficult to maintain an accurate and timely database of these success measures for each project, a summary of the information reported is presented below. The difficulty in compiling data is the loss of contact with the principal investigators soon after the LDRD projects are concluded.

However, in an FY 1995 analysis, it was found that of the 54 projects which were funded during the period FY 1992 - 1994, 22 received follow-on funding, and 5 others were awaiting responses to proposals which have been submitted. The total amount of follow-on funding reported for the 22 projects involved was \$5.3M as compared to funding of these projects of \$2.5M. Other indicators reported during this period were:

Number of Projects with at Least 1 Full-Length Publication	33
Number of Post-Doctoral Students Supported	21
Number of Scientific Associates Hired	7
Number of Copyrights, Invention Disclosures, and Patents Applied For/Granted	12

In fact, only 10 of the 54 projects had none of the aforementioned success indicators to report.

It is estimated that cumulative follow-on funding reported for all projects funded from FY 1985 to FY 1994 is upwards of \$42M versus a total program authorization of \$19.7M during that period. This estimate is conservative since, as mentioned earlier, contact is not generally maintained with the principal investigator once the project has ended.

Summary of FY 1995 LDRD Program

In FY 1995, the BNL LDRD Program funded 28 projects, 13 of which were new starts, at a total cost of \$2,477,694. Following is a table, which lists all of the FY 1995 funded projects and gives a history of funding for each by year.

Several of these projects have already experienced varying degrees of success, as indicated in the individual Project Program Summaries which follow. A total of 27 informal publications (abstracts, presentations, BNL reports and workshop papers) were reported and an additional 34 formal (full length) papers were either published, are in press or being prepared for publication. The investigators on four projects (#94-31, #95-04, #95-25, and #95-44) have filed for patents or disclosures.

Nine of the projects reported that proposals/grants had either been funded or

were submitted for funding including one CRADA.

The complete summary of follow-on activities is as follows:

Follow-on Activity of LDRD Projects	
	Number of <u>Projects</u>
Informal Publications	27
Formal Papers	34
Grants/Proposals/Follow-on Funding	8
Patents/Disclosures Applied For	4
CRADA Application	1

In addition, numerous post doctoral candidates and guest scientists were supported or collaboratively involved in these projects.

In conclusion, a significant measure of success is already attributable to the FY 1995 LDRD Program in the short period of time involved. The Laboratory has experienced a significant scientific gain by these achievements.

Laboratory Directed Research and Development Fiscal Year 1995 - Summary of Projects

Project Number	Project Title	Dept.	Principal Investigator	Approved Budgets by Fiscal Year			FY 1996 est.	Total Funding
				FY 1993	FY 1994	FY 1995		
93-25	Investigation of the utility of max-entropy methods for the analysis of powder diffraction data	PHYS	D. Cox	\$24,431	\$73,342	\$39,778	\$0	\$137,551
93-32	Analysis of structures and interactions of nucleic acids & proteins by small angle X-ray diffraction	BIO	M.S. Capel	42,276	97,690	47,579	0	187,545
93-35*	Relaxographic MRI and functional MRI	CHEM	J.S. Fowler	8,675	93,408	105,161	0	207,244
94-03	Very low temperature infra-red laser absorption as a potential analytical tool	CHEM	G.E. Hall	0	57,142	59,070	0	116,212
94-05	State-resolved measurements of H2 photodesorption: Development of laser probes of H2 for in-situ accelerator measurements	CHEM	M.G. White	0	68,871	77,222	0	146,093
94-06	Siberian snake prototype development for RHIC	RHIC	M.A. Harrison	0	132,139	133,591	220,000	485,730
94-09	Synthesis and characterization of novel microporous solids	DAS	J.A. Hriljac	0	113,862	111,292	0	225,154
94-10	Ozone depletion, chemistry and physics of stratospheric aerosols	DAS	D.G. Imre	0	99,533	103,757	0	203,290
94-31	Understanding the molecular basis for the synthesis of plant fatty acids possessing unusual double bond positions	BIO	J. Shanklin	0	64,808	69,439	0	134,247
94-32	Structure determination of outer surface proteins of the Lyme disease spirochete	BIO	C.L. Lawson	0	76,787	81,508	0	158,295
94-33	Low mass, low-cost multi-wire proportional chambers for muon systems of collider experiments	PHYS	V. Polychronakos	0	87,527	85,717	96,000	269,244
94-34	Theory of self-organized criticality	PHYS	F. Bak	0	61,488	62,532	0	124,020
94-36*	Development of the PCR-SSCP technique for the detection, at the single cell level, of specific genetic changes	MED	K. Rithidech	0	85,114	88,141	0	173,255
94-37*	Feasibility of SPECT in imaging of F-18 FDG accumulation in tumors	MED	G.J. Wang	0	15,806	99,776	110,000	225,582

* Project involves animal vertebrates or human subjects.

Laboratory Directed Research and Development Fiscal Year 1995 - Summary of Projects

Project Number	Project Title	Dept.	Principal Investigator	Approved Budgets by Fiscal Year				Total Funding
				FY 1993	FY 1994	FY 1995	FY 1996 est.	
94-43	Visible free electron laser oscillator experiment	NSLS	I. Ben-Zvi	0	70,000	100,008	30,000	200,008
95-01	Study of possible 2+2 TeV muon-muon collider	PHYS	R.B. Palmer	0	0	149,580	200,000	349,580
95-03	Ultraviolet FEL R&D	NSLS	E.D. Johnson	0	0	100,005	100,000	200,005
95-04	Precision machining using hard X-rays	NSLS	E.D. Johnson	0	0	100,005	100,000	200,005
95-07*	New directions in in-vivo enzyme mapping: Catechol-O-Methyltransferase	CHEM	Y.S. Ding	0	0	98,779	103,000	201,779
95-10	Proposal to develop a high rate muon polarimeter	PHYS	M. Diwan	0	0	49,990	0	49,990
95-11	Development of intense, tunable 20-femtosecond laser systems	CHEM	E. Castner Jr.	0	0	66,937	65,000	131,937
95-13	Use of extreme thermophilic bacterium <i>thermatoga maritima</i> as a source of ribosomal components & translation factors for structural studies	BIO	F.W. Studier	0	0	92,696	98,000	190,696
95-15	Biochemical & structural studies of chaperon proteins from thermophilic bacteria	BIO	J.M. Flanagan	0	0	75,762	100,000	175,762
95-25	Magnetic mapping of rebars and piping in infrastructure systems	DAT	J. Powell	0	0	99,829	0	99,829
95-33*	Low dose gamma imaging facility for in-vivo molecular medicine	MED	R. Ma	0	0	109,736	110,000	219,736
95-40	Atmospheric degradation of halogenated compounds	DAS	Z. Zhang	0	0	94,245	37,000	131,245
95-44	Extraction & destruction of hazardous & toxic chemical pollutants during soil/sludge remediation using innovative technologies	S&EP	S. Chalasani	0	0	75,555	75,000	150,555
95-45	Study of high power density compact target design and associated moderators, beam ports and shielding for a 5 Mw pulsed spallation neutron source	DAT	H. Ludewig	0	0	100,004	0	100,004
				\$75,382	\$1,197,517	\$2,477,694	\$1,444,000	\$5,194,593

* Project involves animal vertebrates or human subjects.

LABORATORY DIRECTED RESEARCH AND DEVELOPMENT
1995 PROJECT PROGRAM SUMMARIES

Investigation of the Utility of Maximum-Entropy Methods for the Analysis of Powder Diffraction Data

D.E.Cox

93-25

PROJECT DESCRIPTION:

The application of the maximum-entropy (MaxEnt) method to the detailed analysis of powder diffraction data has been explored. MaxEnt has first been applied to high-resolution synchrotron x-ray data as a means to locate light atoms in inorganic compounds containing heavier ones, which is a very common problem in structural studies of polycrystalline inorganic materials such as complex high T_c oxides and heavy metal oxide catalysts. Other goals were to use MaxEnt to provide details of the bonding electron density distribution, and for the ab-initio solution of unknown structures. Experimental work was aimed at developing optimum strategies for the collection of suitably accurate powder data at beam-line X7A at the NSLS in order to get the best possible structural information.

TECHNICAL PROGRESS AND RESULTS - Fiscal Year 1995:

Purpose: The development of high resolution synchrotron x-ray powder diffraction techniques at beam-line X7A at the NSLS over the past few years has demonstrated the utility of such data for the detailed structural characterization of a wide range of inorganic materials, including many high T_c systems and complex oxides of interest in catalysis. These studies have generated growing interest in the application of powder data to the ab-initio solution of unknown crystal structures, traditionally a technique requiring suitably-

sized single crystals. However, because of limitations inherent to powder compared to single crystal data, such as poorer counting statistics, peak overlap and inferior peak-to-background discrimination, the information contained in a set of structure factors is generally less complete and of lower accuracy. Fourier maps derived from these data tend to be quite noisy, and information about light atoms, thermal fluctuations or bonding effects may be obscured.

Most generally, MaxEnt is the nonparametric method of choice to retrieve information from sparse and noisy data sets. The great enhancement possible with the use of MaxEnt stems from its ability to reduce truncation and noise effects by orders of magnitude. The method works best when the data relate linearly to the physical information sought. Some recent papers in the literature have demonstrated that MaxEnt can be a very powerful tool in the analysis of powder data, for it is the least-biased with respect to missing data and may reveal details not seen on Fourier maps. Over the period of the project, which is now completed, the MaxEnt method has been successfully used for several typical problems, i.e. the localization of weak scatterers, the characterization of thermal and static disorder and ab-initio structure solution using resonant scattering techniques. The necessary software has been installed on a DEC Alpha computer in user-friendly form, and will be an important component of the suite of programs routinely used for the analysis of powder data.

Approach: There are two difficulties to be faced in structure determination from powder diffraction data: the general problem of non-linear phases and the specific problem of overlapping of Bragg peaks. The use of MaxEnt to solve the former is a topic of current interest, although phasing the data can

frequently be accomplished with standard techniques.

In the first stage of the project, MaxEnt was applied to selected reference materials as a benchmark test of the level of detail that can be extracted for simple systems. Particular attention was given to the minimization of systematic errors in the data collection process, and to a realistic evaluation of the estimated standard deviations (esd's). As a result of this work, significant improvements have been made in experimental strategies for data collection and analysis at X7A. In the second stage of the work, MaxEnt methods were used in conjunction with structure refinement for a variety of more complicated real-world materials, and in the final stage to ab-initio structure solution based on the construction of partial Patterson maps of anomalously scattering atoms.

Technical Progress and Results: The work described in this report has been carried out by Dr. Robert Papoular, a Visiting Scientist on leave from CEN, Saclay, France. The main thrust of his work has been directed towards three objectives, I) to locate weak scatterers in inorganic materials where part of the structure is known through the use of entropic Fourier maps rather than traditional difference Fourier maps ii) to retrieve electron density distributions from high-resolution powder patterns as accurately as possible iii) to devise optimal experimental strategies for data collection, in particular at a synchrotron beam-line such as X7A.

The most significant advance achieved this year is the successful ab-initio solution of a test structure, SrSO₄, from high-resolution powder diffraction data (Fig. 1), using resonant x-ray scattering following a recent suggestion by W. Prandl (Acta Cryst. A50, 1994). We believe this experimental study to

be the first of its kind. Beyond Prandl's original theoretical work, the study also sheds light on inherent practical difficulties and the ensuing resulting limitations of this kind of experiment.

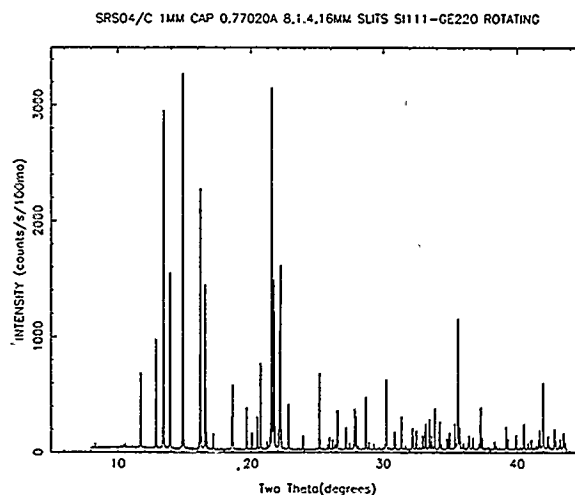
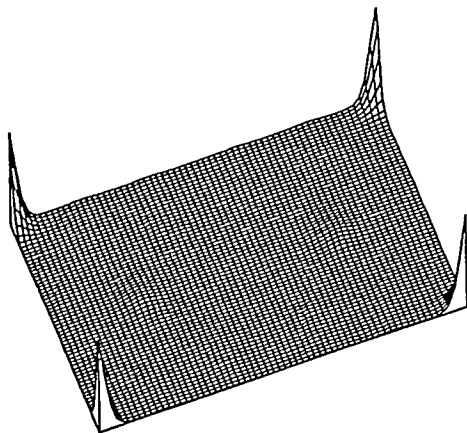


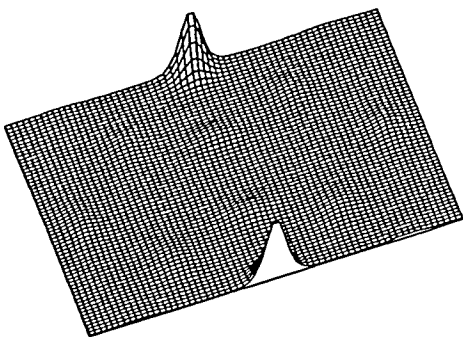
Fig. 1 One of the three high-resolution experimental spectra used to phase SrSO₄ ab-initio. The data were taken at about 13 keV, just below the Sr K-edge (≈ 16 keV).

The idea is to locate the anomalous scatterer first, Sr in this instance. Following Prandl's prescription, three wavelengths must be used in this specific centrosymmetric case, two close to the Sr K-edge and one away from it. The partial Patterson map from Sr atoms alone can therefore be obtained by a selective contrast variation-like method. Maximum Entropy plays a first key-role here in allowing for the reconstruction of the Patterson map (Fig. 2) from non-overlapping or overlapping Fourier data which is as noiseless and as free of truncation effects as possible. In this simple case, the coordinates of the Sr atom can be read (almost) directly from the entropic Patterson sections.

Sr only PATTERSON - Z=0



Sr only PATTERSON - Z=0.19



Sr only PATTERSON - Z=0.50

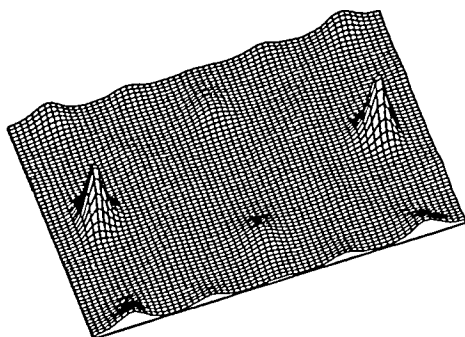


Fig.2(a) Selective Patterson entropic map of Sr alone (section Z=0), from which the coordinate $y_{Sr} \approx 0.25$ is deduced.

Fig.2(b) Selective Patterson entropic map of Sr alone (section Z=.19), from which the coordinate $x_{Sr} \approx 0.16$ is deduced.

Fig.2(c) Selective Patterson entropic map of Sr alone (section Z=.50), from which the coordinate $z_{Sr} \approx 0.19$ is deduced.

Not only does the experimental procedure yield the Patterson Fourier coefficients, but it also gives cross-terms between the normal part of the structure and the purely Sr part, from which the phases of the non-overlapping Bragg reflections of the normal structure (data set measured far from the Sr K-edge) are obtained. We are then left with a partially phased powder data set, for which the Maximum Entropic procedure already implemented and described in last year's report plays a second vital part in order to retrieve the total electron density of SrSO₄ (Fig.3).

A non-anticipated, but inherent, practical difficulty is the normalization of the three data sets taken at various wavelengths. Using an internal polycrystalline diamond calibrant mixed with the sample resulted in substantial micro-absorption effects which cannot be ignored in the data analysis. A second difficulty is the overlap of the intense calibrant (c) peaks with those from the sample being studied SrSO₄, which results in the loss of some of the Patterson and cross-term information due to the fact that part of the powder patterns becomes useless. The former results in an even greater need to use MaxEnt to minimize truncation effects. The unphased information need not be lost if a fourth data set pertaining to SrSO₄ alone is taken far from the Sr K-edge, as was done in the present study. The overall result is that the full SrSO₄ structure could be satisfactorily recovered. This success opens new prospects for similar experiments on unknown compounds.

Two further applications of Maximum Entropy were explored, linked to the unique ability of the latter to yield enhanced Fourier maps incorporating non-trivial Prior Knowledge.

I) The first one is the study of Ca(OH)₂II (Portlandite), for which only powder x-ray

data are currently available (collaboration with SUNY). The problem is to locate the H atoms. The corresponding experiment, which requires a Diamond Anvil Cell, was carried out at CHESS using an image plate. Due to a somewhat restricted and noisy data set, only the Ca and O atoms could be found and refined using standard techniques. A preliminary treatment using MaxEnt could

SrSO₄ DENSITY - Z=0.16

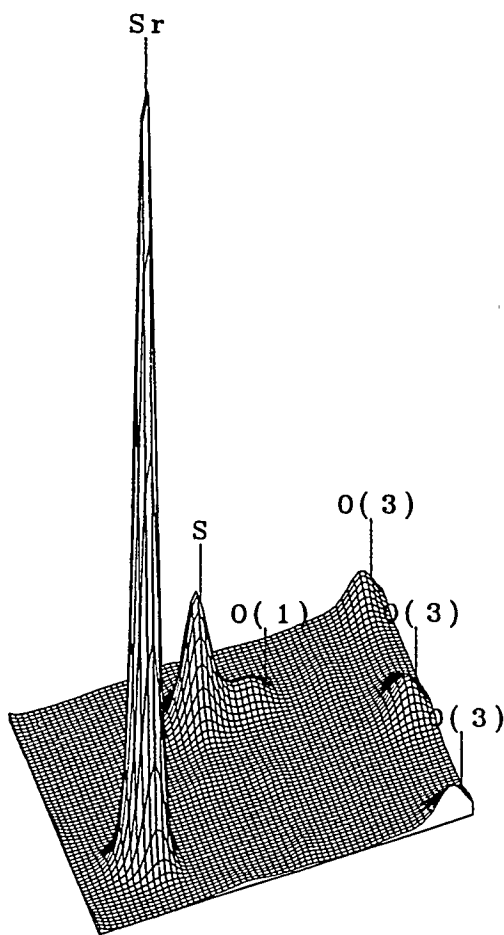


Fig.3 MaxEnt reconstruction of the electron density of SrSO₄ (section z=0.16), obtained from the partially-phased experimental data set obtained at $l = 1.1294 \text{ \AA}$, far from the Sr K-edge. The remaining oxygen O(2) appears in another section ($z=0.03$) and is not visible here.

only give hints of initial position parameters to be further refined by the Rietveld technique. In this case, constraining the H atoms to be found on isotropic spherical shells centered at the oxygen sites greatly improves the electron density reconstruction by eliminating obvious spurious features. Nevertheless, three to four possible H-sites remain on each shell (instead of one). The largest peaks on each shell were used as the initial starting position in the refinement leading to the possible solution.

A neutron experiment being currently out of the question due to the unavailability of a high-pressure cell, a much cleaner and better-resolved experiment is scheduled at X7A. Moreover, the more reasonable estimates of esd's obtainable from this high-resolution powder diffractometer should enable us to find the correct locations of the H atoms.

(ii) The second application aimed at pinpointing, if possible, disordered oxygen atoms in two new oxides of technological interest due to their nonlinear optical properties: Cs(TiAs)O₃ and Cs(TiP)O₃. In this last study, the result is negative and MaxEnt was essentially used to dismiss possible disordered oxygens O(2) found by Rietveld refinement as spurious. Given the high multiplicity of the disordered O(2), it is very unlikely that the latter can be found from powder data by ANY data analysis.

Based on experience gained during this project, a DEC/Alpha 3000 workstation was purchased and installed in June, 1995, two weeks before the completion of the project. Substantial improvements will be possible, since much larger problems can now be tackled, most importantly at much faster computing times (at least a factor of 8 with respect to the 486/66 PC used for this project).

If needed, Maximum Entropy reconstruction can now be carried out almost "on-line" at the NSLS-X7A beam line.

PAPERS/JOURNALS/PUBLICATIONS:

Based on the results described above, five papers have been written (three in press, two submitted) and one is in preparation.

Part of the work mentioned above was presented in an invited talk by R.J. Papoular at the Gordon Research Conference on X-Ray Physics, Plymouth, NH, 7-30-95 to 8-4-95.

R.J. Papoular and D.E. Cox, "Model-free search for cations in zeolites from high-resolution x-ray powder data using the Maximum-Entropy Method," (Europhysics Lett., in press).

D.E. Cox and R.J. Papoular, "Structure refinement with synchrotron data R-factors, errors, and significance tests," (Proceedings of the European Powder Diffraction International Conference (EPDIC IV), in press).

R.J. Papoular, Y. Vekhter and P. Coppens, "The Two-Channel Maximum Entropy Method Applied to the Charge Density of a Molecular Crystal: α -Glycine," (Acta Cryst. A, submitted).

M. Kunz, R. Dinnebier, L.K. Cheng, E.M. McCarron III, D.E. Cox, J. Parise, M. Gehrke, J. Calabrese, P.W. Stephens, T. Vogt and R.J. Papoular, Cs(TiAs)O₃ and Cs(TiP)O₃: "A Disordered Parent Structure of ABOCO₄ Compounds," (Journal of Solid State Chemistry, in press).

M. Kunz, R.J. Papoular and J.B. Parise, "Determination of Hydrogen Positions in Ca(OH₂, II)," (submitted).

R.J. Papoular, D.E. Cox and W. Prandl, "Ab-initio structure solution of SrSO₄ from high-resolution powder data using resonant x-ray scattering," (in preparation).

LDRD FUNDING:

FY 1993	\$24,431
FY 1994	\$73,342
FY 1995	\$39,778

Analysis of Structures and Interactions of Nucleic Acids and Proteins by Small Angle X-Ray Diffraction

Malcolm S. Capel

93-32

PROJECT DESCRIPTION:

Small angle x-ray and neutron scattering are being used to examine the structure of large complexes of biologically relevant macromolecules in solution.

TECHNICAL PROGRESS AND RESULTS - Fiscal Year 1995:

Purpose: Many biologically important processes are mediated by large complexes of proteins, or proteins and nucleic acids. For example, protein synthesis and folding are mediated by the ribosome and chaperonins respectively; while ATP-dependent proteases mediate degradation of damaged proteins. In most cases, these complexes have not yielded to structure determination by x-ray crystallography, thus limiting our understanding of their function. We have shown that small-angle neutron and x-ray scattering combined with scanning transmission electron microscopy (STEM) can provide useful structural information for large complexes in solution. Studies of this type are particularly useful for systems where high resolution structures for the isolated components can be obtained. In these systems, the combined use of low-resolution studies of the complexes and high-resolution studies of the components provides a framework for understanding the function of the complex. A major limitation is in extracting the contribution of a individual

subunit or component. To overcome this problem we have exploited techniques to enhance the contribution of individual components either by selectively labeling the target protein or nucleic acid with either gold clusters, for x-ray scattering studies and STEM, or uniformly labeling with deuterium for neutron scattering. The scattering curves for complexes reconstituted with labeled and unlabeled components can then be compared to gain information about the location of the labeled component.

Approach: Three systems were studied. These are the *Escherichia coli* Hsp60 and Hsp70 chaperonin and the ATP-dependent protease Clp systems. To ensure that the structural studies are biologically relevant, both biochemical and genetic studies were also conducted. These studies required a large amount of purified protein, and to this end each of the components were cloned and overexpressed. In some cases, cysteine residues were introduced into individual proteins to facilitate their labeling with gold clusters. For proteins that possess a free cysteine, labeling was achieved by reacting them with a sulfhydryl-specific gold clusters.

Technical Progress and Results: (a) We have examined the structure of the Hsp60 chaperonin system by neutron and x-ray scattering. This system is formed by two proteins, GroEL and GroES, that together are important for the folding of proteins both *in vitro* and *in vivo*. GroEL is a tetradecamer of 57kDa subunits and GroES is a heptamer of 10kDa subunits. A tight complex is formed between GroEL (801kDa) and GroES (70kDa) in the presence of the nucleotides ATP or ADP, but not in their absence. To determine the stoichiometry and location of GroES in the complex, GroES was uniformly labeled with deuterium, thereby increasing its

contribution to the neutron scattering of the complex in $^1\text{H}_2\text{O}$ solution. The stoichiometry of the ADP-GroEL/GroES complex was found to be 1:1; with GroES being located at the periphery. Moreover, by matching the contribution of deuterated GroES to that of the solvent, we have demonstrated that GroES does not induce a large conformational change in GroEL. This latter observation has important implications for the function of the GroEL/GroES chaperonin system. Modeling studies, using the recently reported crystal structure of free GroEL, are in progress to develop a model for the GroEL/GroES complex in solution.

(b) Structural studies were initiated with the *E. coli* Clp ATP-dependent protease system. The Clp system is composed of two subunits; ClpP, the protease subunits, and ClpA which is required for recognition and presentation of unfolded substrates to ClpP. This system appears to be functionally and structurally related to the 24S proteasome found in most eucaryotic cells. Initial small angle x-ray and neutron scattering, and STEM studies indicate that ClpP exists as a tetradecamer (14-mer) in solution. The structure of the ClpP oligomer is best described as a hollow cylinder having a central axial pore of 36Å. The central pore is sufficiently large to accommodate a portion of an unfolded protein but not most folded proteins. This suggests that the substrates for ClpP must first be unfolded, presumably by the ClpA component of the active protease. Studies of the ClpA component are in progress. The monomeric molecular weight of ClpA is 97kDa; however, it is thought to act as an oligomer of unknown stoichiometry. ClpA possesses an intrinsic ATPase activity that can be stimulated by unfolded substrates. In the presence of ATP, ClpA and ClpP associate to form the active complex. Continuing studies would determine the oligomeric state and low resolution structure

for the functional ClpA complex, and also for the ClpA/ClpP complex. During the course of this work a novel fluorescently labeled protease substrate (rhodamine-casein) has been identified. This substrate may replace the radioactively labeled substrate currently used to assay for Clp function.

(c) Studies were initiated to examine the structure/function of the Hsp70 chaperonin system, which in *E. coli* is made up of the proteins DnaK (70kDa), DnaJ (40kDa), and GrpE (20kDa). The Hsp70 and Hsp60 chaperonin systems are thought to act sequentially in the protein folding pathway *in vivo*. The mechanism of action for the Hsp70 system is not as well characterized as for the Hsp60 system and, in a study undertaken to characterize this system, it was initially observed that DnaK can interact with short hydrophobic peptides, and the unfolded state of a few proteins. Recent studies indicate that the biologically relevant functional complex involves both DnaK and DnaJ (DnaK-substrate-DnaJ). Further, the formation of the ternary complex requires a single round of ATP hydrolysis by DnaK. These studies have lead to the isolation of a complex containing GrpE-ADP-DnaK-substrate-DnaJ that is stable and biologically active in protein folding, and can be produced in sufficient quantities for structural studies. In parallel, high resolution structural studies of DnaJ have lead to a NMR-based model for the N-terminal DnaJ homology domain. Ultimately, we hope that the combined use of low-resolution structures of the complex and high-resolution structural studies of the individual components will aid in understanding the mechanism for this important chaperonin system. During the course of this study, a novel gold-labeled derivative of ATP was synthesized (Dr. J. Hainfeld). This compound may be useful in studying the complexes involving DnaK.

PAPERS/JOURNALS/PUBLICATIONS:

Kriwacki, R.W., Hill, R.B., Flanagan, J.M., Caradonna, J.P., and Prestegard, J.P. "New NMR Methods for the Characterization of Bound Waters in Macromolecules," *J. Amer. Chem. Soc.* 115, 8907-8911 (1993).

Szabo, A., Langer, T., Schroder, H., Flanagan, J., Bukau, B., and Hartl, F.U. "The ATP Hydrolysis-Dependent Reaction Cycle of the *E. coli* Hsp70 System, DnaK, DnaJ, GrpE," *Proc. Natl. Acad. Sci. USA* 91, 10345-10349 (1994).

Flanagan, J.M., Wall, J.S., Capel, M., Schneider, D.K., and Shanklin, J. "Scanning Transmission Electron Microscopy and Small-Angle Scattering Provide Evidence that Native *E. coli* ClpP is a Tetradecamer with an Axial Pore," *Biochemistry* 34, 10910-10917 (1995).

Hill, R.B., Flanagan, J.M., and Prestegard, J. "¹H and ¹⁵N Magnetic Resonance Assignments, Secondary Structure, and Tertiary Fold of *E. coli* DnaJ(1-78)," *Biochemistry* 34, 5587-5596 (1995).

Szabo, A., Korszun, Z.R., Hartl, F.U., and Flanagan, J.M. "A Zinc Finger-Like Domain of the Molecular Chaperone DnaJ is Involved in Binding to Denatured Protein Substrates," *EMBO J.*, in press.

Graziano, V., Capel, M., Schneider, D., and Flanagan, J.M. "Solution Scattering on Complexes of GroES/GroEL: Absence of a Large-Scale Conformational Change in GroEL upon Binding of GroES," manuscript in preparation.

FOLLOW-ON FUNDING:

National Institutes of Health Grant No. GM53181-01, "Structural and Functional Studies of the *E. Coli* Chaperone DnaJ," was resubmitted on July 1, 1995.

LDRD FUNDING:

FY 1993	\$42,276
FY 1994	\$97,690
FY 1995	\$47,579

Relaxographic MRI and Functional MRI

*Joanna S. Fowler and
Charles S. Springer, Jr.*

93-35

PROJECT DESCRIPTION:

This project began in October, 1993. It consists of three separate components:

1. The design and development of a high-field Magnetic Resonance Imaging (MRI) laboratory for the study of humans and animals at Brookhaven National Laboratory (BNL).
2. The continued development of the new form of MRI - *relaxographic* MRI - originated by Professor Springer's research group at the State University of New York at Stony Brook (USB).
3. The extension of a collaboration between Professor Springer's research group and Dr. Nora D. Volkow of the BNL Medical Department in the *functional* MRI (fMRI) studies of anesthetized mice in Professor Springer's animal MRI laboratory in the USB Department of Chemistry.

TECHNICAL PROGRESS AND RESULTS - Fiscal Year 1995

Purpose: The positron emission tomography (PET) laboratory in the BNL Chemistry Department is world-renowned. It is one of the earliest of all PET labs, and many important (and now frequently used) PET techniques, particularly for the brain, were introduced at BNL. In the last ten years, the rapid development of MRI brain studies, of physiology and function as well as anatomy,

has made it an important complement to PET. Together, these two modalities now dominate the practice of *in vivo* neuroscience. It is essential for the vitality of the new *Brookhaven Center for Imaging and Neuroscience* that it have active laboratories for both imaging modalities; so that they can be used synergistically and, indeed, that their respective data can be intrinsically combined.

Approach: Our approach to accomplish this goal has been greatly facilitated by support from the LDRD Program. Professor Springer began a sabbatical leave from USB in the Fall of 1993. He spent a part of each week at BNL. His salary for the Fall Semester was paid by USB. In January, 1994, he moved to the BNL Chemistry Department full time. His salary for the Spring Semester and for the Summer was paid from this LDRD project budget. He spent part of each week at USB in order to maintain his small-animal MRI laboratory there and to supervise his research group of USB Chemistry graduate students.

As FY 1995 began, there was a ground-breaking ceremony for the new high-field MRI laboratory building.

The USB graduate students began to move to BNL to help start the BNL part of the research program. Professor Springer's National Institutes of Health (NIH) Grant had been transferred to BNL in the Summer. In return for teaching a course at USB in the Fall Semester of 1994, USB supported Professor Springer's salary for the Spring Semester of 1995.

Technical Progress and Results: We made significant progress in each of the three components of this project.

Component 1. MRI Laboratory

Siemens Medical Systems, Inc. and its partner in this venture, Spectroscopy Imaging Systems (a subsidiary of Varian Associates, Inc.) are now well into the installation of a very powerful general purpose four Tesla (4 T) whole body MR imaging spectrometer. This is a tremendous accomplishment for BNL. The field strength (measured as flux density) of 4 T for the MR magnet is the largest used for humans. There are only five other instruments in the world with human-sized magnets of this field strength. The \$3.54 million cost of this instrument has been generously supported by OHER and the National Institute of General Medical Sciences of NIH. The magnet was successfully tested at its designed field of 4 T at BNL on 17 September, 1995. If the remainder of the installation proceeds as scheduled, the instrument should begin producing images by the end of 1995.

Component 2. Relaxographic Imaging.

At the beginning of FY 1995, we published a paper introducing and demonstrating the concept of a new fundamental form of MRI, *relaxographic* MRI. This is the production of an image of the spatial distribution of the nuclear spins that comprise only a portion of the distribution of relaxation times that describes the recovery of the entire spin magnetization of an object after an RF pulse. The sum of all relaxographic images of an object is its spin-density image: that is, relaxographic images are spin-density complements.

This approach has great power for *in vivo* MR. Thus, during FY 1995, we have continued to pursue it. While our new MRI instrument is being installed, Ms. Ildiko Palyka, a graduate student in the BNL group, traveled to the University of Minnesota to use

the 4 T instrument there; essentially the twin of the new BNL machine. Working with Dr. Jing-huei Lee, now also a member of the BNL group, she produced the longitudinal relaxogram seen in Figure 1.

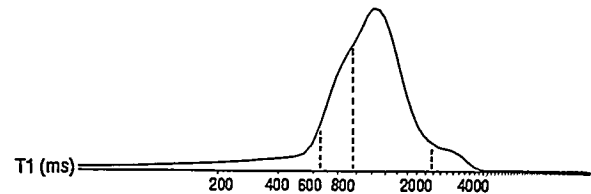


Figure 1

This is the distribution of the longitudinal relaxation time (T_1) values for the $^1\text{H}_2\text{O}$ spins in a chosen axial image slice from a human brain. The T_1 value characterizes the recovery of the equilibrium magnetization projection on the static magnetic field axis. The log-scale abscissa in Fig. 1 reports the T_1 values in ms. Though discrete peaks are not completely resolved in this particular relaxogram, shoulders suggesting distinct spin populations can be discerned. The relaxographic images obtained from these components reveal the natures of these populations. Figures 2 and 3 depict two such images: they are axial (transverse) slices. Fig. 2 is the map of those spins giving rise to the shoulder spanning 625 ms to 950 ms - indicated with dashed lines in Fig. 1. It clearly represents the water of the brain white matter. Only one eye is seen in the image of Fig. 2 (and Fig. 3) because the plane of the axial slice is slightly skewed. The main relaxographic peak, spanning 950 ms to 2350 ms in Fig. 1, gives rise to the relaxographic image of Fig. 3, which shows only gray matter water. Since these two populations compose

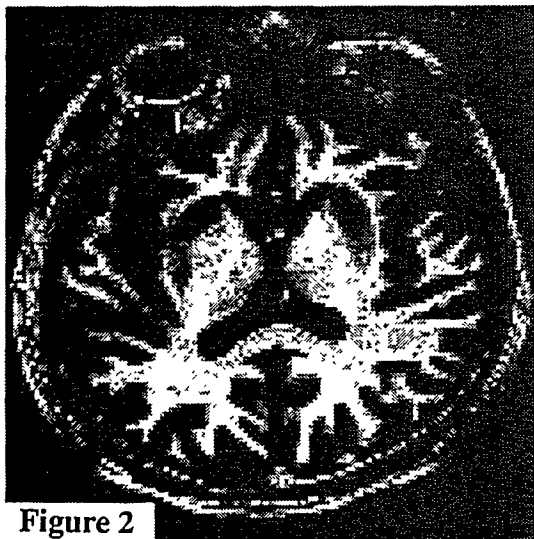


Figure 2

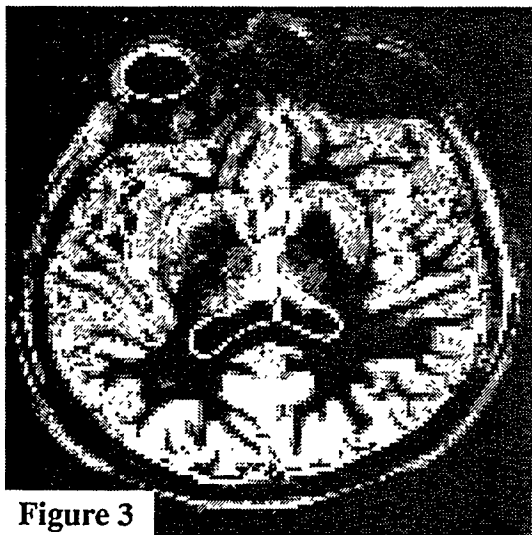


Figure 3

the vast majority of all of the spins (Fig. 1), the complementarity of the two images in Figures 2 and 3 is quite understandable. Relaxographic images (not shown) of the small populations below 625 ms, and spanning 2350 ms and 4000 ms, in Fig. 1 reveal fat ^1H spins, and the ventricular CSF and vitreous humor water spins, respectively.

The relaxographic images of Figures 2 and 3 show the essentially complete discrimination of white and gray matter. The contrast between the two is almost 100%. These two tissue types are "segmented"

naturally; based on the physical properties of their water spins. Tissue water T_1 values depend principally on the concentrations of macromolecules and macro-molecular assemblies, and on the concentrations of paramagnetic species such as iron atoms. These relationships can be quantitated. When relaxographic peaks are more clearly resolved, relaxographic images made from them can also be quite quantitative. Their intensities are proportional to the actual numbers of spins giving rise to them.

Component 3. Functional Imaging.

The term *functional* MRI (fMRI) denotes the direct, noninvasive detection of brain activity by MRI. The detailed mechanism giving rise to the changes observed is not yet certain. However, there is little doubt that at least a significant contribution comes from transient changes in the bulk magnetic susceptibility (BMS) of blood in the relevant brain regions, attendant to changes in the degree of blood oxygenation during mental activation. Professor Springer's USB research group has been studying the underlying principles of BMS effects in NMR and their manifestations in *in vivo* MR since the early 1980s. The small transient changes in blood BMS during cerebral activity are most sensitively detected with higher magnetic field MR instruments. This is one of the main reasons that BNL is installing a human-sized device with a field of 4 T, the largest used for humans. In Professor Springer's laboratory at USB, the MRI instrument has a field strength of 9.4 T, but the magnet bore size restricts *in vivo* studies to mice or smaller animals. Thus, Ms. Palyka and Dr. Wei Huang, then a USB graduate student, decided to try some fMRI studies with mice.

There is an interesting fundamental difference between fMRI investigations of

humans and animals. Animals cannot be instructed in the cognitive protocol and, more importantly, cannot be relied upon to remain motionless inside the magnet. The fMRI signals are particularly sensitive to motion. Animal subjects must be anesthetized in order to conduct the experiment. Having found that a mouse's eyes remain open during anesthesia induced by pentobarbital, Ms. Palyka and Dr. Huang decided to conduct visual stimulation studies of the mouse brain. This led naturally to the question of cerebral response to light during anesthetic-induced unconsciousness. Is it possible that we "see" light when we are not aware that we are seeing it? Ms. Palyka and Dr. Huang obtained very interesting results. Figure 4 depicts two plots of data from a photic stimulation study of an anesthetized mouse. The vertical axes measure the strength of the fMRI response in the visual cortex of the mouse to a flashing white light: the top graph shows simply the signal change, while the ordinate of the bottom graph reports the natural logarithm of the change. The horizontal axis is the same in each graph; the time elapsed since the bolus administration of pentobarbital to the mouse. The top graph demonstrates that during the first hour following administration of the anesthetic agent, there is essentially no response to a flashing light stimulus. After this, a response becomes detectable, and grows in strength as time passes. The curves in the top graph and the straight lines in the bottom graph demonstrate that the recovery of response has a single exponential time course. We suspect that this reflects the wash-out of the anesthetic agent from its active site in the brain. The mouse remains anesthetized during the entire experiment, however. The beginnings of motion due to arousal are quite evident in the fMRI maps, and necessitate the end of the study. As in this case, this usually occurs *ca.* three hours after administration of pentobarbital.

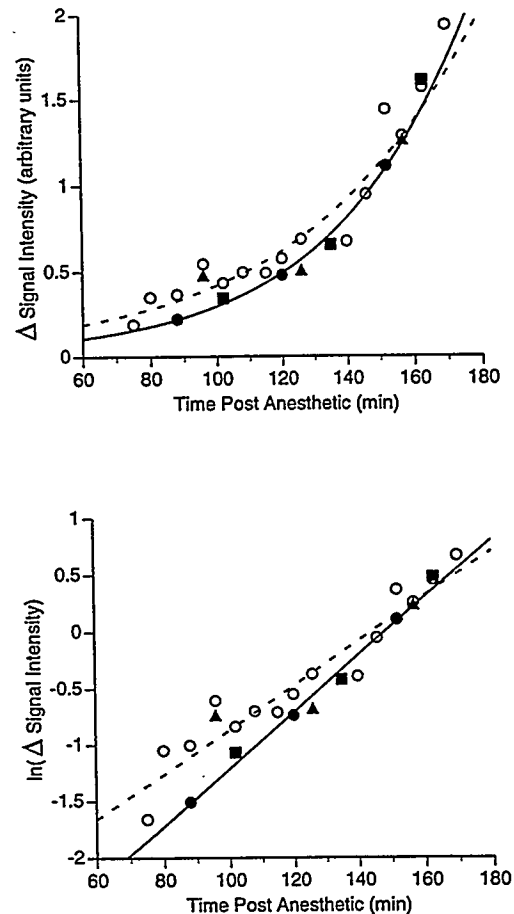


Figure 4

We find these results to be quite exciting. We understand that there really is no quantitative physiological definition of anesthesia. Our results suggest that fMRI can play a significant role in establishing such a definition. We look forward to extending these experiments in a much more rigorous fashion by investigating baboons in the new BNL MRI instrument.

PAPERS/JOURNALS/PUBLICATIONS:

"Relaxographic Imaging," C. Labadie, J-H. Lee, G. Vetek, and C. S. Springer, *J. Magn. Reson. B.* 105 99-112 (1994).

"The Effects of Bulk Magnetic Susceptibility in NMR," I. Palyka, W. Huang, and C. S.

Springer, *Bull. Magn. Reson.*, in press (1995).

"Functional MRI Detection of the Murine Brain Response to Light: Negative fMRI Changes and Temporal Differentiation," W. Huang, I. Palyka, H-F. Li, E. M. Eisenstein, N. D. Volkow, and C. S. Springer, submitted for publication.

"Functional MRI Detection of the Effect of Anesthesia on the Murine Brain Response to Visual Stimulation," I. Palyka, W. Huang, H-F. Li, E. M. Eisenstein, N. D. Volkow, and C. S. Springer, submitted for publication.

Refereed Abstract:

"The Effect of Anesthesia on the Mouse Brain Response to Visual Stimulation," W. Huang, I. Palyka, E. M. Eisenstein, N. D. Volkow, and C. S. Springer, *Proc. Soc. Magn. Reson.* 3 783 (1995)

Presentations:

"Ion Transport," Workshop on Advances in Physiological Chemistry by *In Vivo* NMR; Woods Hole, Massachusetts; 23 March, 1995. (Invited Session Chair).

"The Effects of Bulk Magnetic Susceptibility in NMR," Twelfth Conference of the International Society of Magnetic Resonance; Sydney, Australia; 18 July, 1995. (Invited ASBMB (Australian Society for Biochemistry and Molecular Biology) Lecture).

"The Effect of Anesthesia on the Murine Brain Response to Visual Stimulation," Third Meeting of the Society of Magnetic Resonance; Nice, France; 22 August, 1995. (Poster presentation by Dr. W. Huang).

"Magnetic Susceptibility in MRI: From Brain Artifact to Activation," Inaugural Betts Lecture Series; on Biomedical NMR; Department of Chemistry, University of Manitoba; Winnipeg, Manitoba; 29 September, 1995. (Invited Lecture).

LDRD FUNDING:

FY 1993	\$8,675
FY 1994	\$93,408
FY 1995	\$105,161

Note: This project involves vertebrate animals.

Very Low Temperature Infrared Laser Absorption as a Potential Analytical Tool

Gregory E. Hall and
Trevor J. Sears

94-03

PROJECT DESCRIPTION:

Infrared laser absorption spectroscopy of molecules at temperatures close to 4 K is being studied in a novel collisionally cooled absorption cell. Calculations indicate that there are large benefits to be gained in terms of sensitivity and measurement accuracy compared to experiments at ambient temperatures and measurements are being conducted in prototype systems in order to verify these predictions and characterize the samples. The technique has strong potential for development as an analytical tool as well as providing information of fundamental scientific interest.

TECHNICAL PROGRESS AND RESULTS - Fiscal Year 1995:

Purpose: Spectral congestion caused by an abundance of overlapping lines frequently limits the value of spectroscopic measurements. At room temperature, the infrared absorption spectra of gaseous molecules consist of many Doppler-broadened vibration-rotation transitions. Cooling the sample to cryogenic temperatures can have a dramatic effect. The number of lines will decrease, as the number of thermally populated rotational states decreases. The intensity of the remaining lines belonging to the lowest energy states will increase correspondingly. Each line will also become sharper, as the molecules slow down and have a decreased Doppler width. Cooling from 300 K down to

4 K will decrease the line widths by an order of magnitude. For a typical molecular species of interest, C_2H_5 , the ethyl radical, containing two heavy atoms, the rotational partition function decreases from approximately 20,000 at 300 K to less than 20 at 4 K leading to a further factor of 10^3 in absorption intensity for low lying levels. The peak absorption intensities can thus be enhanced by a factor of 10^4 , allowing greater sensitivity, resolution and measurement accuracy.

Approach: Simply cooling a sample to 4 K, however, does not achieve the enhancement described above, since the equilibrium vapor pressure of virtually all molecular species at 4 K is close to zero. In the condensed phase, all the detailed spectral information present in the gas phase spectrum is lost. Recently however, a novel technique has been demonstrated that allows the measurement of gas phase molecular spectra at cryogenic temperatures. In this technique, the molecule of interest is introduced into a low pressure sample of helium gas, held at approximately 4 K, via an insulated needle injector that connects the low temperature cell containing the helium to an external ambient temperature reservoir. The injected molecules suffer collisions with the cold helium atoms and reach the temperature of the cold buffer gas in fewer than 100. Naturally, the introduced molecules eventually diffuse to the walls of the chamber and condense, however this process involves many more collisions, typically 10,000 at 10 mTorr pressure, and a steady state concentration of cold molecular species can be maintained.

Technical progress and results: The first year of this project was described in the 1994 Annual Report. During 1995, we extended our earlier work to a heavier species, NO_2 , where the benefits of reduced sample temperature are greater. The results are illustrated in Fig. 1 where we show a section

of the $(v_1, v_2, v_3) = (0, 0, 1) \leftarrow (0, 0, 0)$ vibration rotation transition near 1613 cm^{-1} .

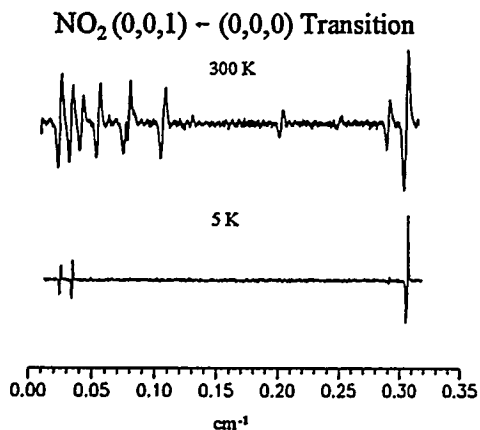


Figure 1. Comparison of warm and cold NO_2 spectra.

The increase in sensitivity and reduction in spectral line widths obtained on reducing the sample temperature from 300 K to a nominal 5 K are clearly apparent. The ambient temperature spectrum was obtained at a sample pressure of 50 mTorr while the low temperature one was obtained in a helium bath gas pressure of 40 mTorr. The transitions in the low temperature spectrum correspond to the two fine structure components of the $3_{12} - 4_{13}$ rotational transition while the large, partially resolved peak at higher wavenumber is due to the two components of the $3_{03} - 4_{04}$ transition. From the relative intensities, we can estimate a rotational temperature of 8 K in this sample. Figure 2 shows a comparison of the integrated low temperature spectrum and theory, illustrating the agreement.

We also investigated two schemes for a multi-pass enhancement of the signal intensity. The first used a confocal mirror arrangement external to the vacuum chamber and cold cell, which required Brewster angle window modifications to the cell and vacuum chamber. The probe laser beam was introduced at a small angle away from the central axis of the cell, achieving 4 traversals

of the sample cell before the beam exits at slightly different angle. The returning beam can be separated from the entry beam and imaged onto the detector. The NO_2 spectra were recorded using this arrangement. Due to imperfect optical materials and the fact that the laser beams are not strictly at Brewster's angle, more than 4 traversals cause unacceptably large reflection loss. The second multipass scheme used reflective optics at the ends of the cold sample cell, and avoided the multiple passes through Brewster angle windows. An arrangement with one flat mirror, silver coated on the inside except for a 2 mm diameter uncoated entrance/exit aperture, and a concave mirror on the opposite end of the cold cell allowed significantly more traversals of the probe beam, up to 14. We found the system hard to use, however, as the alignment inside the vacuum system was hard to verify, and undesired interference fringes masked the absorption lines.

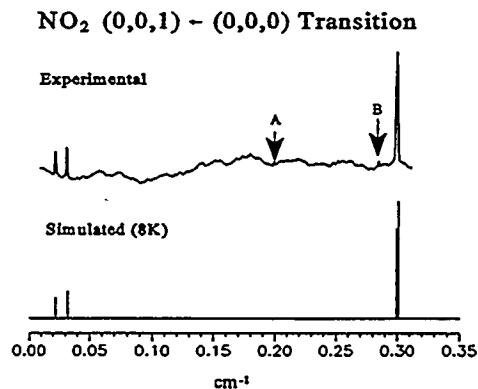


Figure 2. Comparison of experimental and simulated NO_2 spectra.

The results for NO_2 also allow us to estimate the mixing ratio of sample gas from the optically measured column densities, i.e. the molecular density along the integrated along the optical path. Assuming that the cold NO_2 molecules are primarily confined to a 2 cm region around the injector, we found a

partial pressure of NO_2 at 10 K of 0.15 mTorr, corresponding to a dilution ratio of 1:250 in the helium bath. This is a considerably higher concentration than estimated by previous microwave experiments by other workers.

Reverting to a single pass configuration, we could estimate a quantity related to the product of the concentration and temperature of the sample gas as a function of distance from the injector nozzle. Unfortunately, the current design of the chamber results in a fairly small aperture through the center of the cell and it is not possible to extend the measurements more than 2-3 beam diameters (approximately 5 mm) from the injector. At a displacement of approximately 5 mm from the injector axis in a horizontal plane, we found a signal decrease of approximately 1/3 in a strong NO line. It is not possible to separate the contributions from temperature and concentration gradients to this change without a model of the heat and mass flow in the gas sample which we discuss below. Further measurements are also necessary in order to characterize the sample distribution more accurately.

Finally on the experimental side, attempts were made to detect the products of photochemical reactions, initiated by pulsed excimer laser photolysis at low temperatures. As a first system, we chose to look for methyl radicals (CH_3) formed on the photolysis of acetone ($(\text{CH}_3)_2\text{CO}$) at 193 nm. This reaction is known to produce two methyls and a carbon monoxide molecule. Attempts to detect the radical absorption spectrum were not successful, however, we could monitor build-up of CO through transitions in the vibrational fundamental close to 5 microns. While this result demonstrated the presence of acetone in the sample at low temperatures, the gas phase concentration may be significantly lower than that of the more volatile molecules previously

studied. As the acetone flow rates were increased in an attempt to increase the sample density, problems were encountered due to accretion of solid crystalline acetone on the cold cell which eventually blocked the laser beams.

In parallel with the experimental program, we undertook a modeling study of the thermal and mass transport properties of the collision cell. In the presence of strong temperature gradients, the steady-state concentration profiles and temperature profiles depend on a balance of heat transfer through spatially variable thermal conductivity, including a distributed heat load produced by the warm gas flow, and mass transport driven by concentration gradients (Fick's Law diffusion) and by temperature gradients (thermal diffusion). Both analytic and numerical approaches were developed, with the aim of providing predictive aids for optimizing experimental conditions. While important groundwork has been completed in the modeling calculations, further work is still required to make direct contact with experimental measurements. Line-of-sight averaged rotational distributions, Doppler line shapes, total concentrations, and transient properties of photogenerated species can all be compared to experiment for model validation and to suggest experimental improvements. We intend to push ahead with this modeling project, which should be of general use to a growing group of spectroscopists and analytical chemists interested in this technology.

CONCLUSIONS:

The project has demonstrated that this technique has several attractive features:

(a) It fulfills the initial promise of providing a method for studying the spectra of heavier gas

phase molecules whose spectra at ambient temperatures are extremely complicated.

(b) There is a need for better characterization of the sample properties from both experimental and theoretical perspectives.

(c) The prospects for studying gas phase chemistry at cryogenic temperatures are less compelling.

(d) Moving to shorter wavelengths where probe laser sources are more powerful and detectors more efficient would be beneficial.

We anticipate that a new near infrared diode laser system currently under test in our laboratory will be used to investigate this last point.

PAPERS/JOURNALS/PUBLICATIONS:

"Very Low Temperature Infrared Laser Absorption Spectroscopy of N₂O, NO and NO₂" P. Jin, H. Wang, S. Oatis, G. E. Hall and T. J. Sears, *J. Molec. Spectrosc.* 173, 442-451 (1995). (peer reviewed)

"Very Low Temperature Infrared Laser Absorption Spectroscopy" P. Jin, G. E. Hall and T. J. Sears, paper RH01 presented at the 50th Ohio State University International Symposium on Molecular Spectroscopy, June 1995.

FOLLOW-ON FUNDING:

Additional support for the extension and continuation of this project has been obtained through three collaborations. A chemistry graduate from the University of Chicago joined the group as a summer visitor from the undergraduate Summer Student Program, administered through the BNL Education office. We undertook a thermal transport modeling study of the cryogenic gas temperature and density gradients. The steady state temperature and density profiles can be modeled and compared to experimental line-of-sight averages. Secondly, a high school science teacher spent a six week period working on the design of multi-pass optics to be incorporated in the low temperature cell. This was also under a BNL Education Office program.

Finally, Professor Susan Oatis from Long Island University, Southampton has continued her on-going collaboration with the research group, aided by a competitively awarded grant from LIU allowing her a release from teaching for research associated with this project. A proposal to NSF for funding for a semester release beginning in Spring 1996 has also been submitted. This is concerned with the possible use of the technique to study trace atmospheric species.

LDRD FUNDING:

FY 1994	\$57,142
FY 1995	\$59,070

State-Resolved Measurements of H₂ Photodesorption: Development of Laser Probes of H₂ for In-Situ Accelerator Measurements

M. G. White and R. J. Beuhler

94-05

PROJECT DESCRIPTION:

The UV/VUV photodesorption of H₂ and other background gases found in accelerator vacuum systems is being studied by state-selective laser methods. These measurements are pertinent to synchrotron radiation induced desorption which plays a major role in determining the beam chamber vacuum and lifetime of high energy electron/proton storage rings.

TECHNICAL PROGRESS AND RESULTS - Fiscal 1995:

Purpose: The purpose of this project is to explore the dynamics of H₂ production by photodesorption from cryogenic metal surfaces such as those found in superconducting magnets of the next generation particle accelerators. Photodesorbed gases, especially H₂, are expected to play a major role in determining the lifetime of stored beams in large accelerators where synchrotron radiation strikes the surfaces of LHe cooled (4.2K) superconducting bend magnets. We propose to study the desorption of H₂ and other small molecules (CO, N₂, CO₂) by state-selective laser techniques which can provide information on the desorption mechanism and energy distributions of the desorbed molecules. The outcome of this work should result in a

detailed characterization of the photodesorption process as well as a prototype design for in-situ laser measurements in accelerator vacuum systems.

Approach: State-selective laser techniques and mass spectrometry are used to measure the translational energy as well as the internal state distributions of small molecules desorbed from cryogenically cooled metal surfaces. Our approach makes use of coherent vacuum ultraviolet (VUV) radiation to photoexcite desorbed molecules with high sensitivity (10⁶-10⁷ molecules per quantum state) and selectivity (0.7cm⁻¹ bandwidth) through the use of (VUV+UV) resonant multiphoton ionization (REMPI). From a combination of time-of-flight arrival distributions and rovibrational spectra of intermediate electronic states, it is possible to determine the velocity and state distributions of molecules photodesorbed by a second UV/VUV laser. A number of common beam tube materials such as Cu, Al and stainless steel, will be used to evaluate the sensitivity of the desorption properties on metal substrate. The VUV REMPI methods will focus primarily on H₂ desorption but will be extended to detect CO, N₂ and CO₂ which includes the most important desorption gases in UHV vacuum systems. These studies are also useful for evaluating the utility of laser-based *in situ* measurements of H₂ densities in accelerator environments.

Technical Progress and Results: A new, ultra high vacuum (UHV) apparatus was assembled for state-selective detection of desorbed species from cryogenically cooled metal surfaces. The apparatus includes a linear time-of-flight (TOF) mass spectrometer for species identification and translational energy distributions, a triply-differentially pumped, laser VUV radiation source for state-selective excitation of desorbed molecules, and a fully rotatable, LHe cooled sample holder for

mounting metal crystals and angularly dependent desorption measurements. An excimer laser operating at a variety of UV wavelengths (308 nm, 248 nm, 193nm) is used to induce electronically stimulated desorption while an IR laser operating at 1064 nm is employed for studies of laser-induced "thermal" desorption.

Initial measurements have focussed on the IR laser-induced "thermal" desorption of CO from low temperature Cu and Ag surfaces. CO is only weakly physisorbed (~5 Kcal binding energy) to Cu and Ag and only at temperatures below 50K. Consequently, these systems are well suited for exploring the general features of photodesorption of background gases physisorbed on cryogenically cooled beam tubes. Infrared measurements provide information on desorption induced by rapid heating of the metal surface caused by the thermalization of electron-hole pairs excited by the laser.

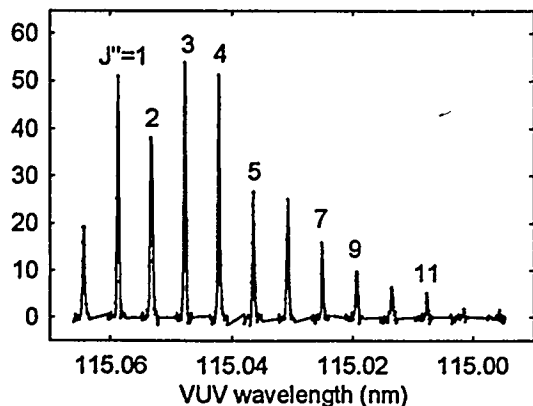


Figure 1: Rotational spectrum of the VUV-induced B-X transition of CO molecules resulting from IR-photodesorption from a Ag (111) surface at 42K. This spectrum yields a Maxwell-Boltzmann rotational state distribution with a rotational temperature of 110 K.

Previous state-resolved measurements for NO and CO chemisorbed on Pt and Ni surfaces

exhibit low energy desorption channels that are attributed to laser-induced surface heating, however, the observed translational and rotational temperatures are considerably different. By contrast, our measurements for IR-desorption of CO from Ag(111) at 42K result in "thermal" (Maxwell-Boltzmann) rotational and translational energy distributions with nearly identical characteristic temperatures (see Figures 1 and 2). The equilibration of rotational and translational temperatures of the desorbed CO is consistent with a thermally activated desorption process for which the desorption rate peaks at the maximum surface temperature induced by laser excitation.

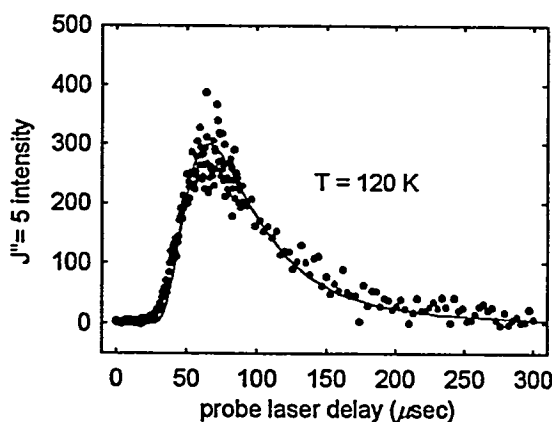


Figure 2: Arrival time distribution of CO molecules in the $J''=5$ rotational state resulting from IR-photodesorption from a Ag (111) surface at 42K. The data is well described by a Maxwell-Boltzmann velocity distribution with a translational temperature of 120K (solid line).

Surprisingly, the rotational and translational distributions were found to be independent of IR laser intensity in apparent disagreement with the accepted heat diffusion model of laser-induced surface heating. The latter results suggest that desorption is not a result of surface heating, but involves electronic

excitation of the surface which is dependent on the photon energy and not the absorbed fluence. Desorption measurements at higher photon energies are currently in progress in an effort to determine the relative importance of surface heating versus surface excitation in photodesorption.

In addition to the above measurements, we have completed implementation of a second-generation LHe cryostat which can be used to routinely cool sample substrates to 4-5K. As a result, it is now possible to extend our desorption studies to physisorbed H₂, which has a desorption temperature of ~8K on most metal surfaces. As the one-photon absorption oscillator strengths for H₂ are significantly greater than for CO, we expect to be able to perform state-resolved desorption measurements on H₂ at partial pressures as low as 10⁻¹⁰ - 10⁻⁹ Torr⁵ (10⁶ - 10⁷ molecules/cm³). These detection limits are well below the H²

partial pressure (~10⁻⁸Torr) found in previous measurements of synchrotron radiation induced desorption of a LHe cooled stainless steel beam tube. Future studies will focus on the photon energy dependence of H₂ desorption including the development of a "white light" plasma source which will be used as a laboratory model for accelerator diagnostics.

PAPERS/JOURNALS/PUBLICATIONS:

L. E. Fleck, B. Niu, R. J. Beuhler and M. G. White, *State-Resolved Dynamics of Infrared Photodesorption of CO from Ag (111)*, in SPIE Conference Proceedings, H.-L. Dai and J. M. Hicks, editors, to be published.

LDRD FUNDING:

FY 1994	\$68,871
FY 1995	\$77,222

Siberian Snake Prototype Development For RHIC

M.A. Harrison

94-06

PROJECT DESCRIPTION:

A helical dipole magnet is one in which the dipole field, rather than remaining vertical, rotates uniformly along the length of the magnet. Such magnets are required to do spin physics at RHIC. The parameters required include the following: $B \sim 4T$, aperture = 100 mm, low current operation ($<500A$) to minimize heat leak through many necessarily separated leads, and a pitch in the helix of approximately 180 degrees in one meter. There is no published record that such magnets have been built in the past; this is not surprising since they serve no useful purpose in normal accelerator or beam transport optics.

TECHNICAL PROGRESS AND RESULTS - Fiscal Year 1995:

Purpose: The purpose of this R&D program is to demonstrate the feasibility of implementing polarized protons in the RHIC accelerator by constructing a prototype Siberian Snake module.

Approach: Design Principles: Various possible ways to build a helical magnet were considered without any particular method standing out as obviously superior. The usual rules of engagement for the building of superconducting magnets still apply: that high forces be contained, that superconductor motion (particularly stick/slip motion) be minimized, that energy be safely extracted from the magnet at quench, that the ends of the magnet be restrained, that cooling be adequate for the operational conditions, etc. The design that is presently being developed

borrowed some concepts developed in the SSC and RHIC magnet programs, in particular the coils of the RHIC sextupole magnet and the assembly methods used for RHIC correctors. However, the critical question of how to build a spiral coil uses a new concept: grooves milled into a thick-walled aluminum cylinder to give a $\cos(\theta)$ current distribution when the grooves are filled with conductor. Unfortunately, this approach mandates that there will be considerable labor required in building model magnets because the many turns forming the coils will have to be wound by hand. The positive side of this approach is that models can be built without a large tooling expense. If this design goes into production, then some relatively straightforward tooling can be built to reduce the labor required to acceptable levels.

Technical Progress and Results: It was found that the superconductor wire being used in the RHIC corrector program could be used for the helical magnet design if it is wound into a 7-strand cable. This conductor, nearly one mm in diameter, would require 382A to produce a 4T field in the present design. By using this existing wire, the need to develop a new superconductor is circumvented. Using a cable in the magnet is preferable to using a single wire: if a break in a wire should occur, the magnet would very likely still operate. The required cable has been manufactured in sufficient quantity for a first model of the present coil design. The required Kapton insulation was also wrapped onto the cable in the manufacturing operation.

As stated, this small diameter cable is hand-wound in an ordered pattern into slots milled into an aluminum cylinder. A piece of prepreg fiberglass cloth is placed between each layer of cables in the slots. Pins at the ends allow the winding to proceed without cables bunching together. When all the turns have been wound onto the cylinder, they are compacted with ring clamps or other means,

and then the entire assembly is placed into an oven to cure at elevated temperature, thereby forming a series of current blocks around the cylinder in which each cable is firmly supported in a fiberglass/epoxy matrix. This design for supporting the cable turns is analogous to that developed for the wire turns in the RHIC sextupole magnet. The ends are then filled with a mineral-loaded epoxy and cured in a follow-on operation, a technique used in the SSC program for adding strength and rigidity to coil ends.

Two of these cylinders, concentric with one another, are required to give the required field of 4T. These two cylinders will be mounted into an iron yoke using a support scheme as is being used for the RHIC corrector magnets. A helium containment shell is then welded in place around the yoke, serving also as the magnet support structure. From this point, the design is similar to that of the arc magnets for RHIC and all the same concepts and methods will be used as appropriate.

It is estimated that the helical magnet operating at 4.2K will have a margin in field of 16% above 4T. This is too slender a margin for an untested design such as this, so an operating field of 3.5T is recommended for this design, giving in the case a margin of 33%. Undesired harmonics are easily minimized in this design by adjusting the thickness of the walls between current blocks, a procedure analogous to adjusting coil wedges in a conventional magnet.

Status: The parameters for a first model have been established. Superconducting cable wrapped with kapton has been delivered to BNL and tested. A suitable magnetic design, including end design, has been made. The engineering design for one of the required two cylinders has been completed, material has been procured, and the cylinder has been manufactured in the BNL shops. The winding

and curing of the cylinder has been completed, and an initial test to measure quench performance has been conducted. It was found that this coil quenched near short sample, with some modest training and some most variation in the achieved quench currents. This result was quite encouraging and has pointed the way to some changes in the assembly to enhance the quench performance.

Future Work: *Lab:* After making some small changes and additions in the coil construction (recure with increased pressure, overwrap with kevlar), the coil will be retested for quench performance. In addition, tests will be performed to measure the temperatures reached in the coil during quench, and the magnetic field along the length of the coil will be measured.

Design: Based on experience gained with the construction of the initial prototype, some changes are being made in the design of the ends of the coil. Otherwise, the design appears good, and it is planned to build both inner and outer coils, and to assemble them into a complete cold mass for testing later in the year. In parallel, new design is being developed that will have increased margin (~10% in field) by increasing the number of turns in the inner coil and by increasing the operating current in the outer coil. Accelerator physics requirements will dictate the actual design that is finally built..

FOLLOW-ON FUNDING:

Negotiations for full project funding are underway with the Japanese research institute at RIKEN.

LDRD FUNDING:

FY 1994	\$132,139
FY 1995	\$133,591
FY 1996 est.	\$220,000

Synthesis and Characterization of Novel Microporous Solids

J. A. Hriljac

94-09

PROJECT DESCRIPTION:

Synthetic routes to new large-pore microporous solids are being developed and these, and related materials, are being studied using powder and microcrystal diffraction techniques.

TECHNICAL PROGRESS AND RESULTS - Fiscal Year 1995:

Purpose: Crystalline large-pore molecular sieves are important materials for a variety of industrial applications in traditional fields such as catalysis and sorption, and are also needed as new hosts for hybrid inclusion compounds (such as those formed with semiconductor, organometallic, or organic molecules) with novel electronic or optical properties. The rational synthesis of new frameworks presents a tremendous scientific challenge due to a limited knowledge of the crystallization mechanism(s) and the metastable nature of molecular sieves. The work in this program is aimed at increasing the understanding of the formation of these compounds as well as synthesizing and characterizing new materials. It relies heavily on the ability to perform crystallographic work on powders or small single crystals, and includes the development of the appropriate techniques, instrumentation, analysis methods, and their implementation at the NSLS and HFBR.

Approach: Two related studies are being undertaken to elucidate the chemical factors which produce large-pore molecular sieves. The first of these is the role of templates. It is

well known that one can influence the products formed from a reactive gel via 'structure directing' or 'templating' by the addition of appropriate cations. The nature of this process and the details of the gel chemistry are not well understood, and further work is clearly needed if the rational design of new molecular sieves is going to be achieved. To elucidate the template-solid relationship a series of related molecular sieves will be prepared and the crystal structures determined before any calcinations or treatments. Attempts will then be made to correlate the template shape and siting with the pore structure. The second study will explore the synthesis of materials with unusual chemical compositions, particularly borates. The approach is based on the postulate that in the aluminosilicate zeolites there is a limit on the possible topologies that is imposed by the strictly tetrahedral coordination of silicon, the connectivity of the tetrahedra only through corners, and a rather narrow range of observed Si(Al)-O-Si(Al) angles. These constraints are relaxed in the alumino- and gallophosphates and one finds not only aluminum in 5- and 6-coordinate sites but also a greater number of well defined large-pore sieves. Microporous borates should offer a rich diversity of topologies, as boron is often three- or four-coordinate and forms a variety of ring and cage compounds.

The crystallographic work includes the continuing development of techniques for solving structures *ab initio* from high resolution powder diffraction data and refining the structural models against synchrotron X-ray and neutron data. It also includes the development and implementation of the use of imaging plates for the collection of diffraction data from micron-sized single crystals.

Technical Progress and Results: (a) As discussed in the FY 94 report, the supposedly

well defined aluminophosphate AIPO-5 was chosen for the template crystallographic studies as it has a reasonably simple structure and can be crystallized using a large variety of organic cations. Work at the NSLS in collaboration with Jon Hanson included collecting imaging plate data sets on both the as-prepared crystals with Et_3N as the template, and crystals that were calcined. Data reduction and structure solution has been complicated due to uncertainties in the true crystal symmetry and space group. In order to provide further information high-resolution powder data were collected at beam line X7A on powdered batches of the same materials, as well as samples that were freshly calcined, fully dehydrated and sealed under nitrogen, and dehydrated then rehydrated, respectively. There are clear changes in crystal symmetry as shown in Figure 1. We still have not been able to fully index these powder patterns (which sometimes include weak supercell reflections) and unravel this surprisingly rich and complex set of phase changes.

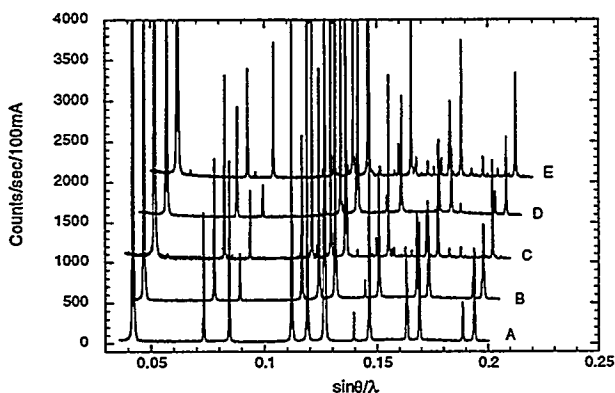


Figure 1. Powder scans of various samples of AIPO-5 where (A) is as-synthesized, (B) is calcined and exposed to ambient conditions, (C) is calcined and dry, (D) is sample C rewetted, and (E) is freshly calcined.

(b) Exploratory syntheses of microporous materials continued, but no longer concentrated on borates, as no further progress was made on solving the structures of those solids prepared in FY 94. Instead, the synthesis of new aluminophosphates was attempted utilizing

novel templates such as R_3BzN^+ (Bz = benzyl, R = methyl, ethyl, or butyl) or tetraarylphosphonium cations. The former series led to AIPO-5 while the latter only provided condensed phases. This was undertaken by Dr. Cahit Eylem, a postdoctoral researcher working half time on this program

(c) A second project with Dr. Eylem was the analysis of high resolution synchrotron X-ray powder diffraction data on a sample of ZSM-5 loaded with bithiophene that was prepared by D. R. Corbin and coworkers at DuPont. This is a precursor to a hybrid material that can be formed by the subsequent polymerization and doping of the organic intercalate. The material thus obtained is a so-called 'molecular wire' which contains isolated strands of conducting polymers. In this work we were able to determine the siting of the sorbed organic. From this information it is clear that cross-linking is a possibility during polymerization. We predict longer oligomers will alleviate this problem and lead to materials with better conductivity.

(d) In a continuing collaboration with C. C. Torardi at DuPont Central Research, the powder neutron data collected at beam line H1A at the HFBR on $\text{BiMo}_2\text{O}_7 \cdot 0.2\text{D}_2\text{O}$ was analyzed using the Rietveld method. This material is of interest as a potential oxidation catalyst. The heavy atom part of the structure was solved previously using *ab initio* methods from high-resolution synchrotron X-ray data, and from the neutron data the deuterium atoms were located and the hydrogen bonding has been described. By analogy to the known bismuth molybdate catalysts and with this structural information, we have conceptualized how to transform this solid into an active catalyst. Future work will test the hypothesis.

(e) In FY 95 the work with Jon Hanson at beam line X7B using imaging plates for

collecting diffraction data on small single crystals continued. The study of a novel high-pressure silicate, in collaboration with John Parise at SUNY - Stony Brook, was completed and a manuscript has been accepted. In this work, we were able to show the power of the imaging plate technique by comparing in detail the results of a standard in-house structure refinement and one at the NSLS. Even though the exposure time for the latter experiment was only ca. 6 minutes an excellent refinement was obtained.

PAPERS/JOURNALS/ PUBLICATIONS:

A high resolution powder neutron diffraction study of the novel layered oxide $\text{BiMo}_2\text{O}_7(\text{OD})\cdot 2\text{D}_2\text{O}$. J. A. Hriljac, C. C. Torardi, and T. Vogt, *J. Phys. Chem. Solids* **56**, 1339-1343 (1995).

Synthesis and structure of the novel high pressure silicate $\text{Na}_{1.8}\text{Ca}_{1.1}\text{Si}_6\text{O}_{12}$. T. Gasparik, B. Eibsen, J. B. Parise, and J. A. Hriljac, *Amer. Mineral.* (in press).

Structure of a zeolite ZSM-5-bithiophene complex as determined by high resolution synchrotron X-ray powder diffraction. C. Eylem, J. A. Hriljac, V. Ramamurthy, D. R. Corbin, and J. B. Parise, *Chem. Mater.* (submitted).

LDRD FUNDING:

FY 1994	\$113,862
FY 1995	\$111,292

Ozone Depletion, Chemistry and Physics of Stratospheric Aerosols

*Dan G. Imre and
Ignatius N. Tang*

94-10

PROJECT DESCRIPTION:

The goal of this proposal is to initiate a new research program to study the physics and chemistry of stratospheric aerosols. Many atmospheric processes are thought to proceed via heterogeneous reactions between gas phase molecules and aerosol particles. Aerosols have been implicated as major participants in the formation of the Polar Ozone hole. Furthermore, by converting reactive Nitrogen to Nitric Acid, they also play a very important role in maintaining the Stratospheric Nitrogen balance. Since all atmospheric reactions involve reactive Nitrogen, aerosols therefore indirectly also control the entire atmospheric chemical balance.

We propose to construct a novel experimental setup in which the physics and chemistry of single levitated aerosol particles under stratospheric conditions will be studied. Using Mie scattering as well as Laser Raman Spectroscopy we will observe and map exact points of phase transition. We will be able to generate and study states of super saturation and super cooling which are unique to aerosols. Furthermore, Raman spectroscopy will enable us to document the various crystal structures and compositions of frozen particles, as well as to follow in detail heterogeneous chemical processes. This will be the first set up of this kind, providing the first glimpse into the chemistry of single levitated aerosol particles.

TECHNICAL PROGRESS AND RESULTS - Fiscal Year 1995:

Purpose: Few recent scientific observations have captured our attention as did the discover of the Ozone hole in 1985. It sparked an enormous amount of research and controversy. The proposed research program addresses one of the crucial steps in the mechanism believed to lead to the destruction of the Ozone layer. It will develop a novel experimental approach to investigate the physics and chemistry of aerosols under stratospheric conditions. Participants in the most recent IPCC WGI/OZONE Assessment Workshop (May 1993), identified an *urgent* need to have information concerning basic thermodynamic properties of stratospheric aerosols, whose importance is not limited to the Ozone issue alone, but extends to many climatological phenomena. Surprisingly to date, not a single laboratory study on stratospheric aerosols is available. Even the most fundamental of properties - the physical state of stratospheric particles can not be unambiguously predicted.

The discovery of the Antarctic Ozone hole in 1985 by Farman et al. came as a complete surprise; every available study to that date predicted Ozone depletion at high altitudes (~40km) and at mid latitude. The observation could not possibly be explained by considering gas phase chemistry alone. In 1987 a new mechanism involving heterogeneous chemistry catalyzed by stratospheric cloud particles was proposed, and has served as the prevalent explanation for polar Ozone depletion ever since. The extreme low temperatures of the polar winters are known to result in the formation of Polar Stratospheric Cloud (PSCs) which are ice, or Nitric Acid/ice particles. The surface of these particles was hypothesized to serve as a catalyst for the conversion of inactive

Chlorine-HCl and ClONO₂, to its reactive forms that destroy Ozone. The supporting evidence for this mechanism is based on laboratory experiments in which, stratospheric aerosols are simulated by thin ice films, with not even an attempt at surface characterization. To date there has not been a single case where the proposed Ozone depletion chemistry has been shown to work on actual aerosols.

Approach: Developing a new experimental set up that will trap a *single* isolated aerosol and keep it under stratospheric conditions (temperature as low as 160 k and pressure of 50 torr). This set up will enable the control, and cycling of temperature, relative humidity and gas phase constituents much as they occur in the ambient stratosphere. This experimental setup will combine light scattering with Raman spectroscopy of single levitated particles. Precise thermodynamic properties of super cooled and super saturated droplets will be determined using Mie scattering. Chemical properties will be studied using laser Raman spectroscopy, a highly sensitive tool for distinguishing one chemical state from another. For example we should, for the first time, be able to determine the exact crystalline states of ice clouds.

Technical Progress and Results: A six window low temperature single particle cell has been designed and constructed. The cell is LN₂ cooled, heat exchange with the electrostatic trap is achieved using variable number of heat conductors. The cell is configured such that it floats at 160 k. Temperature is controlled using two 50 ohm heaters. Temperature is monitored using diodes at three locations to insure even heating. Temperature can be scanned or held fixed using a feedback loop. An ultrahigh vacuum system incorporating the cryostat was constructed. The entire system is designed to

allow gas flow. The mie scattering laser was mounted and a data collection system was constructed, with the entire system being computer controlled. The system was tested and calibrated using the well known salt of ammonium sulfate.

To simulate stratospheric particles sulfuric acid was the next target system. It has been proposed that stratospheric particles composed of sulfuric acid and water serve nucleation sites for the formation of PSCs. The idea being that as the temperature in the Antarctic winter lowers, sulfuric acid particles accue water diluting the sulfuric acid content in the process and eventually freeze at ~190K to form H₂SO₄•4H₂O (SAT). The stable form of sulfuric acid and water at this temperatures.

On the basis of these predictions many laboratory experiments have been conducted on SAT surfaces to simulate stratospheric conditions. Our original goal in constructing the system was first to test the above predictions of: first, the freezing temperature and second, the composition of the solid formed.

Contrary to the original predictions we find that sulfuric acid and water particles do not freeze at ~190K. We have kept aerosols under these stratospheric conditions for many hours and none have frozen. These particles can however, be made to freeze by cooling down to 166K where the 45% solution finally freezes. Surprisingly, the solid formed is not SAT but instead H₂SO₄•8H₂O (SAO).

Attempts to convert SAO to SAT by warming to 190K and holding the particle under these conditions for over 4 days proved unsuccessful. These particles under our conditions deliquesce at 213K to form a 37% sulfuric acid particle. The entire cycle is summarized in Figure 1.

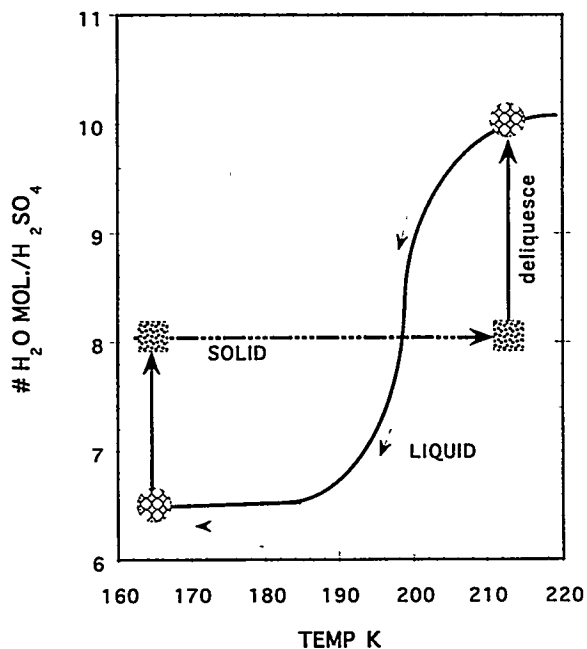


Fig. 1: The hydration and dehydration cycle for a sulfuric acid particle at low temperatures at 100% relative humidity (with respect to water ice). The particles do not "freeze" until the temperature reaches 166K at which point they form a metastable solid with ~6.5 water molecules per sulfuric acid molecule. This solid absorbs water to form the SAO which remains stable all the way to 213K at which point it deliquesces.

PAPERS/JOURNALS/PUBLICATIONS:

A paper titled: "Phase Transformation and Metastability of Hygroscopic Microparticles," summarizing the room temperature results has been published in *Aerosol Science and Technology* 23 443-453 (1995).

A paper describing the recent low temperature observations is in preparation.

A preliminary report on the low temperature results was presented at the 1995 Gordon Research conference in an invited talk.

LDRD FUNDING:

FY 1994	\$99,533
FY 1995	\$103,757

Understanding the Molecular Basis for the Synthesis of Plant Fatty Acids Possessing Unusual Double Bond Positions

John Shanklin

94-31

PROJECT DESCRIPTION:

Acyl-acyl carrier protein (ACP) desaturases catalyze the introduction of the first double bond into plant fatty acids. As such, these enzymes are one of the primary determinants of the industrial and nutritional value of unsaturated vegetable oils. A number of acyl-ACP desaturases exist in nature that are structurally similar yet use fatty acids of different chain-lengths as substrates and insert double bonds into different positions in acyl chains. Using site-directed mutagenesis, we are attempting to identify structural features that contribute to the differing substrate recognition properties of these variant acyl-ACP desaturases. With this knowledge, it may be possible to rationally design new acyl-ACP desaturases that catalyze the synthesis of novel types of monounsaturated fatty acids in order to enhance the economic value of existing vegetable oils.

TECHNICAL PROGRESS AND RESULTS - Fiscal Year 1995:

Purpose: The chain-length and position of the double bond of a monounsaturated fatty acid strongly influences its physical properties as well as its potential industrial and nutritional uses. For example, oleic acid (18:1 Δ^9) and petroselinic acid (18:1 Δ^6) are both 18 carbon monounsaturated fatty acids but their double bonds are located at different positions within the acyl chain. Because of this small structural

difference, the melting point of petroselinic acid (m.p. 30°C) is twice that of oleic acid (m.p. 14°C). With a melting point above room temperature, vegetable oils rich in petroselinic acid can be used in the manufacture of unsaturated margarines without requiring chemical hydrogenation, as is the case for oils rich in oleic acid. Also, the presence of its double bond at the sixth carbon atom from the carboxyl end of the molecule allows petroselinic acid to be used as an industrial starting material for nylon 66 precursors and lauric acid, a component of detergents and surfactants.

The double bond of monounsaturated fatty acids of plant oils results primarily from the activity of acyl-ACP desaturases. The ability to alter the chain length and double bond positional specificities of acyl-ACP desaturases would allow for a means of producing vegetable oils with new physical and industrial properties, as illustrated in the example above. To achieve this, requires an understanding of the structural features of desaturases that influence how these enzymes recognize and interact with their fatty acid substrates. Available to address this question are cDNAs encoding structurally related but functionally variant acyl-ACP desaturases: Δ^9 -stearoyl (18:0)-ACP desaturase, Δ^4 -palmitoyl (16:0)-ACP desaturase, and Δ^6 -16:0-ACP desaturase. These plant enzymes share a high degree of structural similarity and presumably function through the same catalytic mechanism. Despite this, these desaturases, display substrate preference for fatty acids of different chain-lengths (16:0 vs. 18:0) and insert double bonds into different positions of acyl chains (Δ^4 , Δ^6 , or Δ^9).

The goal of this work is to understand the structural basis for the different fatty acid chain-length and double bond positional specificities of these variant acyl-ACP

desaturases. Information gained from this research may allow for the design of fatty acid desaturases that are capable of producing industrially useful isomers of monounsaturated fatty acids. Genes encoding these "new" desaturases will then be engineered into existing oilseed crops to produce high-value vegetable oils.

Approach: Site-directed mutagenesis studies have been conducted to understand how structural differences between variant acyl-ACP desaturases relate to the different substrate recognition properties displayed by these enzymes. cDNAs for the Δ^9 -18:0-ACP and Δ^6 -16:0-ACP desaturases have been used as tools for mutagenesis studies. The polypeptides encoded by these cDNAs share >80% amino acid sequence similarity. Comparisons of the primary structures of these desaturases, however, reveal no obvious regions of amino acid differences that account for the different activities catalyzed by these enzymes. Our mutagenesis work has therefore first involved combining or "swapping" large portions of the cDNAs for the Δ^9 and Δ^6 desaturases. These cDNAs are then expressed in *Escherichia coli* to obtain chimeric forms of the Δ^9 and Δ^6 desaturases.

The resulting chimeric desaturases are assayed *in vitro* to determine whether a given mutagenesis step has resulted, for example, in the conversion of a Δ^9 -18:0-ACP desaturase into a Δ^6 -16:0-ACP desaturase. From these results, more defined regions of the acyl-ACP desaturases are mutated to determine the effect on substrate chain-length and double bond positional specificities. The ultimate goal is to identify specific amino acid differences that distinguish the activity of a Δ^9 -18:0-ACP desaturase from that of a Δ^6 -16:0-ACP desaturase.

To facilitate the screening of mutants, a system is being developed that will allow

acyl-ACP desaturases to function in *E. coli*. Plants and *E. coli* have a similar fatty acid biosynthetic system. *E. coli* cells, however, lack the ability to produce unsaturated fatty acids through an acyl-ACP desaturation pathway. We are attempting to introduce this pathway into *E. coli* by the expression of plant acyl-ACP desaturases together with ferredoxin and ferredoxin-NADP oxidoreductase, which are required as the oxidation-reduction component of desaturation. Such a system should allow one to assess whether a mutation has resulted in an alteration in the fatty acid chain-length or double bond positional specificity of an acyl-ACP desaturase by simply monitoring the fatty acid composition of recombinant *E. coli* by gas chromatography.

Technical Progress and Results: Through mutagenesis studies, a region of 30 amino acids has been identified in the Δ^6 -16:0-ACP desaturase that contributes to the ability of this enzyme to recognize and interact with acyl-ACP substrates. More specifically, replacement of this 30 amino acid domain in the Δ^6 -16:0-ACP desaturase with that present in the Δ^9 -18:0-ACP desaturase results in an enzyme that catalyzes both the Δ^9 and the Δ^6 desaturation of 16:0- and 18:0-ACP. Within this 30 amino acid region, there are nine amino acids that differ between the Δ^9 -18:0-ACP desaturase and the Δ^6 -16:0-ACP desaturase. Changing various combinations of these nine amino acids in the Δ^6 -16:0-ACP desaturase to those present in the Δ^9 -18:0-ACP desaturase results in a variety of phenotypes. One mutant obtained by "swapping" two specific amino acids catalyzes the Δ^6 desaturation of 16:0- and 18:0-ACP with nearly equal efficiency. This mutant therefore offers a potential means of producing the industrially important fatty acid petroselinic acid (18:1 Δ^6) in transgenic oilseed crops. Another mutant obtained by changing six specific amino acids in the Δ^6 -16:0-ACP desaturase functions primarily as

a Δ^9 -18:0-ACP desaturase. This mutant desaturase catalyzes both the Δ^6 desaturation of 16:0-ACP and the Δ^9 desaturation of 18:0-ACP. However, the Δ^9 -18:0-ACP desaturase activity of this enzyme is approximately two- to four-fold higher than the Δ^6 -16:0-ACP desaturase activity. In total, results obtained from these mutants point to this 30 amino acid region as the primary domain that determines the fatty acid chain-length and the double bond positional specificity of acyl-ACP desaturases. This opens up the possibility of targeting this region for further mutagenesis studies with the goal of designing "new" acyl-ACP desaturases that produce monounsaturated fatty acids of potential economic value.

We have also succeeded in engineering *E. coli* to produce monounsaturated fatty acids through the plant acyl-ACP desaturation pathway. By expressing the Δ^6 -16:0-ACP desaturase together with a plant-type ferredoxin, *E. coli* cells accumulate the monounsaturated fatty acid 16:1 Δ^6 to levels of 10 to 12% of their total fatty acid content. Additional studies and work by others suggests that this system is a viable *in vivo* means of assaying the activity of acyl-ACP desaturases that recognize substrates containing 16 carbon atoms or less (*e.g.* a Δ^6 -16:0-ACP desaturase functions in *E. coli*, but a Δ^9 -18:0-ACP desaturase does not). The plant acyl-ACP desaturation pathway has also been introduced into a mutant strain of *E. coli* that cannot grow without the addition of unsaturated fatty acids to its media. We have complemented this mutation by co-expressing

a plant Δ^9 -14:0-ACP desaturase (kindly provided by D. Schultz and J. Medford, Penn State University) and ferredoxin. This result suggests that it may be possible to use this *E. coli* mutant to rapidly select for functional acyl-ACP desaturases produced in mutagenesis studies. For example, a Δ^9 -18:0-ACP desaturase is not capable of complementing the unsaturated fatty acid requirement of the *E. coli* mutant. However, if this enzyme can be converted into a 14:0- or 16:0-ACP desaturase through random mutagenesis, these altered forms of the Δ^9 -18:0-ACP desaturase can be rapidly identified by their ability to sustain the growth of the *E. coli* mutant in the absence of unsaturated fatty acids.

PAPERS/JOURNALS/PUBLICATIONS:

A manuscript describing the functional expression of the plant acyl-ACP desaturation system in *E. coli* has been submitted for publication in the *Journal of Bacteriology*. A manuscript describing results obtained from mutagenesis studies of acyl-ACP desaturases is in preparation. We are also in the process of submitting an invention disclosure form to explore the possible patenting of a portion of our results.

LDRD FUNDING:

FY 1994	\$64,808
FY 1995	\$69,439

Structure Determination of Outer Surface Proteins of the Lyme Disease Spirochete

Catherine L. Lawson

94-32

PROJECT DESCRIPTION:

The structures of major antigenic outer surface proteins of the Lyme disease spirochete are being determined by X-ray crystallographic methods.

TECHNICAL PROGRESS AND RESULTS - Fiscal Year 1995:

Purpose: Our goal is to obtain detailed structural information needed for rational design of broad spectrum vaccines against the various strains of the *Borrelia* spirochete. OspA, OspB, and OspC are major antigenic outer surface proteins of *B. burgdorferi*; OspA and OspB share 53% amino-acid sequence identity, and so almost certainly share a common three-dimensional fold. The structures of OspA (or OspB) and OspC must be determined *de novo* because they have no significant sequence homology to other proteins of known structure.

Approach: OspA, OspB, and OspC are readily purified from recombinant clones obtained from J.J. Dunn (Biology, BNL). The emphasis of our work has been to search for diffraction quality crystals over a broad range of experimental conditions, and to then proceed with structure determination efforts. Several methods are employed to solve the crystallographic phase problem.

Technical Progress and Results: (a) Crystallization and Preliminary Crystal Analysis. CocrySTALLIZATION of OspA with the Fab fragment of a monoclonal antibody (α LS184.1) was reported in FY 1994. The crystals belong to space group $P2_12_12_1$, have unit cell dimensions $a = 89.4 \text{ \AA}$, $b = 91.6 \text{ \AA}$, and $c = 103.1 \text{ \AA}$ and there is one Fab/OspA complex per crystal asymmetric unit. The solvent content is 54%. The crystallization procedure has now been improved to routinely provide single, diffraction quality crystals for structure determination efforts.

Crystals of OspC with thin-plate morphology have also been grown. At 4°C , they are extremely sensitive to radiation. Conditions were found to flash freeze OspC crystals in a nitrogen gas stream using a novel support composed of a nylon loop coated with formvar. The space group has been determined to be P1 with cell dimensions $a = 34.1 \text{ \AA}$, $b = 48.1 \text{ \AA}$, $c = 144.1 \text{ \AA}$, $\alpha = 94.2^\circ$, $\beta = 90.9^\circ$, $\gamma = 95.1^\circ$. Crystal diffraction is anisotropic, with reflections observed to 1.7 \AA near the a^*b^* -plane, but to only 3.5 \AA along the c^* -axis. We continue to search for a more suitable crystal form of OspC for structure determination efforts.

(b) Data collection. Several X-ray diffraction data sets for crystals of the Fab184.1-OspA complex have been collected at NSLS beamlines X12B and X12C. Initially, crystals were mounted in capillaries and kept at 4°C during data collection, but resulting data statistics were poor. Crystals presoaked in a cryoprotectant mother-liquor and then flash-frozen in a nitrogen-gas stream were found to provide superior quality diffraction data (Table I).

Table I. Comparison of X-ray diffraction data from capillary-mounted vs. flash-frozen crystals of the Fab184.1-OspA complex.

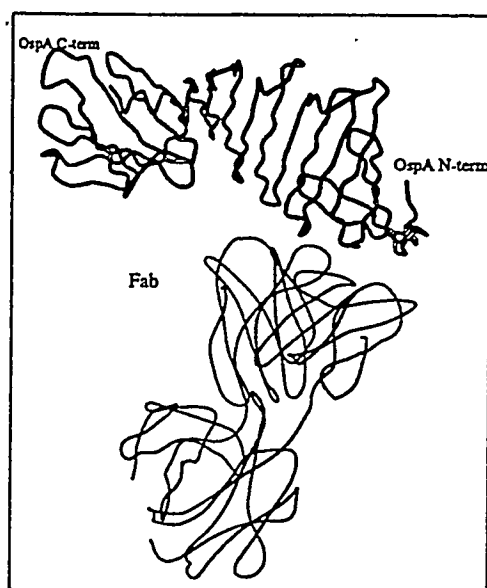
data set temp. (°C)*	4	-173
resolution limit (Å)	3.2	2.7
measured reflections	56987	89601
unique reflections	13608	23461
completeness (%)	94.6	99.0
$\langle I/\sigma(I) \rangle^{**}$	5.6	10.2
$R_{\text{merge}}(\%)^{***}$	14.2	6.9

*Data set 1 was collected from a native, capillary mounted crystal, data set 2 was collected from a flash-frozen crystal presoaked in a tri-methyl lead solution.

**Average ratio of observed intensity to estimated error in intensity measurement.

*** $R = \frac{\sum_h [\sum_l |I_{h,l} - \langle I_h \rangle|]}{\sum_h \langle I_h \rangle}$ where $I_{h,l}$ is the intensity of the l th measurement with Miller indices h and $\langle I_h \rangle$ is the mean intensity of that reflection.

Figure 1. Ribbon trace of the Fab184.1-OspA complex.



(c) Structure determination. An atomic model for the Fab184.1-OspA complex has now been obtained (Fig. 1), and is currently being refined. A summary of the structure determination process follows.

A molecular replacement model provided the first estimated phases for the Fab184.1-OspA crystal structure factors. The model was derived from an anti-lysozyme antibody Fab structure (PDB entry 2HFL), with amino-acid side-chains of the hypervariable loops corrected according to the gene-sequence of the 184.1 light and heavy chains. Resulting maps showed electron density for OspA in and near the antibody-combining region of the Fab, but they were not sufficiently clear to trace the OspA polypeptide chain.

Diffraction data from several heavy-atom derivatives (K_2PtCl_4 , trimethyl-lead, iodotyrosine) were used to obtain an independent set of MIRAS (multiple isomorphous replacement with anomalous scattering) phases to 2.8 Å. Combining these phases with molecular replacement phases and then performing a solvent flattening density-modification procedure produced much improved electron density maps, finally allowing the main-chain of OspA to be traced.

The high ratio of surface area to volume for the OspA structure combined with an unusual amino-acid composition has made incorporation of the OspA amino-acid sequence into the three-dimensional model one of the most challenging aspects of the structure determination. The strongest platinum site has provided the position of the single methionine residue; difference Fourier peaks from two serine-cysteine mutants have

provided further sequence anchors. Refinement of the structure against a recently obtained 2.3 Å data set is expected to improve model quality. We also hope to obtain higher resolution data in the near future on the NSLS wiggler beamline X25.

PAPERS/JOURNALS/PUBLICATIONS:

Li, H. and Lawson, C.L. "Crystallization and Preliminary X-ray Analysis of *Borrelia burgdorferi* Outer Surface Protein A (OspA) Complexed with a Murine Monoclonal Antibody Fab Fragment," *J. Structural Biology*, in press.

A manuscript describing the structure of the Fab-OspA complex is in preparation.

FOLLOW-ON FUNDING:

National Institutes of Health Grant No. AI37256-02, "Vaccine Intervention for Lyme Borreliosis," Pending Award 10/1/95 - 9/30/96, \$121,168 Total Funding.

LDRD FUNDING:

FY 1994	\$76,787
FY 1995	\$81,508

Low Mass, Low Cost, Multiwire Proportional Chambers for Muon Systems of Collider Experiments

V.A. Polychronakos

94-33

PROJECT DESCRIPTION:

Development of economical, mass production techniques of Multiwire Proportional Chambers (MWPC) appropriate for use with Muon Systems covering large solid angles in modern Collider Experiments. These chambers would utilize modern lightweight composite materials and provide all functions needed in a Muon System, i.e. precision momentum measurement, transverse coordinate, timing, and trigger.

TECHNICAL PROGRESS AND RESULTS - Fiscal Year 1995:

Purpose: Multiwire Proportional Chambers have been in use for many years. Their spatial resolution is generally limited by the anode wire spacing and is of the order of one millimeter. This is inadequate for precision measurements of high momentum particles in planned or future High Energy Hadron Colliders where resolutions at the 100 micron level are needed.

Additionally, coverage of large solid angle requires chambers with the smallest possible dead space in the perimeter of the device. Ordinary proportional chambers usually feature massive frames in order to withstand the significant anode wire tension. The chambers under development in this project would provide all necessary functions required by a Muon System, i.e.:

- Precision coordinate for the momentum determination (<70 microns).
- The transverse coordinate with coarser resolution (1mm or coarser, as required by the particular application).
- Bunch crossing timing (3ns).
- Primitives for Level 1 trigger.

In addition they will be constructed using modern, lightweight composite materials resulting in high precision construction necessary for achieving spatial resolutions better than 100 microns while minimizing dead area in their perimeter.

Approach: The basis of our design is a low mass flat panel made of a parer (nomex) honeycomb core and copper-clad, 0.5 mm fiber epoxy facings forming the cathodes of the proportional chambers. These panels are approximately 2 cm thick and weigh about 1Kg per square meter. Three such panels, for example, would form a two layer chamber. One face in each gap is lithographically segmented into readout strips, typically, on a 5 mm pitch. Interpolation of the charge induced on these strips provides the precision momentum measurement coordinate. These panels are enclosed by suitable frames which provide the necessary features to complete the chambers. These are the 2.5 mm steps for the attachment of the anode wires, the printed circuit boards for the electrical connections, gas manifolds, a gas seal, bolt holes, etc. These frames are quite narrow (less than 5 cm for example) because the panels are stiff enough to withstand the wire tension of about 60 Kg/m. Even though the size of the frames has thus been dramatically reduced, they would still dominate both the weight of the detectors as well as their cost if ordinary materials such as fiberglass epoxy composites requiring

extensive precision machining are used. Multiple Coulomb scattering is also the dominant factor limiting the momentum resolution of such detectors. In this project we have been investigating alternate materials and fabrication methods for the construction of proportional chambers. The use of lightweight polymer concrete had been extensively investigated during the first year of this project. Low density casting materials with appropriate physical properties were identified and a series of samples were fabricated. Casting of the panels with such materials would drastically reduce the additional machining required, significantly reducing the fabrication cost. The initial cost of the casting forms, however, makes this techniques suitable for very large experiments where such cost would represent a relatively small fraction of the total cost. During the past year (FY 1995) other materials such as rohacell foams were also investigated and results from prototype work are summarized below. These materials would be appropriate for smaller experiments where the somewhat increased fabrication costs would still be below the required initial expenditure for the casting forms.

Technical Progress and Results: During the past year a possible alternative to polymer concrete appropriate for smaller projects has been investigated. An easily machinable, rigid polymethacrylimide foam was selected as a possible candidate for the closeout frames of the honeycomb/glass epoxy panels. Encouraging results demonstrating sufficient strength of the prototype panels led us to construct a functioning prototype detector to demonstrate feasibility of the concept.

A possible follow-up of this work might be the construction of a Cathode Strip Chamber system for the forward endcap muon system in the ATLAS experiment at CERN. This experiment employs a toroidal magnetic

field which would require azimuthal strips in the endcap chambers measuring the muon coordinate in the bending plane. The optimum chamber geometry featuring azimuthal strips would require radial wires so that the strips are always perpendicular to the wires eliminating parallax errors. Then, in order to maintain constant gas gain, the anode-cathode distance has to vary in accordance with the wire to wire separation. Constructing such chambers using the honeycomb/rohacell panels proved to be quite easy. Figure 1 shows an exploded view of the prototype where the various components comprising the lightweight panels are indicated.

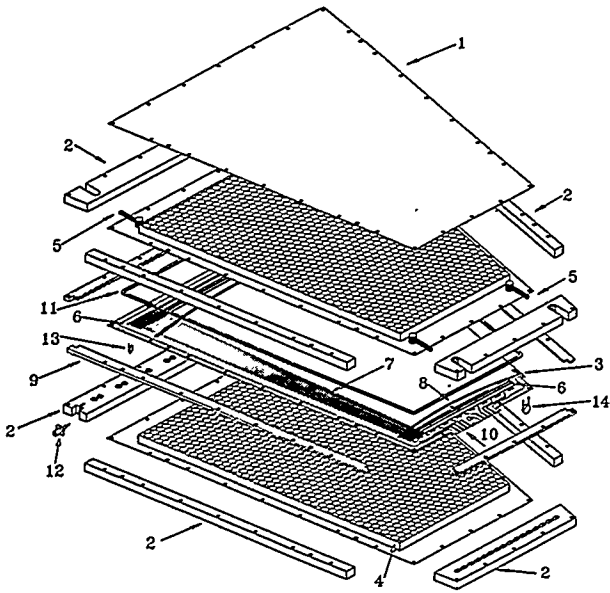
Figure 2 shows a plane view of one of the chambers where the radial wires are shown along with a detail of the cathode strip plane. The numbers shown represent percent variations of the gas gain from a mean. These measurements were performed using an Americium source with a Molybdenum filter which produces 17.4 KeV X-rays which are energetic enough to penetrate the panels. It can be seen that the root mean square variation is of the order of 10% more than adequate for the operation of the chamber. Preliminary data from a test of this prototype using minimum ionizing particles in a test beam at CERN last summer indicate spatial resolution better than 70 micrometers.

FOLLOW-ON FUNDING:

Proportional chambers of this design have been accepted as the baseline technology covering the high eta region of the Muon System of the ATLAS experiment at the CERN Large Hadron Collider. BNL participates in this experiment and, pending approval of the whole project, DOE funding for further development of these chambers would be a realistic possibility.

Figure 1

**ONE GAS GAP CSC CHAMBER
EXPLODED VIEW**

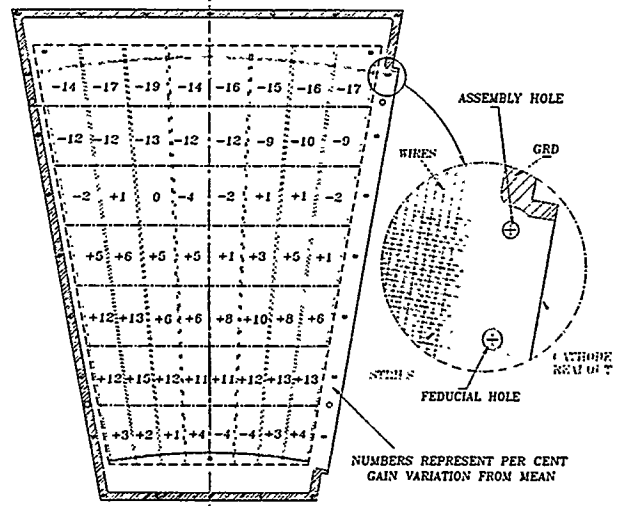


- 1.G-10 LAMINATE
- 2.ROHACELL BAR
- 3.CATHODE READOUT
- 4.NOMEX HONEYCOMB
- 5.GAS INLET/OUTLET
- 6.WIRE FIX. BAR
- 7.WIRES

- 8.STRIPS
- 9.SPACER BAR
- 10.ANODE READOUT
- 11.SEALING RUBBER
- 12.HV-CONNECTOR
- 13.HV-RESISTOR
- 14.HV-CAPACITOR

Figure 2

Plane view of one of the chambers.



LDRD FUNDING:

FY 1994	\$87,527
FY 1995	\$85,717
FY 1996 est.	\$96,000

Theory of Self-Organized Criticality

Per Bak

94-34

PROJECT DESCRIPTION:

The purpose of the proposed research is to help in developing theories of models exhibiting self-organized criticality in order to enhance our understanding of complex dynamical systems.

TECHNICAL PROGRESS AND RESULTS - Fiscal Year 1995:

Purpose: The purpose of the research is to help in developing theories of models exhibiting self-organized criticality in order to enhance our understanding of complex dynamical systems. The funding supports Dr. Peter Thomas, who has been hired as a research associate for a period of two years.

Approach: (a) Further numerical studies were performed on a modified version of the model of biological evolution invented by Per Bak and Kim Sneppen in an attempt to understand punctuated equilibria. Peter Thomas' study has so far been quite successful: the model does not exhibit the expected behavior, but locks into some spurious oscillating states. However, in an unexpected happy turn of events, Maya Paczuski, a DOE distinguished postdoctoral fellow, and Stefan Boettcher were able to construct a similar model and solve it analytically. The model exhibits the expected behavior, with non trivial exponents for the distribution of periods of stasis. This work will be followed up by the two authors.

b) The phenomenon of "contact line depinning" has been studied in a collaboration between Peter Thomas and Maya Paczuski. Contact line depinning is the phenomenon that the line separating a droplet on a surface is displaced intermittently as the droplet grows. The model also describes crack propagation. The idea is to apply concepts derived from a more general study of surface depinning to this specific problem. The study lead to some novel and quite unexpected results. The phenomenon is governed by exponents which are different from theoretical estimates based on functional renormalization group methods, but agree with a new theory which was derived.

PAPERS/JOURNALS/PUBLICATIONS:

Peter Thomas has completed two manuscripts:

- (1) "Exact results on a lattice model of a binary reactant mixture."
- (2) "Exchange effects in the Wigner Solid," on subjects not directly related to the topic of this project.

A third manuscript on contact line depinning is in progress.

LDRD FUNDING:

FY 1994	\$61,488
FY 1995	\$62,532

Development of the PCR-SSCP Technique for the Detection, at the Single Cell Level, of Specific Genetic Changes

K. Rithidech

94-36

PROJECT DESCRIPTION:

In recent years, the polymerase chain reaction (PCR), in combination with other molecular techniques, has played a significant role in the molecular characterization of gene damage resulting from exposure to genotoxic agents. However, relevant studies have been generally carried out in heterogeneously pooled samples. Thus, it could be highly advantageous to establish PCR-based techniques for use in the detection of genetic damage in individual cells following exposure to toxic agents.

TECHNICAL PROGRESS AND RESULTS-FISCAL YEAR 1995:

Purpose: We propose to investigate the feasibility of using the polymerase chain reaction-single stranded conformational polymorphism (PCR-SSCP) technique for the detection, following irradiation, of specific genetic changes in single cells. Although, the PCR-SSCP method has been successfully used to identify gene-harboring mutations in a pooled samples, and even though it is highly promising as an approach to identifying small numbers of cells harboring mutated genes, its use in single cells has not as yet been reported. The approach also has the potential for use as a rapid molecular screening method for the early detection of cancer cells, and thus for observing clonal expansion and progression.

Such information has important applications for diagnostic, prognostic, and possibly therapeutic purposes, e.g., for the detection of drug resistant cells. More importantly, this study, if successful, will open a vital approach to the analysis of genetic damage at potentially critical sites for untoward outcomes following exposure to genotoxic agents at the single cell level.

Approach: In the first year of the project, our focus will be on the establishment of the PCR-SSCP methodology using pooled samples. These samples are radiation-induced myeloid leukemic (ML) cells that were collected from mice with ML resulting from exposure to monoenergetic fast neutrons, γ rays, or X rays over the years that our ongoing studies on radiation leukemogenesis have been ongoing. These ML cells are cryopreserved and thus suitable for DNA analyses. They are also perpetuated by transplantation into syngeneic mice. We then shall use the PCR-SSCP for the study of N-ras mutations in DNA isolated from these ML cells. Subsequently, we shall attempt to demonstrate that the PCR-SSCP analysis can be used to detect N-ras mutations in DNA isolated from cells of mice exposed to different doses of X rays. The N-ras gene is selected for our initial study because it is known to play an important role in both murine and human oncogenesis. Furthermore, this gene has been extensively studied; therefore, its DNA sequence, mutational spectra, and appropriated DNA primers for PCR amplification have been well characterized.

Following the establishment of the PCR-SSCP method for the detection of N-ras mutations, we shall illustrate further that a selected region of the mouse hypo-xanthine-guanine phosphoribosyl transferase (HPRT) gene can be amplified in both normal and X-irradiated cells. Thereafter, we shall use the

SSCP method for the detection of damage at this specific site in these PCR products. The HPRT gene is included in this project because it is the only locus that can be used for studying *in vivo* mutagenesis, both in human beings and experimental animals. Furthermore, its mutations has been known to be associated with the human Lesch-Nyhan syndrome.

In the second year of this project, we shall apply the PCR-SSCP technique for the detection of gene changes following exposure to X rays at the single cell level. To do this, it is imperative that we first optimize the PCR conditions for amplifying selected genes, i.e. N-ras and HPRT, in single cells. We shall begin with cells from non-exposed mice. A serial dilution or micromanipulation will be used to isolate single cells from the mouse bone marrow. Painstaking experimental strategies will be implemented to circumvent potential shortcomings of the use of PCR in single cells. After the development of a single cell PCR has been achieved, we shall continue on experiments involving the use of SSCP analysis for the detection of N-ras or HPRT mutations on a cell-by-cell basis, in DNA isolated from mice exposed to different doses of X rays.

Technical Progress and Results: The PCR-SSCP technique is tremendously sensitive for the detection of base changes. However, it has some technical limitations. These include conditions for PCR amplification (e.g. effects of primers and annealing temperature) and for SSCP analysis (e.g. effects of polyacrylamide concentration in the gel, power, temperature, and gel running time). In spite of these technical difficulties, we have made steady progress in the past two years to establish the PCR-SSCP technique for the detection of mutations at specific sites of the genome, based on pooled samples. We began to use the PCR-SSCP technique as a rapid screening

method for the N-ras gene mutations in radiation-induced ML cells. Our results indicate that involvement of mutations of the N-ras gene in radiation leukemogenesis occurs in Exon 2 (a 103 bp long portion) but not in Exon 1 (a 128 bp long portion) or Exon 3 (a 107 bp long portion). We also detected N-ras changes in DNA samples isolated from mice exposed to different doses of X rays (as low as 0.5 Gy). Similarly, we observed changes in Exon 9 of the HPRT gene (172 bp) in DNA samples of mice exposed to different doses of X rays.

We expanded the use of the PCR-SSCP method to detect possible changes in the DNA sequence of the p53 gene within Exon 4 (a 220 bp long portion) and exon 5 (a 180 bp long portion). Results from these experiments show no mobility shifts in either Exon 4 or Exon 5 of the P53 gene.

In FY 1995, we attempted to develop a single cell PCR of the N-ras gene (Exon 2, 103 bp). Due to the minute amounts of DNA available, many more PCR cycles were needed, which resulted in many bands of products. Thus, the PCR process in single cells is technically difficult and more susceptible to not only contamination but also errors in fidelity of the enzyme Taq polymerase. Therefore, currently the single cell PCR is not feasible in our laboratory because some technical problems limit its use. However, we have had remarkable success in developing a unique PCR-based technique namely the MULTIPLEX-TOUCH DOWN PCR as a rapid screening of minisatellite polymorphisms. Polymorphisms of minisatellites have been found to be one of the important genomic instabilities associated with carcinogenesis. Their detection is usually done by radioisotopic PCR amplification of repeat sequences, using primers specific for the flanking genes. PCR products are then

analyzed on a denaturing polyacrylamide gel electrophoresis (PAGE). Using this protocol, however, a number of bands usually result that could complicate genotypic interpretation. To overcome such a problem, we have established a non-radioisotopic "TOUCHDOWN" PCR (T-PCR) technique for the detection of mouse minisatellites. This strategy markedly improved the quality of PCRs, i.e., spurious bands detected on the non-denaturing PAGE stained with ethidium bromide were eliminated. The "TOUCHDOWN" PCR, however, is tedious and time-consuming. Thus, we further established the "MULTIPLEX-TOUCHDOWN PCR" (MT-PCR) to simplify the detection of minisatellite length polymorphisms. Different minisatellites can be amplified simultaneously and analyzed unambiguously on the non-denaturing PAGE. We found that MT-PCR is simple, rapid, economical, powerful, and highly efficient. A minute amount of DNA template, as low as 10 ng, can be used in one reaction with 3 different pairs of primers (TRIPLEX-TPCR). However, an increase in the amount of DNA template is required if more primer sets are used.

PAPERS/JOURNALS/PUBLICATIONS:

Rithidech, K., J.J. Dunn, V.P. Bond, E.P. Cronkite and Gordon, C.R. (1994) Detection of N-ras gene mutations in radiation-induced murine myeloid leukemia by the PCR-Single strand based technique. *Environmental and Molecular Mutagenesis, Vol. 23, Suppl. 23:57.*

Rithidech, K. J.J. Dunn, V.P. Bond, E.P. Cronkite, and C.R. Gordon (1995) Rapid screening of minisatellites using multiplex-touchdown PCR protocols. To be presented at the 27th Annual meeting of the Environmental Mutagen Society, to be held in British Columbia, Canada, Mar. 24-28, 1996.

LDRD FUNDING:

FY 1994	\$85,114
FY 1995	\$88,141

*This project involves the use of vertebrae animals.

Feasibility of SPECT in Imaging of F-18 FDG Accumulation in Tumors

*Gene-Jack Wang and
Peter H.M. Kuan*

94-37

PROJECT DESCRIPTION:

To evaluate the feasibility of SPECT in imaging of ^{18}F FDG accumulation in tumors, we compare the sensitivity and specificity of PET and SPECT on ^{18}F FDG imaging of breast tumors. Patients who are suspected of having breast cancer following mammography will be recruited for this study. The patients will have a PET scan following injection of ^{18}F FDG. Images of chest and axillary region will be obtained using a SPECT system with high energy collimators following the PET scan.

TECHNICAL PROGRESS AND RESULTS - Fiscal Year 1995:

Purpose: Prior to patient SPECT studies, systemic F-18 phantom studies were performed in order to document the detectable sizes (10 to 15 mm) and activity (μCi) at varying background condition.

Approach: The phantom studies were done using Jackzack brain phantom (Figure 1a) and hot sphere phantom (Figure 2a). Inner space (240 cc of water) of the brain phantom was filled with 4.8 mCi of F-18 chloride and outer space (500 cc of water) was free of radioactivity as background. The hot sphere phantom was a 20-cm diameter cylinder, which was filled with water, with 6 spheres on a circle of 11.5 cm diameter. Diameters of the spheres were 1.3, 1.6, 1.8, 2.5, 3.2, and 3.8 cm,

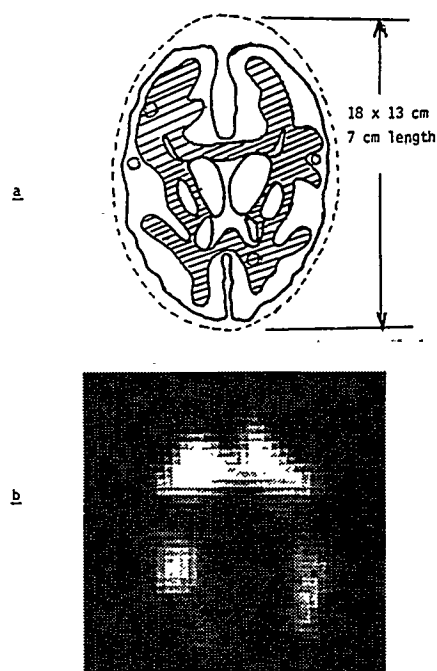


Figure 1.

a. Illustration of Jackzack Brain Phantom. b. F-18 SPECT image of inner space of Jackzack Brain Phantom (image pixel size = 4 mm).

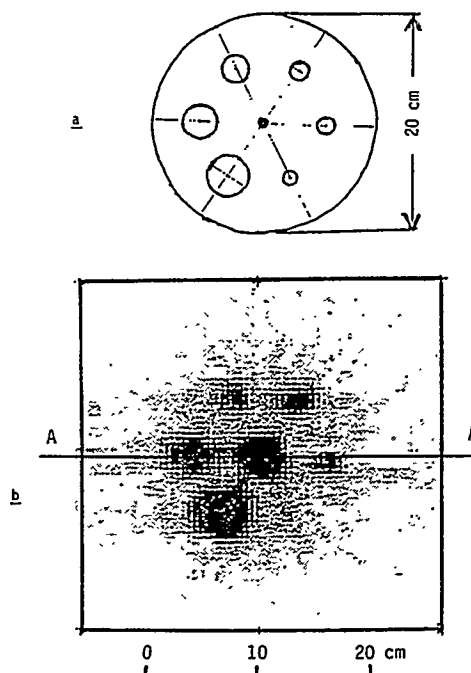


Figure 2.

a. Illustration of a Hot Sphere Phantom. The inner diameters of the Hot Sphere Phantom are 1.3, 1.6, 1.8, 2.5, 3.2, and 3.8 cm. b. F-18 SPECT image of Hot Sphere Phantom (image pixel size = 4 mm).

3.8 cm respectively. Each sphere was filled with 20 $\mu\text{Ci/cc}$ of F-18 chloride. There was also a line source at center of cylinder with activity of 300 $\mu\text{Ci/cc}$.

The phantom studies were performed at The Stony Brook University Hospital using a dual headed SPECT scanner (ADAC) with a high energy collimator designed for 511 keV gamma-ray. The phantoms were scanned with set up of both detectors. Each detector rotated 180° on a non-circular orbit and recorded 32 images with data collection time of 40 seconds per image. The matrix was set at 128x128x16 and field of view was 15"x20".

Point-source studies were also performed to evaluate the integral uniformity of the system. The point-source studies were done using a Na-22 point source on Tc-99m generated map, Na-22 point source on Na-22 generated map and F-18 point source on Na-22 generated map. The point source spread function was measured at 10 cm from collimator for both detectors.

The F-18 phantom SPECT data were collected with an uniformity map created by Na-22 511-keV gamma ray. The pixel size was 3.97 mm² and voxel size was 3.97 mm³.

Technical Progress and Results: Uniformity analysis showed the best integral uniformity with Na-22 point source on Na-22 generated map with integral uniformity at central field of view (FOV) of 1.5% and full FOV of 3%, followed by F-18 point source on Na-22 generated map with integral uniformity at central FOV of 7% and full FOV of 11%. Na-22 point source on Tc-99m generated map showed an integral uniformity at central FOV of 13% and full FOV of 20%.

Full width half maximum (FWHM)

measured from the point source spread function studies showed that the SPECT with 511-keV collimators can achieve a resolution of 1.0 mm at 10 cm (Figure 3).

Structure of inner space can be visualized in the Jackzack brain phantom with acceptable quality (Figure 1b). Radioactivity in the hot sphere phantom can be visualized with the size of sphere larger than 16 mm (Figure 2b) with 1 $\mu\text{Ci/voxel}$ of 4 mm³.

The point source studies indicated that the SPECT scanner with a 511 keV collimator can achieve an integral uniformity of 1.5% at central FOV and 3% at full FOV using Na-22 point source on Na-22 generated map. F-18 point source on Na-22 generated map did not have acceptable integral uniformity (2%). Since Na-22 is an isotope with gamma energy of 511 and 1270 keV, decreased integral uniformity could be due to penetration of higher energy gamma ray through 511 keV collimator. We plan to perform F-18 phantom SPECT studies based on uniformity map generated by Ge-68 point source.

The phantom studies and point source spread function tests are consistent with the expected resolution of 9.9 mm at distance of 10 cm. In clinical patient settings, the expected distance is 10 to 30 cm and the observable resolution should be above 1.6 cm. We will recruit patients with tumors larger than 1.6 cm to evaluate the feasibility for detecting the tumors. However, higher concentration of radioactivity at center rod was visualized in spite of smaller size indicating that patients with a smaller tumor and high FDG uptake can also be visualized. Further studies with higher concentrations of sphere and various background activities in the cylinder of the hot sphere phantom will

be performed to assess its feasibility. We will compare the results obtained so far using the ADAC scanner to that using a Picker triple-headed scanner with 511 keV collimator to be installed at Medical Department toward the end of the year before performing patient studies.

LDRD FUNDING:

FY 1994	\$15,806
FY 1995	99,776
FY 1996 (est.)	110,000

Note: This project involves the use of human subjects.

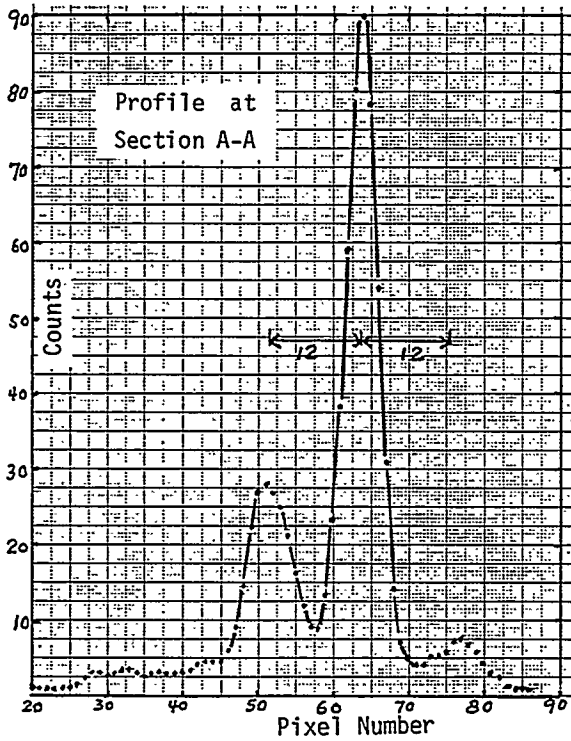


Figure 3.

The profile of Hot Sphere Phantom at section A-A indicated in Figure 2b, demonstrating the ability to detect the small size of lesion with appreciable uptake of F-18.

Visible Free-Electron Laser Experiment

I. Ben-Zvi

94-43

PROJECT DESCRIPTION:

A Free-Electron Laser (FEL) oscillator is being studied at the short wavelength limit of the electron-beam-brightness. The wavelength is made short through the use of a very short-period undulator (micro-undulator). The 50 to 70 MeV electron beam of the BNL Accelerator Test Facility is being used in beam-line 3 of the ATF. Two types of undulators are available for the experiment: a pulsed electromagnet undulator made by MIT and a superferric undulator built at BNL. Both have a period of 8.8 mm. A successful demonstration of this short wavelength FEL oscillator will be an important step towards the realization of high power, tunable very short wavelength radiation sources in the VUV and X-rays. These sources may have important R&D applications in photochemistry, atomic and surface physics, biology and other sciences.

TECHNICAL PROGRESS AND RESULTS - Fiscal Year 1995:

Purpose: In recent years, the emergence of research applications requiring intense, coherent, high brightness radiation sources beyond existing state of the art, has driven a wave of accelerator research and development. The NSLS has developed a proposal for the construction of a Deep Ultra-Violet FEL. An advisory panel chaired by Andrew Sessler of LBL recommended, among other things, the demonstration of the Visible FEL Oscillator Experiment. The motivation is the operation of a FEL near the emittance limit of the

accelerator and, possibly, extension to the near UV provided the beam brightness is as calculated.

Approach: The hardware of the Visible Free-Electron Laser experiment includes two 60 cm long microundulator with a period of 0.88 cm. One is a BNL built superconducting device and the other is a MIT built pulsed device. The superconducting undulator technology has been developed at the National Synchrotron Light Source at BNL under a previous LDRD (91-22) project. We use a ferromagnetic yoke machined out of a solid block of low carbon steel. A superconducting NbTi coil is wound continuously along the yoke, with the winding direction alternating every half period. The magnetic field of this undulator is very uniform even for operation above saturation. The experiment is installed on beam line number 3 of the BNL Accelerator Test Facility (see figure). The FEL output will be at a wavelength of 500 nm at an electron beam energy of 50 MeV. The ability of the ATF to reach 70 MeV makes it possible to extend the operation of this FEL to the UV, about 250 nm. The FEL interaction and resonator design were studied in detail. An output power of 10 MW peak and a gain of about 25% are expected at the ATF beam parameters but with only 50 A peak current and a rms normalized emittance of 7p mm mrad .

Technical progress and results: (a) The beam line of the experiment has been assembled and surveyed, including support stands, beam line magnets), vacuum hardware, electron beam diagnostics, beam dump and optical diagnostics.

(b) The MIT pulsed microundulator has been measured, installed and surveyed.

(c) A precision alignment system of the

FEL has been installed and tested (see Fig. 1). A green HeNe laser alignment is mode-matches into the optical resonator of the FEL. With this system we can align with a very high precision the cavity mirrors, the electron beam line and the undulator magnetic axis to coincide. The cavity mirrors are aligned by an interferometric technique for high precision. The cavity length is being adjusted to the electron beam's repetition period by mode-matching the doubled (green) light of the photocathode Nd:YAG laser into the FEL cavity and adjusting the cavity's length to resonate with the YAG's pulse train (see Fig. 2)

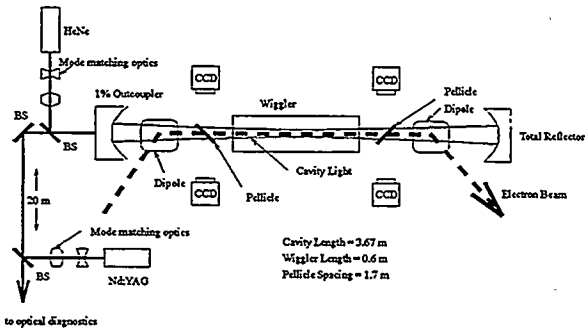


Fig. 1. The FEL Oscillator alignment system

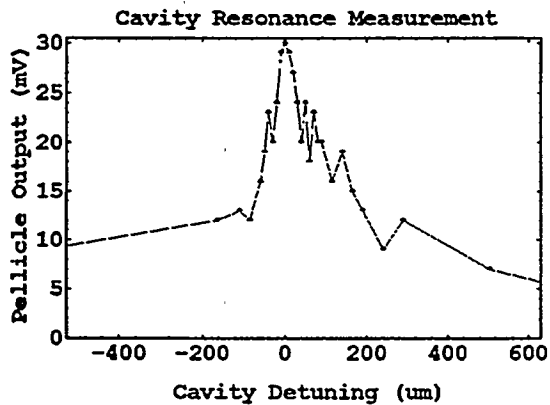


Fig. 2. Determining the resonator length

(d) A diagnostic system to analyze the radiation of the FEL has been built and tested. This system includes photomultiplier and photodiodes for the detection of the light, a spectrometer for the measurement of a

spectrum, a CCD camera for the measurement of pointing stability and mode quality and a streak camera for time resolved measurements on a picosecond scale. The resonator losses were measured to be within specifications by observing the ring-down of a laser pulse injected into the resonator. (See Fig. 3)

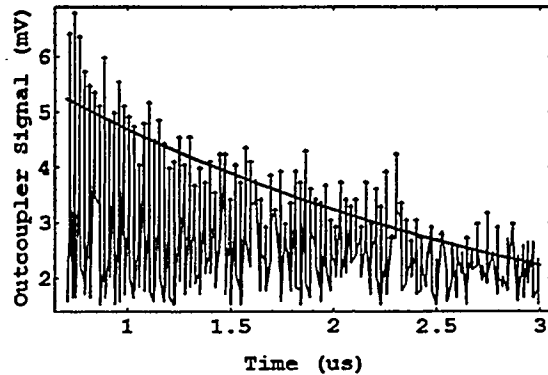


Fig. 3. The optical resonator ring-down

(e) A number of ATF accelerator runs were done and the beam transport was studied. The spontaneous emission of the microundulator has been measured, with and without the optical resonator (see Fig. 4). The spectrum was at the calculated wavelength but slightly broader than the theoretical limit. We have searched to see gain in the FEL but so far have not observed any. The plans for the near future are to make improvements in the alignment, electron beam transport, bunch train length and beam current and continue with the experiments in an attempt to demonstrate lasing.

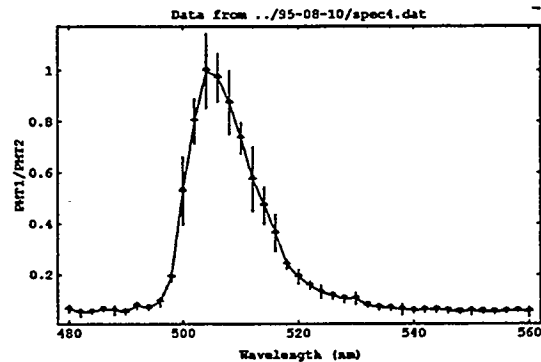


Fig. 4. Spontaneous radiation spectrum

PAPERS/JOURNALS/PUBLICATIONS:

LDRD FUNDING:

Radiation from Relativistic Electron Beams in Periodic Structures, M. Babzien et. al., to be published in Nucl. Instr. and Meth. in Phys. Res. A

FY 1994	\$ 70,000
FY 1995	\$ 100,008
FY 1996 est.	\$ 30,000

Optical Alignment and Diagnostics for the ATF Microundulator FEL Oscillator, M. Babzien et. al., to be published in Nucl. Instr. and Meth. in Phys. Res.

Study of Possible 2 + 2 TeV Muon-Muon Collider

R.B. Palmer & R.C. Fernow

95-01

PROJECT DESCRIPTION:

The muon collider is being studied as a possible means of reaching the TeV energy regime at less cost than using hadron-hadron or electron-positron colliders. A conceptual design of a complete collider facility will be worked out of all the necessary components starting from the muon production and ending with the collider detector.

TECHNICAL PROGRESS AND RESULTS - Fiscal Year 1995:

Purpose: Muon colliders represent a possible approach to extending the high energy frontier of particle physics. Electron-positron colliders are believed to be constrained by energy loss due to beamstrahlung radiation and the expense of building two full energy linacs. The muon collider has negligible beamstrahlung and might be more economical, since it can make use of circular collider rings. A 2 + 2 TeV machine would be of moderate size (it would fit on the BNL site) and does not require the use of any exotic technologies.

However, many difficulties must be addressed. To fully understand the feasibility of this concept, it is important to simulate a complete facility from particle production to the intersection in the collider. Experiments should be performed to measure the efficiency of proposed pion production and collection ideas. The number of collected muons per incident proton on target is a crucial parameter

for determining the ultimate luminosity of the collider. Another crucial measurement is the efficiency of ionization cooling in reducing the emittance of the muon beam.

Approach: We have organized a design group, which meets weekly to discuss muon collider problems and concepts. We are collaborating in this work with groups at FNAL and LBL, as well as with interested individuals in other labs and universities. Work is presently concentrating on the design of a high energy 2+ 2 TeV collider and on a smaller 250 + 250 GeV collider.

Technical Progress and Results: A complete conceptual design for a 2 + 2 TeV collider has been determined, including a detailed parameter list. A Monte Carlo program has been written to simulate many aspects of the muon production and acceleration.

The pion production spectrum has been studied by comparing analytic models, computer codes and existing data. We are currently organizing a collaboration to measure the pion production spectra in the appropriate kinematic regions at the MPS spectrometer at the AGS. A collection system based on a target inside a high field solenoid has been designed.

An RF phase rotation system has been designed that reduces the momentum spread of the muon beam. A cooling system, which increases the transverse and longitudinal phase space density of the muon beam, has been worked out analytically. We have submitted a Letter of Intent to the AGS Program Advisory Committee to perform a demonstration of ionization cooling.

Work has begun on the conceptual design of multi-pass dipoles for use in the return arcs of a recirculating accelerator.

Work has been done on the conceptual design of the accelerator lattice near the intersection regions of the collider ring.

A physics group has begun work on (1) physics processes that can be measured at a muon collider, (2) the expected backgrounds at the intersection region due primarily to muon decays, and (3) the design of a generic detector.

PAPERS/JOURNALS/PUBLICATIONS:

We have organized a workshop on muon collider ideas and problems, which took place at Montauk, NY, in October 1995.

R.B. Palmer et al, High energy, high luminosity muon-muon collider design, BNL report 62041, 1995.

D. Kahana & Y. Torun, Analysis of pion production data from E-802 at 14.6 GeV/c using ARC, BNL report 61983, 1995.

V. Barger et al, Physics goals of a muon-muon collider, BNL report 61593, 1995.

R.B. Palmer et al, Monte Carlo simulations of

muon production, BNL report 61581, 1995.

R.B. Palmer et al, Beam dynamics problems in a muon collider, BNL report 61580, 1995.

R.C. Fernow & J.C. Gallardo, Validity of the differential equations for ionization cooling, BNL report 61579, 1995.

R.C. Fernow, Comparison of the Wang and Wachsmuth models for pion production with measurements at 12 GeV/c,

R.C. Fernow et al, A possible ionization cooling experiment at the AGS, BNL report 61577, 1995.

R.C. Fernow & J.C. Gallardo, Muon transverse ionization cooling: stochastic approach, BNL report 61576, 1995.

R.C. Fernow et al, Targets and magnetic elements for pion collection in muon collider drivers, BNL report 61575, 1995.

LDRD FUNDING:

FY 1995	\$149,580
FY 1996 est.	\$200,000

Ultra-violet Free Electron Laser R&D

Erik D. Johnson

95-03

Ilan Ben-Zvi

Richard Heese

Sam Krinsky and

Li-Hua Yu

PROJECT DESCRIPTION:

The NSLS has identified short wavelength Free Electron Lasers as a possible new source for its synchrotron radiation research community. Considerable research and development work has already taken place at BNL on many of the component technologies necessary to prototype such a device. Key among these elements is an accelerator designed to produce low emittance, high peak current, short pulses of electrons. Several types of synchrotron radiation sources can utilize such a machine, including a coherent transition radiation source, a coherent synchrotron radiation source, as well as a short wavelength Free Electron Laser. This suite of experiments is now known collectively as the Source Development Laboratory (SDL). The SDL utilizes equipment recovered from various terminated projects notably the ARPA 210 MeV linac, and the 10 meter long NISUS undulator from the Army SSDC. The function of this LDRD project is to support the integration these existing technologies into an accelerator designed to prototype an UV-FEL.

TECHNICAL PROGRESS AND RESULTS-Fiscal Year 1995:

Purpose: A full CDR has been developed for an ultra-violet free electron laser designed to operate into the deep UV. The so-called DUV-FEL proposal cost estimate is roughly \$30M for its full implementation. Much of the

pre-construction R&D it would require can be accomplished on existing or loaned equipment, running at reduced repetition rate, and tuning capability. This experiment, called the ultra-violet project free electron laser (UP-FEL) seeks to perform a reduction to practice in a proof of principle experiment. Many of the existing components must be adapted or improved from their present form. This LDRD project covers some of the R&D required to execute the proof of principle experiment for the FEL

Approach: The DUV-FEL Conceptual Design Report forms the basis for the design of the Source Development Lab accelerator. It requires the production and delivery of a very bright electron beam to an amplifier, in this case comprised initially of the NISUS undulator. To generate the electron beam, the 'Gun III' design developed in an Accelerator Test Facility (ATF) collaboration has been adopted. Since the final objective is to drive a seeded beam FEL (either in fundamental or harmonic mode), phase stabilization of the accelerator is critically important. Improving the relative stabilization to a level below 1 ps requires investigation of stabilization of the gun/seed laser phase with respect to the accelerator RF system, and development of the accelerator control system to derive the benefits made possible by the laser oscillator stabilization. Expertise for addressing many aspects of these problems lies outside the laboratory, so much of the work is undertaken through collaboration and R&D subcontracts.

Technical Progress and Results: The 'Gun III' collaboration was established prior to the funding of this LDRD, so much of the conceptual design work had already been performed. The gun is basically a simplified version of the well established ATF RF photocathode electron gun. The SDL project benefits from this previous work, and has recently contributed to supporting the testing

of the first prototype gun, which was fabricated during FY 95. Simulations of the gun performance, initial cold testing, and tuning have been reported [1]. The conceptual design of the injector system, including emittance compensation solenoid is now well underway [2]. During FY 96, it is anticipated that the prototype injector system can be assembled and tested.

The SDL project similarly benefits from prior work conducted by the BNL Chemistry department for its Center for Radiation Chemistry Research (CRCR) facility in specifying a gun laser system. An electron gun similar to that for the SDL is employed in the CRCR which required the specification of a gun laser system. After considerable investigation of alternatives, a Spectra Physics Titanium:Sapphire (Ti:Sap) laser was selected. To maintain some commonality between the facilities, the same basic laser system was specified for the SDL. For the CRCR, this laser provides the opportunity for multi-color experiments, while at the SDL, radiation from the gun laser can be split off for seeding the FEL, resulting in very low timing jitter.

For the SDL, some enhancements of the performance of this system are however required. In particular, the SDL accelerator design includes an electron pulse compressor which demands phase stability between the laser system and accelerator RF at or better than 1 ps rms. To see if such a system could be delivered, an R&D subcontract was let to Spectra Physics [3]. They have found that the addition of a computer controlled coarse adjustment of the oscillator cavity length, coupled with the piezo fine adjustment achieves significant long term stabilization with respect to the drive clock (81.6 MHz). The reason for the improvement is that the coarse adjustment is used to keep the PZT translator in the middle of its travel. This improves the stability of the PZT. The scheme

also has the additional advantage that the phase stabilization is now a completely automated 'hands off' function. This is very beneficial considering the distance between the laser and the end user experiment (~50 m).

During FY 95 considerable effort was also invested in setting up a control system for the SDL which is based on the same hardware as the NSLS accelerator plant. The commonality of hardware and software (once the low level interface development is complete) has several benefits. Software modification and maintenance should be comparatively straight forward. New features developed for the NSLS control system should be directly compatible with the SDL control system. Perhaps most important is that staff members familiar with the NSLS control system should find it comparatively easy to operate the SDL accelerator.

PAPERS/JOURNALS/PUBLICATIONS:

[1] "Microwave measurements and beam dynamics simulations of the BNL/SLAC/UCLA emittance-compensated 1.6-cell photocathode RF gun," by D.T. Palmer, R.H. Miller, H. Winick, X.J. Wang, K. Batchelor, M.H. Woodle, I. Ben-Zvi, **SPIE Proceedings 2522**, p 514, (10-14 July 1995 San Diego, CA)

[2] Design review meetings have been held, 3/6/95, 6/22/95, and 10/25/95.

[3] Spectra Physics Report to BNL on 'Computer interface of Lok to Clock Synchronization' 28 September 1995, by A.M. Del Gaudio.

LDRD FUNDING:

FY 1995	\$100,005
FY 1996 est.	\$100,000

Precision Machining using Hard X-rays

*Erik D. Johnson and
D. Peter Siddons*

95-04

PROJECT DESCRIPTION:

Preliminary work has indicated that hard x-rays can indeed extend the lithographic processing of resist materials to the scale of several centimeters while maintaining precision at the level of microns. Combining the characteristics of a hard x-ray source, such as the NSLS X-27B beamline used for this work with techniques of coupled scanning of substrate and mask has proven to be a viable method for producing fully figured three-dimensional structures in plastic. This project is a systematic study of these techniques and the processing parameters required to operate with confidence in this high aspect ratio regime. Apart from the basic research interest of understanding the materials science aspects of this problem, a demonstration and reduction to practice of this technology should provide potent motivation for its commercialization.

TECHNICAL PROGRESS AND RESULTS-Fiscal Year 1995:

Purpose: The idea of using the lithographic techniques developed by the microelectronics industry to fabricate micromechanical components began to take shape in the mid-80's. By 1988 a group in Germany was sufficiently convinced of its future importance to float a commercial enterprise to capitalize on the techniques developed by the research group based at the Karlsruhe Nuclear Research Center working on the BESSY storage ring in Berlin. At roughly the same time a group headed by Prof. H. Guckel at the

University of Wisconsin at Madison began to develop their own techniques in this area, using the ALADDIN storage ring at Madison. Currently, these two groups lead the field worldwide in technique development and successful applications. Recently, exposure in the mass media has raised the profile of these developments and several other groups have begun to initiate programs.

Almost all of the programs existing or proposed make use of soft x-rays to fabricate tiny structures which are essentially 2-dimensional. Our work is directed at developing methods for the very precise manufacture of macroscopic, three-dimensional structures using hard x-rays in a lithographic process. Such a technology, if carried through to production scale, would be revolutionary, allowing complex 3-dimensional objects to be machined with sub-micron precision.

Approach: Early in this work, we made some test objects which showed that fully figured plastic masters could be made. To proceed to the manufacture of 'real devices' one must be able to transfer the mask pattern to the plastic while holding dimensional tolerances. This can not be done without a suitable measurement tool. We have obtained access to an electron microscope, and an optical microscope with an encoded translation stage which allows us to make comparisons between the mask and exposed parts. We can also systematically investigate the effect of varying the exposure and development conditions using this tool.

We have for our initial work limited our choice of resist material to polymethylmethacrylate (PMMA) as it is readily available and well studied with regard to its properties as a thin film photo-resist. It is a 'known' quantity within the micro-electronics community, and therefore we reasoned, would

be more readily adopted as part of a new technology. We have also selected 2-methyl-4-pentanone, commonly known as methyl-isobutyl-ketone (MIBK) as our developer for similar reasons. In the micromechanics field other, more complex developers are used, but our initial investigations have shown that the MIBK actually performs better in thick resist processing than the alternative development systems.

In pursuing this research, we are making both tolerance test structures, for studying processing parameters, and fabricating structures directly in plastic for selected applications. This is done to gain an understanding not only of the resist and processing properties, but to maintain an awareness of manufacturability issues throughout the course of the research.

Technical Progress and Results: The following photographs are test objects from our preliminary experiments, and provide some idea of the potential for the technique. When we first started exploring the use of hard x-rays for lithographic processing of materials, we made devices not unlike existing LIGA technology, in as much as they were essentially figured only in two dimensions.

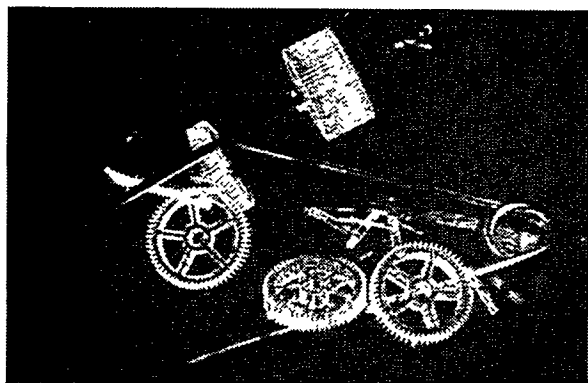


Figure 1 PMMA gears up to 3mm thick with diameters ranging from $50\mu\text{m}$ to 5mm are shown with a pin and needle for scale. Note the small gear through the eye of the needle.

The first obvious difference is the thickness of the parts. We have exposed samples many mm thick, including producing a square hole 1mm across, but over 100 mm deep.

In addition, many processing advantages are realized from the use of hard x-rays. For example, our first mask was a $50\mu\text{m}$ thick gold pattern on a standard silicon wafer. As a mask, this object is far more robust than any used for conventional soft-xray lithography. The shorter wavelength also means that diffraction blurring is negligible. In fact the only source of aberration comes from the source size, and the ratio of working distance to source distance. As a practical matter, at the NSLS, this means working distances of a few mm will result in sub-micron image blurring. This is a far cry from the $10\mu\text{m}$ working distances which are required for x-ray lithographic processing of semiconductor devices.

It didn't take long for us to realize that the enormous penetration depth of hard x-rays could be utilized to make fully figured three dimensional objects. We turned first to the manufacture of solids of rotation. The set up involves a rotary stage which holds the sample to be exposed with its axis nominally parallel to the plane of the storage ring. The mask is placed between the source and the sample with a typical working distance the order of a few cm. It is also important to note that for these devices, the masks can be quite simple. In the case of the spherical shape in figure 2, the mask was a steel dowel pin set in a block of brass. The edge of the block was slightly above the axis of rotation so a continuous shaft is produced, and the dowel is oriented along the beam to provide a smooth round mask for the sample. The mask and sample are scanned vertically through the beam, then the sample is rotated and the process repeated.

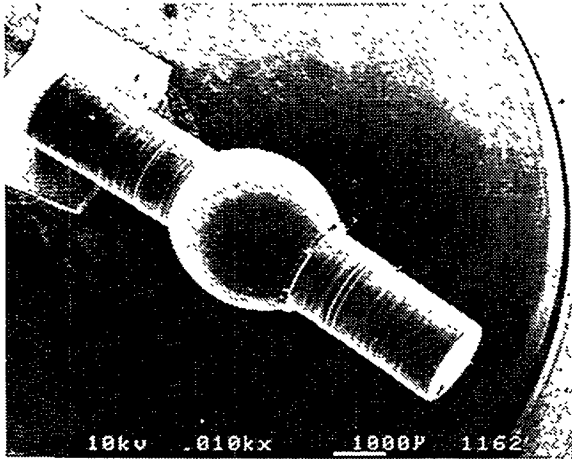


Figure 2 Electron micrograph of the ball on pin in PMMA.

By constructing a mask from several stacked dowel pins, complex shapes such as those shown in micrographs 1208 and 1201 can be produced. These samples were made from sheets of PMMA. Since the mask extended beyond the thickness of the sheet, the piece provides a good comparison of the photo-machined surface finish to that of the as-finished sheet (where the shape is truncated).

There is no reason to believe that these ideas can not be successfully extended to make

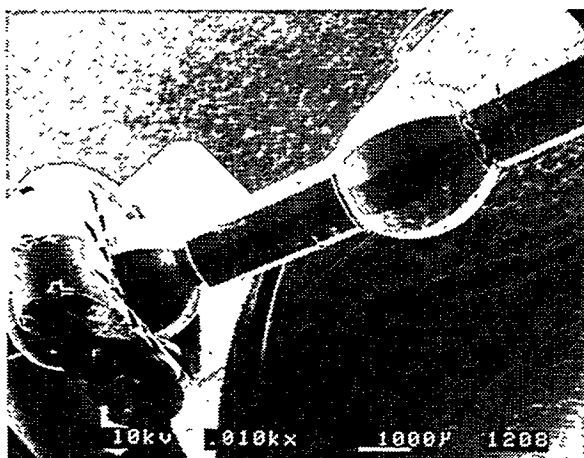


Figure 3 Overview of rotational test sample.

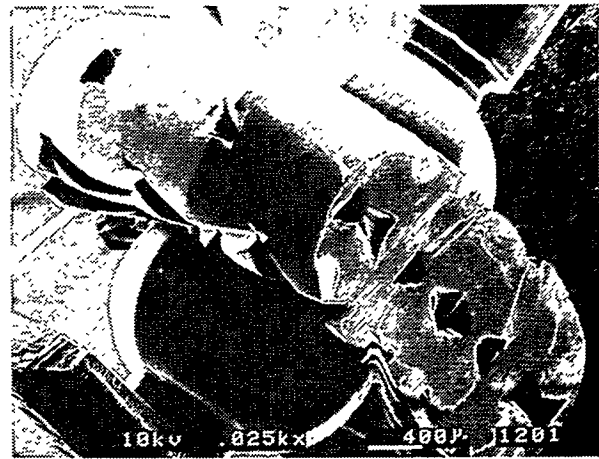


Figure 4 Close-up view of area at the left of figure 3. It clearly shows small channels, and reentrant surfaces.

practical devices including integrated optical systems, sensors, actuators, and transducers. It can also be seen from the micrographs that it is possible to produce parts which have re-entrant geometries.

Fabrication of re-entrant structures simply amounts to understanding the processing characteristics of the plastic, and arranging the exposure in such a way that material to be removed has received sufficient (usually multiple) exposure to be developed while the surrounding material is under exposed, and remains intact. To prove the point, we manufactured a wine glass shape, in effect removing the inside from the outside. For this test, we made six-fold symmetric parts as illustrated in figure 5. The masking was actually accomplished in two stages. First, similar to the other parts already described, the outside shape was figured. In the second step, part of the mask was removed to leave only a wire to outline the shape of the bowl of the glass. It can be seen by inspection that the central portions of the part would be in the beam three times per turn, while the bowl would experience the beam only twice.

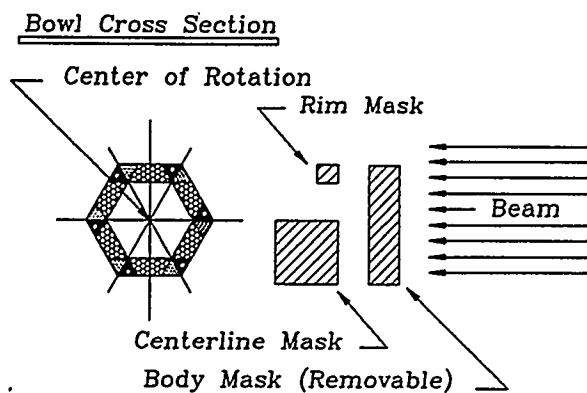


Figure 5 Three exposure levels are shown by the different hatching patterns in the plastic which will remain in the finished part. The central portion, which experiences a fourth and higher level of exposure, is removed in the development process.

Collectively, these results lead to the filing of a patent which details the fundamental principles, and possible applications of hard x-ray lithographic manufacturing [1]. The patent contains some 21 descriptive figures and 70 claims which relate to this work.

The large working distances which can be used allowed us to make rather crude masks, which would be too bulky to function for soft x-ray lithographic methods. We have refined the implied concept of 'kinematic' masks by prototyping a hard x-ray mask direct writing tool. This device is essentially remotely controlled precision x-ray apertures, coupled with scanning stages to manipulate the resist.

One application of this writer has been to fabricate a series of long channels in 1mm PMMA sheet, as prototypes for high density Gel-electrophoresis columns. This work was undertaken in connection with a CRADA between LI-COR and the BNL Biology department, with J.C. Sutherland as the principle investigator [2]. The prototype track arrays we have manufactured are a series of 50 or more channels through 1mm thick PMMA

sheet, which are 40 mm long by $125 \pm 3 \mu\text{m}$ wide, with a $500 \mu\text{m}$ spacing between channels. While the compactness of this array is impressive, the more important feature is the smoothness of the sidewalls, which would be difficult to achieve by conventional machining methods. This finish of these surfaces is important to minimize wall drag and elution spread in the macromolecules being driven through the channel. For a functional device, the technique will need to be extended to allow fabrication of channels up to 500 mm long.

As previously mentioned, the high energy of the x-rays employed in our work allows the use of substantial mask supports, such as silicon wafers. This in turn allows large area masks and large area exposures. As already shown, the high energy also allows exposure of a significant thickness of resist. This resist need not be in a single sheet.

We have recently described a possible operating mode for 'conventional' LIGA technology where multiple, large area samples may be simultaneously exposed [3]. The implication is that the mastering and injection molding necessary in present practice with soft x-rays may be eliminated in an economically viable manufacturing technology. Parts manufactured in this way would also possess superior precision, since the loss of fidelity associated with replication steps is avoided.

During the course of this work, we have evaluated a variety of exposure and processing parameters which are beginning to evolve into design rules for precision machining using hard x-rays. It is our expectation that we will continue to follow this line of investigation. In addition, we have now been approached by a variety of potential collaborators with interest in various aspects of this research. We hope to cultivate their

interest in the coming year as the basis for establishing a permanent research program.

PAPERS/JOURNALS/PUBLICATIONS:

[1] US Patent Application 'Method and Apparatus for Micromachining using Hard X-rays' D.P. Siddons, E.D. Johnson, H. Guckel, J.L. Klein co-inventors. 21 Figures, 70 Claims, Assigned jointly to BNL, and WARF (Wisconsin Alumni Research Foundation)

[2] BNL CRADA BNL-C-95-07 'Instrumentation for High Throughput DNA

Sequencing', J.C. Sutherland PI.

[3] 'Very High Aspect-Ratio Micromachining using Hard X-rays' E.D. Johnson, J.C. Milne, D.P. Siddons, H. Guckel, J.L. Klein, Invited workshop presentation at the 1995 Synchrotron Radiation Instrumentation meeting, Argonne Illinois, 18 October 1995.

LDRD FUNDING:

FY 1995	\$100,005
FY 1996 est.	\$100,000

New Directions in *in vivo* Enzyme Mapping: Catechol-*O*- Methyl-transferase

Yu-Shin Ding

95-07

PROJECT DESCRIPTION:

Catechol-*O*-methyltransferase (COMT; EC 2.1.1.6) regulates the concentration of important catecholamine neurotransmitters such as dopamine. It is also a new molecular target in the development of drugs to treat Parkinson's disease (PD). Though the major function of COMT was described first in the 1950's and its structure was recently elucidated, there is limited information on its regional distribution or functional significance in the living body or of changes in its activity occurring in diseases. With the recent development of selective and potent COMT inhibitors, we now have the opportunity to probe the distribution of COMT *in vivo*.

TECHNICAL PROGRESS AND RESULT - Fiscal Year 1995

Purpose: The goal of this proposal is to develop and validate the methodology for mapping COMT activity *in vivo* using PET. Specific aims include:

- (1) Synthesis and evaluation of the first positron emitter labeled COMT inhibitor as a radioligand for mapping COMT *in vivo*.
- (2) Exploration of the potential of the new COMT radioligand as a tool in pharmaceutical development and for monitoring COMT inhibitor therapy for Parkinson's disease.

Approach: In order to examine the

distribution and functional activity of COMT in the living system, Ro41-0960 (2'-fluoro-3,4-dihydroxy-5-nitrobenzo-phenone), a fluorine containing, potent and selective COMT inhibitor, was chosen for labeling. Enzyme kinetic studies indicated a reversible tight binding type interaction between COMT and Ro41-0960. These characteristics generally fit a major requirement for mapping COMT *in vivo*; namely, that the binding of the labeled inhibitor to the enzyme should be tight enough to allow of visualization of the enzyme-substrate complex. Additionally, reports that Ro41-0960 crosses the blood-brain barrier (BBB) inhibiting brain COMT activity supported the development of a rapid synthetic route to [¹⁸F]Ro41-0960 as a radiotracer for central and peripheral COMT distribution.

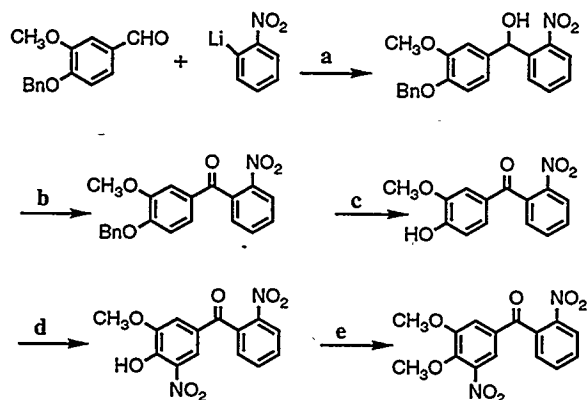
Technical Progress and Results: Over the past year, we have completed the first synthesis of a F-18 labeled ($t_{1/2} = 110$ min) COMT inhibitor ([¹⁸F]Ro41-0960) and have initiated PET studies. Preliminary studies of COMT are summarized in the following sections and include: (1) synthesis of [¹⁸F]Ro41-0960; (2) studies of [¹⁸F]Ro41-0960 in baboon (brain imaging with PET, measurements of blood compartments and lipophilicity); (3) studies of [¹⁸F]Ro41-0960 in mice (biodistribution and blocking studies).

(1) Synthesis of [¹⁸F]Ro41-0960

[¹⁸F]Ro41-0960 was synthesized by a fluoride-for-nitro group nucleophilic aromatic substitution reaction using no-carrier-added (NCA) [¹⁸F]-fluoride, followed by hydrolysis with HBr (Scheme 2). The synthesis time was 100 min; radiochemical yield 5-7%, specific activity 2-5 Ci/ μ mol (EOB), and radiochemical purity of >98%. A flow chart for the preparation of the protected precursor (3,4-dimethoxy-5,2'-dinitrobenzophenone) is shown in Scheme 1.

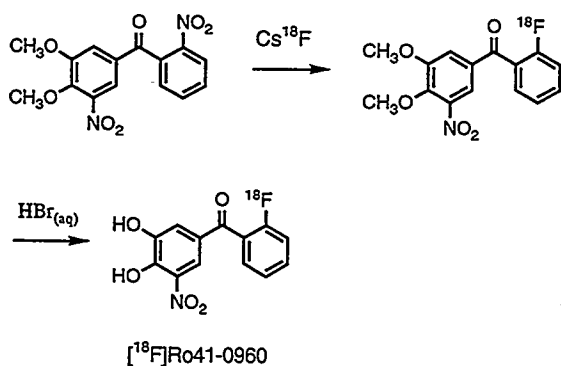
(2) PET Studies of [¹⁸F]Ro41-0960 In Baboons

Scheme 1: Synthesis of Precursor for F-18 Labeled COMT Inhibitor Ro41-0960



a) THF; (b) PCC, CH₂Cl₂; (c) HBr/HOAc; (d) HNO₃/HOAc; (e) NaH, (CH₃)₂SO₄, DMF.
Bn = benzyl; PCC = pyridium chlorochromate

Scheme 2: Synthesis of F-18 Labeled COMT Inhibitor (Ro41-0960)



Baboon Brain Studies: Two adult female baboon (*Papio anubis*) were anesthetized and used for PET studies. One baboon was injected with NCA [¹⁸F]Ro41-0960 (2.1 mCi) and another baboon was injected with [¹⁸F]Ro41-0960 (1.2 mCi) diluted with unlabeled Ro41-0960 (1.4 mg/kg).

The brain uptake of F-18 after the injection of [¹⁸F]Ro41-0960 was negligible at all times through a 90 min experimental interval both at a tracer dose (no-carrier-added, NCA) and with addition of unlabeled drug (1.4 mg/kg, carrier added (CA)) as is shown in Figure 1. In contrast to the brain, the whole body scan of the baboon at 90 min after injection of [¹⁸F]Ro41-0960 showed high uptake in kidneys, liver, gall bladder and bladder.

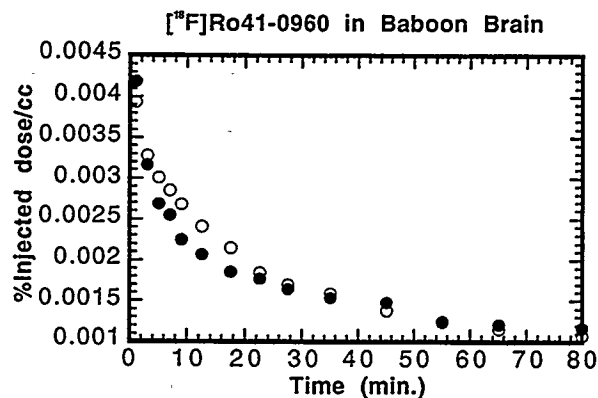


Figure 1. Time-activity Curves of [¹⁸F]Ro41-0960 in the Brain both at a Tracer Dose (No-Carrier-Added (NCA), open circles) and with Addition of Unlabeled Drug (1.5 mg/kg, Carrier Added (CA), solid circles).

Data Analysis: The following analysis was also carried out in order to separate the radioactivity in tissue from that contributed from blood. Measured radioactivity in the ROI at time t is considered to be the sum of radioactivity in tissue plus a contribution from the blood volume so that

$$\text{ROI}(t) = (1 - V_B) \times C_T(t) + V_B \times C_p(t)$$

Where V_B is the vascular fraction, C_T is the radioactivity in tissue and C_p is the plasma radioactivity including labeled metabolites.

Kinetic analysis demonstrated that the transfer of [^{18}F]Ro41-0960 through the BBB is negligible both in the NCA and CA studies (Figure 2a & 2b), as indicated by the low net brain concentrations after correction for the vascular contribution. Radioactivity in the brain was found to be adequately described by the blood volume component alone, assuming that the blood volume is 4% of the total brain volume.

This is a significant observation calling into question the common assumption that Ro41-0960 crosses the BBB.

Blood Compartments and Lipophilicity:

After incubation with whole baboon blood, [^{18}F]Ro41-0960 was predominantly associated with plasma proteins (Table 1). The plasma free fraction was <1%, and less than 5% was associated with the erythrocyte fraction. Mouse blood behaved similarly. The octanol/water partition coefficient was 3.97 ± 0.14 .

Table 1: Blood Compartments

	Mouse	Baboon
Plasma Free Fraction	$0.5 \pm 0.07\%$	$0.86 \pm 0.20\%$
Plasma/Erythrocytes	16	24

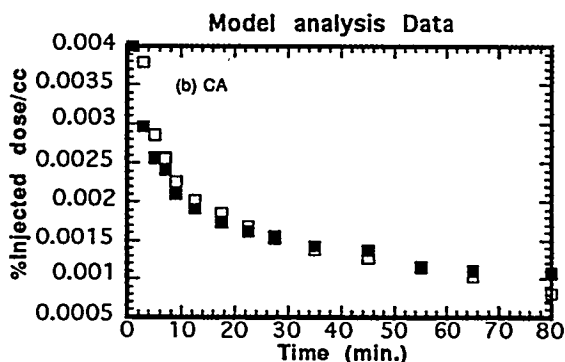
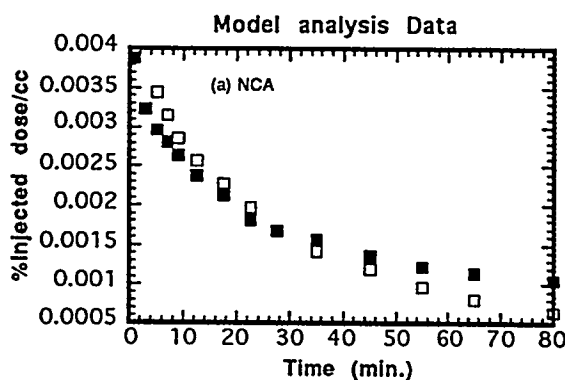


Figure 2. Time-activity Curves of Model Analysis for (a) NCA and (b) CA studies. Solid squares represent ROI (global brain region); open squares represent the model of ROI as $V_B \times C_p$, where V_B is the vascular fraction and C_p is the plasma radioactivity including labeled metabolites.

(3) Studies of [^{18}F]Ro41-0960 In Mice

Biodistribution: Outbred Swiss-Webster mice (25-38g males, $n = 4-5$ per group) were injected intravenously with [^{18}F]Ro41-0960 (5 μCi) alone or pretreated intraperitoneally 30 min before radiotracer with unlabeled Ro41-0960 (25 mg/kg).

Preliminary biodistribution data were obtained in mice sacrificed 5, 30 and 60 minutes after intravenous administration of [¹⁸F]Ro41-0960 (data were expressed as percentage of injected activity per gram; %IA/g). At 5 minutes, blood contained a higher concentration of F-18 than other tissues. The blood F-18 fell progressively between 5 and 60 minutes, while F-18 in liver and kidney remained approximately constant. At 30 minutes, the following decreasing rank order of F-18 concentration was observed: (>7 %IA/g) urine, kidneys, liver, blood; (2-5 %IA/g) small intestines, lungs, adrenals, salivary gland; (1-2 %IA/g) stomach, heart, spleen; (<1 %IA/g) skin, bone, muscle, gonads, fat, eyes, brain. The brain contained very little F-18 (<0.5%) compared to other tissues. The bone contained about 1% IA/g at all times. Urine contained a higher concentration of radioactivity than blood at all times. F-18 in the small intestines rose between 5 and 60 minutes, and was about 5% of the injected radioactivity at 60 minutes.

Blocking Studies: In order to assess if the binding is saturable, mice were pretreated with unlabeled Ro41-0960 prior to [¹⁸F]Ro41-0960 administration. In mice pretreated with 25 mg/kg unlabeled Ro41-0960, the F-18 concentrations in blood and brain were about half those seen in control mice, at each time-point. Most other tissues also contained less F-18 in the treated animals. In contrast, F-18 in the small intestine more than doubled, and F-18 in urine rose several fold. This was probably due to drug-induced effects on excretion pathways. Stomach also contained 2-3 times more F-18 in pretreated than in control animals.

SUMMARY AND CONCLUSION:

Our preliminary studies demonstrate that (1) we can synthesize [¹⁸F]Ro41-0960 in sufficient yield for PET studies; (2) [¹⁸F]Ro41-0960 has low cerebral bioavailability, in contrast, to the many claims of its central activity in the literature; (3) a significant low plasma free fraction and high erythroplasmatic ratio as indicated in Table I suggests that high degree binding to plasma protein rather than binding to erythrocyte may explain, at least in part, the exclusion of [¹⁸F]Ro41-0960 from the brain; (4) tracer uptake is highest in kidney and liver which is consistent with high levels of COMT in these peripheral organs; (5) it labels the COMT sites in periphery; (6) its uptake in mouse organs known to have high COMT can be blocked with unlabeled Ro41-0960. These studies support this proposal to (1) further characterize [¹⁸F]Ro41-0960 as a tracer for peripheral COMT *in vivo*; (2) to examine the pharmacodynamics of COMT inhibition with PET. These studies will form the groundwork for investigating the role of COMT in disease and will serve as a tool in drug research and development.

PAPERS/JOURNALS/PUBLICATIONS:

Y.-S. Ding, Y. Sugano, S.J. Gatley, J.S. Fowler, J. Koomen, N. Volkow, R. Chen, C. Shea, D.J. Schlyer. Synthesis of [¹⁸F]Ro41-0960, a potent COMT inhibitor, for use in *in vivo* mapping with PET. 42nd Society of Nuclear Medicine Meeting (Abstract), June 1995.

Y.-S. Ding, S.J. Gatley, J.S. Fowler, R. Chen, N.D. Volkow, J. Logan, C.E. Shea, Y. Sugano, J. Koomen. PET Radiotracers for Studies of Catechol-O-methyltransferase. 11th

International Symposium on Radiopharmaceutical Chemistry (Abstract), August 1995.

Y.-S. Ding, S.J. Gatley, J.S.Fowler, R. Chen, N.D. Volkow, J. Logan, C.E. Shea, Y. Sugano, J. Koomen. Mapping Catechol-*O*-methyltransferase in vivo: Initial Studies with [¹⁸F]Ro41-0960. *Life Sciences* (in press).

LDRD FUNDING:

FY 1995	\$ 98,779
FY 1996 est	\$103,000

*This project involves animal vertebrates.

Proposal to Develop a High Rate Muon Polarimeter

*Milind Diwan and
Hong Ma*

95-10

Muon polarization is a sensitive probe of CP and T symmetries in many kaon decay processes. In particular, the out of plane polarization of muons in $K^+ \rightarrow \pi^0 \mu^+ \nu$ is T violating. The measurement of the transverse polarization of the muon in $K^+ \rightarrow \pi^0 \mu^+ \nu$ is of interest for two reasons: 1) The out of plane polarization of the muon can only be caused by a new source of time reversal violation outside the minimal standard model of particle physics, 2) The spurious polarization caused by the final state interaction between the pion and the muon is negligible in this case because the pion is neutral. Recent theoretical reviews [1] suggest that a measurement at 10^{-3} level could yield interesting results.

The previous best experiment was carried out at the BNL-AGS and yielded a measurement of $P_T = (-3.1 \pm 5.3) \times 10^{-3}$ [2]. A new experiment at the KEK-PS in Japan will try to measure this number with a sensitivity of 9×10^{-4} [3]. The higher beam intensity at the AGS combined with a high acceptance detector should make it possible to measure this number with a sensitivity down to 10^{-4} .

PROJECT DESCRIPTION:

Recent upgrades to the AGS have made it possible to obtain enough kaon decay events to perform muon polarization measurements with unprecedented sensitivity if appropriate detectors can be built. A polarimeter that can be operated in a high

intensity environment with large analyzing power is essential for these experiments. We have proposed a polarimeter that combines several functions in one. It will measure the range of the muons of interest, measure the decay positron track and energy to identify it from random backgrounds and help the analyzing power, and also measure the time of the decay.

We have built a small muon polarimeter to test these ideas. Figure 1 shows a schematic of the polarimeter with a cosmic ray data event. The apparatus consists of ten extruded aluminum muon chambers stacked on top of each other. Each chamber is about 2 meters long and has 64 cells with a cross section of 1 cm by 1 cm (filled with a mixture of 90% Argon and 10% methane) with a wire in the center. The cells are arranged in a staggered fashion so that there are no inefficient gaps between them. To save readout electronic channels two staggered cells are combined into one electronic channel; thus the 64 cells correspond to 32 readout channels. The chambers are entirely made from aluminum, which does not depolarize muons and is therefore the material of choice for a polarimeter. The two skins, the middle structural plate, and the walls between the cells are 2 mm, 3 mm, and 3 mm thick, respectively. Therefore, a muon traversing vertically will be slowed down by at least 5 mm of aluminum in each chamber. Indeed, the event shown in Figure 1 shows a muon that stopped in the stack and decayed to an electron. As the figure shows we have placed three scintillation counters on top of the stack to trigger on incoming muons. There are also scintillator planes on the sides and the bottom of the stack to veto on muons that leave the stack without stopping. The muon chambers were borrowed from the AGS experiment E865.

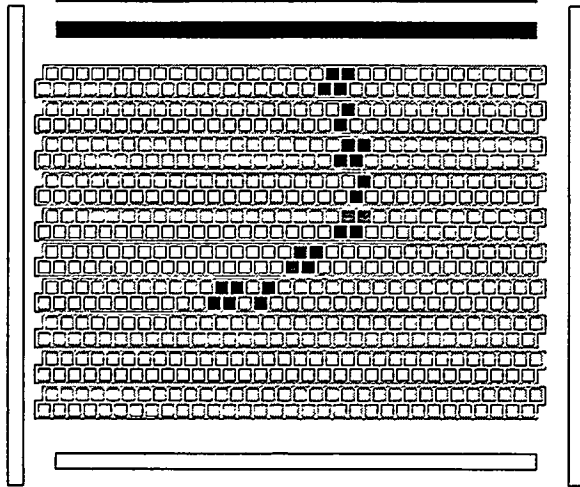


Figure 1: Schematic of the muon polarimeter with a superimposed cosmic ray data event. The dark shade hits are prompt hits from muon, and the light shade hits are delayed hits from electrons.

Figure 2 shows a schematic of the readout electronics for the apparatus. The signals from the polarimeter chambers were amplified and then discriminated. The trigger and veto scintillators were read out by photomultiplier tubes (PMT). The discriminated signals from the PMTs were sent to fast trigger electronics that produced a signal when a cosmic ray muon entered and did not exit through the bottom or the side scintillators. This stopping muon trigger was sent to LECROY-1879 pipeline TDCs, which recorded the times of all signals from the muon chambers and the scintillators for 8 μ s after the detection of the stopping muon. This data was sent to a micro-VAX computer where it was later analysed.

Muon Polarimeter Readout Electronics

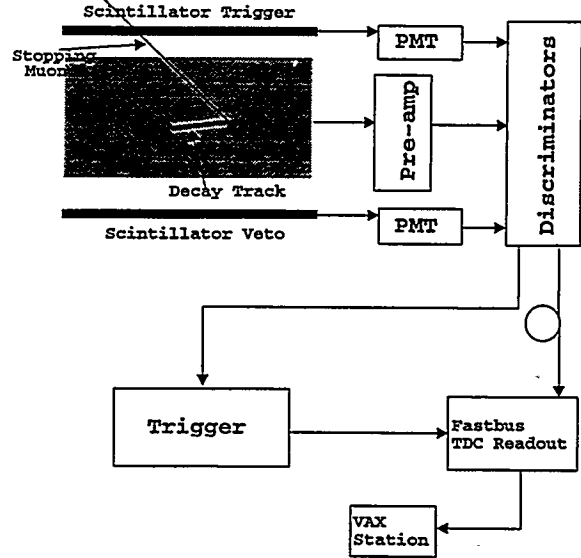


Figure 2: Schematic of the muon polarimeter read out electronics.

TECHNICAL PROGRESS AND RESULTS - Fiscal Year 1995:

We have collected approximately 10,000 cosmic ray muon decays with our apparatus. Figure 3 shows the measured decay time of the muons. The fitted lifetime of the cosmic ray muons is $1.80 \pm 0.04 \mu$ s. The effective lifetime of stopping cosmic ray muons is shorter than the lifetime of muons in vacuum (2.2μ s). This is because the μ^- , which form 30-40% of the cosmic ray muon flux, are absorbed in nuclei through inverse beta decay. Inverse beta decay of μ^- competes with the decay process causing the lifetime of stopped μ^- to be smaller. The lifetime of stopped μ^+ , on the other hand, should be 2.20μ s, since there are no absorption processes for the μ^+ .

Figure 3 also shows the spectrum of polarimeter hits for the muon decay electrons. More than half of the electrons produce 4 or more hits. Measurement of the electron direction is necessary to measure the

polarization of the stopped muon. Since the electrons produce more than 4 hits on the average we should be able to measure the electron direction well. The multiple scattering of the electron, however, will limit the analyzing power. Our future analysis will focus on understanding the spectrum and the analyzing power.

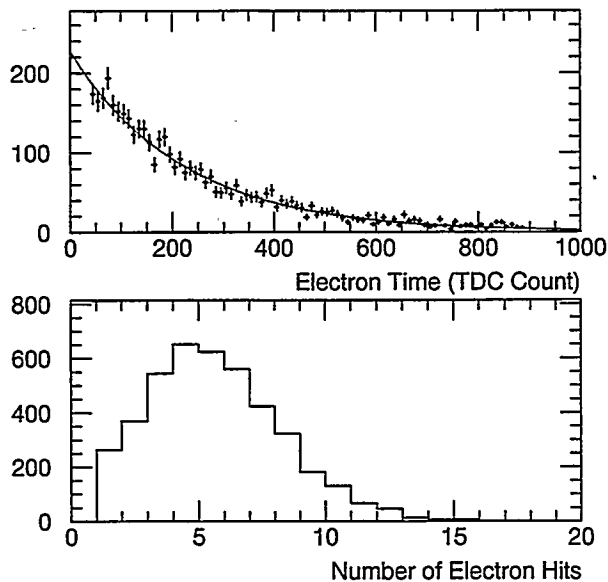


Figure 3: Cosmic ray muon decay data from the test polarimeter. a) Lifetime of the cosmic ray muons stopped in the aluminum of the polarimeter. The time is measured in units of TDC bins. The conversion factor is 8ns/bin . The fitted lifetime is $1.80 \pm 0.04\mu\text{s}$. b) Distribution of the number of hit channels by the muons decay electrons.

To measure a component of the muon polarization with an error of 10^{-4} requires us to collect and analyze at least 10^9 decays. Such an experiment must be done in an intense kaon beam with much accompanying soft background radiation. A fine grained polarimeter that produces several hits for each decay electron should be satisfactory for such an experiment.

The event rate in such an experiment is so large that one must contemplate analyzing all 10^9 events on line. Therefore, we are developing a hardware trigger and analysis system for the test polarimeter. The polarimeter will be divided into sections that produce a prompt signal for the stopping muon and a delayed signal for the decay electron. The trigger electronics will respond only to this delayed signal within $7\mu\text{s}$ of the prompt and produce a bit pattern indicating the direction of the electron with respect to the incoming muon.

References

1. G. Belanger and C.Q. Geng, Physical Review D44 (1991) 2789.
2. S.R. Blatt, et al., Physical Review D27 (1983), 1056.
3. J. Imazato, et al., KEK-PS research proposal Exp-246, June 6, 1991.

PAPERS/JOURNALS/PUBLICATIONS:

The results from the data gathered in our test apparatus so far will be the subject of an undergraduate senior thesis of Steve Madonna from California Polytechnical University.

FOLLOW-ON FUNDING:

We are writing a proposal for measuring the T-violating muon polarization in $K^+ \rightarrow \pi^0 \mu^+ \nu$ decays. Our experience with the test polarimeter will influence the design of this experiment.

LDRD FUNDING:

FY 1995

\$49,990

Development of Intense, Tunable 20-femtosecond Laser Systems

Edward Castner Jr.

95-11

PROJECT DESCRIPTION:

Novel ultrashort pulse laser systems producing pulse durations less than 20 femtoseconds (2.0×10^{-14} s) are being designed and built at BNL. In parallel with the laser system development, we are also developing new time-resolved absorption and emission spectrometers. The new laser systems and spectroscopic instrumentation are being used to study photo-induced chemical reactions in solution with ultrashort time resolution.

TECHNICAL PROGRESS AND RESULTS- Fiscal Year 1995:

Purpose: Bursts of light energy from ultrashort pulse lasers are required in a number of research applications at BNL. Our application of femtosecond light pulses is to generate and probe transient photochemical species in solution. We are also adding capabilities for new laser spectroscopy experiments by generating sub-20 fs light pulses in a BNL-built Ti:sapphire laser oscillator with an added acousto-optic cavity dumper, and by extending our present Ti:sapphire laser regenerative amplifier technology. Two-color pump/probe transient absorption experiments, and femtosecond upconversion gated fluorescence experiments will allow the monitoring of photo-induced charge transfer reactions in solution with unprecedented time resolution, on a time scale shorter than the molecular motions of the photo-reactants and surrounding solvent medium.

Approach: Ultrashort pulse lasers are essential tools in a number of current research areas, including optical spectroscopy, coherent control of chemical reactions, time-resolved holography and scanning microscopy, and novel electron-accelerator development. In my lab in the Chemistry Department, femtosecond lasers are used for several applications in the search for understanding the details of electron-transfer processes in solution. In particular, by using a laser pulse of 15-25 femtoseconds, one can initiate photochemical events by creating a coherent wavepacket on the reactive excited state potential energy surface of the molecule and then monitoring the evolution of the photo-induced reaction by absorption, fluorescence, or Raman spectroscopy experiments using one or more time-sequenced femtosecond light pulses.

Generation of reliable ultrashort laser pulses of 10 to 20 femtosecond duration is now possible with the Titanium-doped sapphire gain material. Chirped-pulse regenerative amplification in Ti:sapphire allows the amplification of these pulses to very high peak powers, at the milliJoule energy level and beyond, while preserving the spatio-temporal characteristics of the high-quality oscillator pulses. Acousto-optic cavity-dumping of a laser oscillator is a means of obtaining about one order of magnitude greater laser pulse energy, with no change at all in the other laser pulse characteristics.

Technical Progress and Results: During the course of the LDRD research, we have developed and built a Ti:sapphire laser oscillator with substantially shorter light pulse output than can be generated in commercially available Ti:sapphire laser systems. The laser produces pulses at 800 nanometer center wavelength, with a spectral bandwidth of 53 nm, full-width, half-maximum (FWHM). The

pulse duration as measured by second harmonic generation (SHG) autocorrelation techniques is <21 femtoseconds, FWHM. The laser output energy is 3 nJ/pulse, at a pulse repetition frequency of 85 MHz. A 3 nJ pulse with 20 fs duration carries a peak power of 150 kW. The temporal profile of the pulse as measured by the SHG autocorrelation technique is shown in Figure 1, and the laser pulse intensity spectrum is shown in Figure 2.

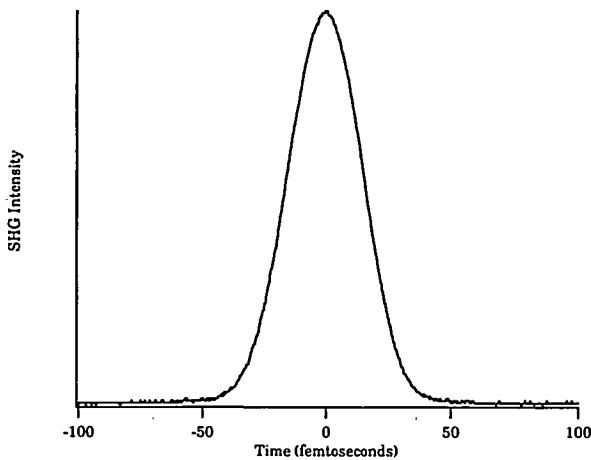


Fig. 1. 21 fs laser pulse SHG time autocorrelation.

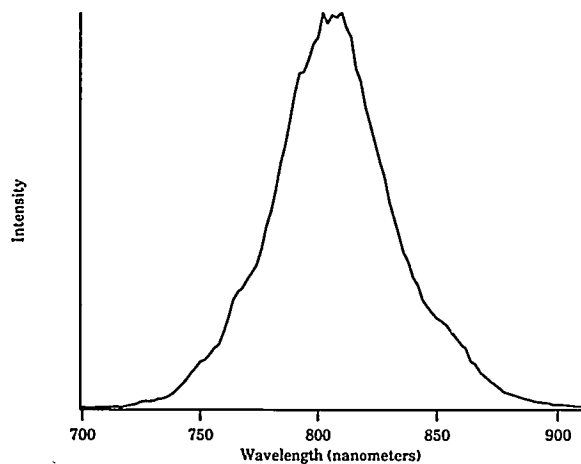


Fig. 2. Laser pulse intensity spectrum.

When focused, the pulse energy from this Ti:sapphire laser oscillator is sufficient for many experiments. However, nonlinear

optical experiments often require higher energy pulses, and the use of frequency conversion schemes (harmonic, sum and difference, and optical parametric frequency generation) in nonlinear optical crystals. Another way to obtain higher energy ultrashort light pulses is to use chirped-pulse regenerative amplifier technology. However, even with the greatest efforts, regenerative amplifiers can only produce pulses as short as 35 fs, because of group-velocity dispersion and gain saturation fundamental limits.

By using a cavity-dumping scheme in the Ti:sapphire laser oscillator directly, the original bandwidth and pulse duration of the laser oscillator are preserved. This means that by reducing the pulse output repetition frequency by means of an acousto-optic switch, one can obtain the same laser characteristics, but at an energy that is larger by an order of magnitude than the laser alone. Such a cavity-dumped Ti:sapphire laser oscillator will operate at up to only 1 MHz pulse repetition frequency, but at an increased pulse energy of up to 100 nJ/pulse. For experiments such as sum-frequency gated fluorescence upconversion and transient grating spectroscopy, the experimental signal depends on the third power of the laser pulse peak power. Thus, cavity dumping can increase our signal levels conservatively by three orders of magnitude, greatly expanding the range of experiments we can perform.

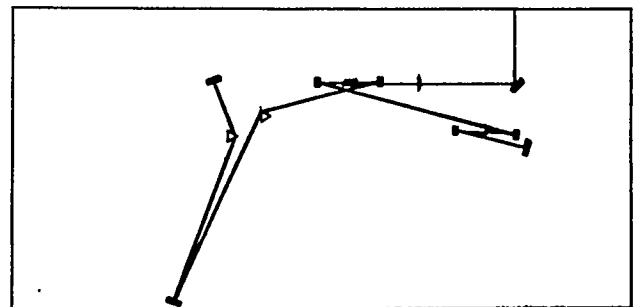


Fig. 3. Optical layout of the cavity-dumped Ti:sapphire laser.

The free-running (non-cavity-dumped) Ti:sapphire laser oscillator has been designed, built, and characterized, as discussed above. By performing laser resonator design calculations using a Gaussian ABCD matrix beam-propagation formalism, we have designed a cavity-dumped configuration for the Ti:sapphire laser oscillator. A schematic diagram of the laser beam path within the resonator is shown in Figure 3. By using an acousto-optic Bragg diffraction cell within a focusing fold in the laser cavity, we can selectively diffract out a pulse from the laser, discriminating it from the pulses arriving just before and after the selected 'dump' pulse. The cavity-dumper radio-frequency drive electronics and Bragg diffraction cell have been procured and satisfactorily tested. The Ti:sapphire laser oscillator has been rebuilt to incorporate the acousto-optic switching technology, and normal laser output has been regained. Acousto-optic cavity dumping of the laser has been successfully demonstrated. The cavity-dumped Ti:sapphire laser will be complete on a final realignment when modelocking is reached, to produce ultrashort laser pulses once again.

Two ultrafast laser experiments have been designed and are presently underway to make use of our current ultrashort pulse lasers and the upcoming cavity-dumped laser. One experiment will use the Ti:sapphire regenerative laser amplifier system to allow for femtosecond transient absorption. The second experiment will use the cavity-dumped Ti:sapphire laser system to produce and measure photoemission from excited states of molecules with femtosecond time resolution.

We have designed a transient absorption spectrometer, capable of initiating a photochemical reaction with a femtosecond laser pulse, and detecting the time-dependent concentrations of reactants and products by absorption spectroscopy with a variably-delayed white-light probing femtosecond

pulse. The instrument is based on our standard femtosecond Ti:sapphire regenerative laser amplifier system, used at 1 kHz pulse repetition frequency to produce three independent femtosecond laser pulses: a fundamental (790 nm) pulse for laser diagnostics, a SHG pulse (395 nm) for optical excitation, and a white-light continuum beam extending from about 450-1000 nm for transient absorption probing.

A demonstration of the capabilities of the new femtosecond transient absorption spectrometer is given by the transient shown in Figure 4. The experimental sample is a solution of Co²⁺OEP in toluene (where OEP = octaethyl porphyrin). A drawing of the molecular structure of Co²⁺OEP is shown in Figure 5. The Soret band of the sample is photoexcited and a white-light continuum beam to probe the absorption spectrum of the sample before, during, and after photoexcitation. In this example, the probe wavelength was restricted to a 10 nm slice of light at 550 nm. The signal-to-noise is adequate to resolve the 6 picosecond exponential decay time. Improvements in the signal-to-noise ratio of the experiment are presently in progress, including more sophisticated signal modulation and detection schemes.

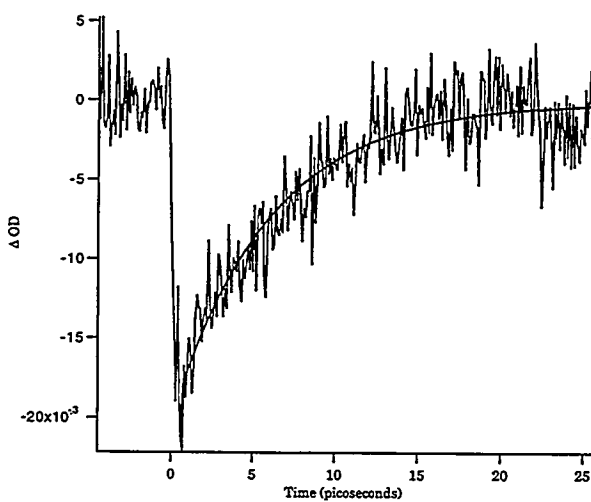


Fig. 4. Absorption transient for Co^{II}OEP.

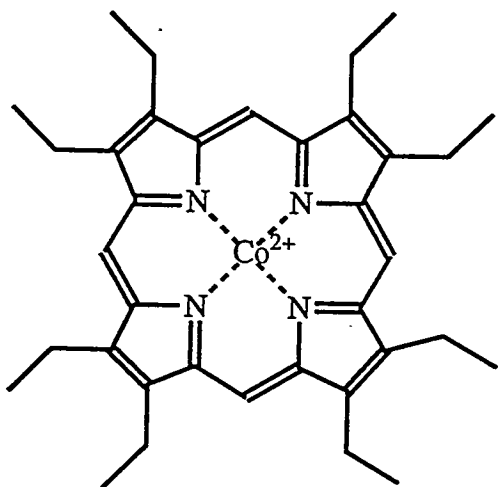


Fig. 5. Drawing of the molecular structure of Co²⁺ OEP.

The femtosecond fluorescence upconversion experiment is being set up to stimulate and detect emission from photoexcited states of electron-transfer

chromophores in solution. An all-reflective fluorescence collimation scheme will be used, to minimize the group velocity dispersion effects on the time-resolved emission. Use of the cavity-dumped laser system should allow greatly enhanced signal levels, perhaps up to 3 orders of magnitude more than with the non-cavity-dumped Ti:sapphire laser. Also, by reducing the repetition rate from 82 MHz to 1 MHz, we are then enabled to use electronic gating on the single-photon-counting detection system, to further enhance the signal-to-noise ratio. The performance of this instrument will be described in detail in the subsequent year final report.

LDRD FUNDING:

FY 1995	\$66,937
FY 1996 est.	\$65,000

Use of Extreme Thermophilic Bacterium *Thermotoga maritima* as a Source of Ribosomal Components and Translation Factors for Structural Studies

F. William Studier, PI

95-13

and Venki Ramakrishnan, Co-PI

PROJECT DESCRIPTION:

We are engaged in a long-term study of the ribosome, and in particular in the crystallography of ribosomal proteins and initiation factors. It has been the general experience that thermophilic bacteria yield proteins that are more easily crystallizable than those of mesophilic organisms such as *Escherichia coli*. In order to investigate the possibility of working on extremely thermostable proteins, we decided to use the organism *Thermotoga maritima*, which is a eubacterium unlike the other hyperthermophiles, and is closely related to bacteria such as *E. coli*. However, it can grow at the astonishingly high temperature of 90°C.

We had just solved the structure of initiation factor IF3 in two separate halves, because the whole protein would not crystallize. As a first step, therefore, we decided to isolate IF3 from *T. maritima*, to attempt to crystallize it.

TECHNICAL PROGRESS AND RESULTS - Fiscal Year 1995:

Rather than trying to purify IF3 from large amounts of *T. maritima* cells, we decided to clone the gene for IF3 and overexpress it in *E. coli*.

A small region of the *T. maritima* IF3 sequence was known from the random sequencing studies of Jeffrey Miller and colleagues at UCLA. We used this small known sequence to probe restriction digests of genomic *T. maritima* DNA that was a gift from Dr. Janet Westpheling of the University of Georgia. A band that contained the IF3 gene was then cloned into a plasmid. The plasmid library was screened for the insert that contained the IF3 gene, and was then used to sequence the entire gene.

Once the gene sequence had been determined, the gene was transferred to one of the T7-based expression vectors developed at Brookhaven, pET-13a. The gene could be well-expressed in *E. coli* upon induction in the strain BL21(DE3).

A comparison of the sequence of *T. maritima* IF3 with other prokaryotic sequences reveals several highly conserved stretches, but also shows that *T. maritima* has a shortened loop at the junction between the N- and C-terminal domains of IF3 (Fig. 1). As this loop is what gives the protein flexibility between the two domains, the *T. maritima* IF3 could thus be a less flexible and more easily crystallizable protein.

Thus as a result of this work, we are in a position to begin crystallizing IF3 from *T. maritima*. The knowledge gained from this study could be used to identify and clone the genes for other ribosomal components from the organism.

PAPERS/JOURNALS/PUBLICATIONS:

The results will be included in a comprehensive publication when crystals of *T. maritima* IF3 are obtained.

LDRD FUNDING:

FY 1995	\$92,696
FY 1996 est.	\$98,000

Biochemical and Structural Studies of Chaperon Proteins from Thermophilic Bacteria

John M. Flanagan

95-15

PROJECT DESCRIPTION:

High resolution structural studies of the Hsp70 chaperone system from thermophilic bacteria.

TECHNICAL PROGRESS AND RESULTS - Fiscal Year 1995:

Purpose: The Hsp70 chaperone system is comprised of three proteins: Hsp70, Hsp40, and Hsp20. Homologues of the Hsp70 system are found in all organelles and cell types, and the system is thought to play key roles in the cellular protein folding process. *In vitro*, protein folding occurs spontaneously, and proceeds to the thermodynamic minimum state. In contrast, the folding of many proteins, *in vivo*, requires the assistance of molecular chaperones that aid this process, but are not themselves incorporated into the final folded state. A detailed mechanism for the action of molecular chaperones in assisting folding is not known, however, most current models hold that chaperones act to minimize "off-pathway", non-specific protein-protein interactions that lead to aggregation. Very little is known about the three-dimensional structures of the components in the Hsp70 molecular chaperone system, or for their complexes. To date, only the structures of the ATPase domain of Hsp70, and the J-homology domain of Hsp40 are known. These studies have provided important clues to the mechanism of Hsp70 and Hsp40 action, although, additional structural information will

be required to fully understand these important proteins.

Approach: The three-dimensional structure of a protein can be determined either by NMR spectroscopy, or by single crystal x-ray diffraction. The relatively large size of the individual components in the Hsp70 chaperone system limits their study by NMR spectroscopy, and x-ray diffraction studies are hampered by the lack of suitable crystals. Some of the difficulties in crystallizing these proteins may be related to their specific functions. First, both Hsp70 and Hsp40 possess protein binding activities that result in their aggregation at high concentrations. In addition, both Hsp70 and Hsp40 are multidomain proteins, and biochemical evidence indicates that the links between domains are relatively flexible. To circumvent these problems, studies were initiated to identify, clone, and overexpress, in *Escherichia coli*, thermophilic homologues of Hsp70, Hsp40, and Hsp20. The thermophilic homologues may be better suited for crystallization trials, in part, because these experiments are conducted in a range of temperatures (4 to 25°C) far from the optimum temperatures (70 to 90°C) for their activity.

Two approaches are being employed to identify the genes encoding the Hsp70 system from three thermophilic bacteria: *Thermotoga maritima* (TM), *Thermus thermophilus* (Tth), and *Bacillus stearothermophilus* (Bst). One approach, is to design degenerate oligonucleotide primers that are complimentary to the DNA sequence encoding 7-10 residue long stretches of absolutely conserved amino acids. These oligonucleotides are used to amplify regions of the genomic DNA of the organism by PCR. The amplified PCR products can then be used to screen a genomic library from this organism.

The second approach, is based upon the high degree of functional conservation in the Hsp70 system. Specifically, Hsp70 and Hsp20 form a tight complex involving highly conserved residues that are not contiguous in the linear amino acid sequence. However, the high degree of functional conservation in these two proteins means that heterologous complexes, containing Hsp70's from one species and Hsp20's from another, can be formed, and provides a means to identify Hsp20 homologues from various sources. To date, both approaches have been tried with limited success.

Technical Progress and Results: (a) Degenerate oligonucleotide primers were synthesized that should prime at three distinct and highly conserved regions in the sequence of Hsp70. The primers were used amplify genomic DNA from *TM*, *Tth*, and *Bst* by PCR. DNA fragments of the appropriately sizes were observed in reactions containing genomic *TM* and *Tth*, but not *Bst* DNA and these were cloned and the inserts are currently being sequenced. At least one candidate clone, amplified from *Tth* DNA, appears to be an authentic Hsp70 homologue. This DNA fragment will be used to probe a genomic library of *Tth*. New primers are currently being synthesized that take into account the known patterns of codon usage in *TM* and *Bst*. It is hoped that these primers may allow us to clone regions of the DNA from the Hsp70 homologues in *TM* and *Bst*.

(b) In most prokaryotic organisms, Hsp70 and Hsp40 are found in the same operon. Based upon this assumption, genomic libraries from *TM*, *Tth*, and *Bst* were obtained or constructed, containing large DNA inserts (6-10kb). Clones for Hsp70, derived from these libraries, may also contain all or part of the

Hsp70/Hsp40 operon.

(c) In a few cases, the Hsp70/Hsp40 operon also contains Hsp20, in this case the above strategy may also lead to the cloning of Hsp20. However, to increase the chances of finding Hsp20, we are also employing an alternative strategy. Here, we will exploit the ability of Hsp70 and Hsp20 from different species to form heterologous complexes. In a pilot study, the ATPase domain of the *E. coli* Hsp70 homologue, DnaK, was immobilized by chemical crosslinking on an affinity column matrix. In the presence of ADP, the *E. coli* Hsp20 homologue, GrpE, was purified to near homogeneity from a crude cell lysate. Moreover, the yeast mitochondrial Hsp20 homologue was identified from a yeast extract by this approach. We plan to use the DnaK affinity column to purify the Hsp20 homologue from *TM*. If successful, the amino terminal sequence of this protein will be determined and this information will be used to clone the gene from a genomic library of *TM*.

PAPERS/JOURNALS/PUBLICATIONS:

Hill, R.B, Flanagan, J.M., and Prestegard, J. "¹H and ¹⁵N Magnetic Resonance Assignments, Secondary Structure, and Tertiary Fold of *E. coli* DnaJ(1-78)," *Biochemistry* 34, 5587-5596 (1995).

Szabo, A., Korszun, Z.R., Hartl, F.U., and Flanagan, J.M. "A Zinc Finger-Like Domain of the Molecular Chaperone DnaJ is Involved in Binding to Denatured Protein Substrates," *EMBO J.*, in press.

LDRD FUNDING:

FY 1995	\$75,762
FY 1996 est.	\$100,000

Magnetic Mapping of Rebars and Piping in Infrastructure Systems

J. Powell

95-25

PROJECT DESCRIPTION:

MAGI (MAGnetic Imaging) is a proposed new method for determining the condition of internal steel reinforcement or underground piping by magnetic mapping. MAGI is based on the use of the very sensitive and precise magnetic measurement techniques and sophisticated 3-D magnetics computer codes that have been developed for high energy accelerator systems.

MAGI involves the measurement of magnetic fields close to the particular structure or sub-surface zone under investigation, when it is immersed in a low-level applied background field. The background field can be spatially and temporally varied in a controlled manner. The presence of iron/steel sources (rebars, pipes, etc.) locally perturbs the background field. By comparing the measured perturbations with those predicted from 3-D computer codes, the specific parameters for the iron/steel sources, i.e., the geometry of the sources (locations and sizes) and their local states (degree of corrosion and cracking, weld integrity, etc.) can be determined. The initial estimates for these parameters are iteratively corrected by comparison.

The sources experimentally investigated in Tasks 1 and 2 will be laboratory arrangements that are representative of those found in actual infrastructure construction, and will include single and multiple pipes and rebars. After

establishing and validating the field measurement and computer analysis methods, measurements will be carried out to test how well the source geometry and conditions predicted by the iterative convergence technique agrees with the actual "unknown" (to the experimenters) source geometry and conditions.

TECHNICAL PROGRESS AND RESULTS - Fiscal Year 1995

Purpose: The purpose of the project is to determine the capability of high performance magnetic sensing techniques to remotely determine the location, diameter, and path of underground metal pipes and cables using equipment located at the surface.

Magnetic sensing of underground pipes and cables was identified by the NICEST (National Infrastructure Center for Engineering Systems and Technology) group at BNL as a key new technology that could dramatically improve infrastructure in the U.S. The location and conditions of much of the underground piping (e.g., water, gas, sewers) and cable systems in urban areas is unknown. In general, these systems are old, deteriorated, and subject to increasing frequency of failure. New York City, for example, has millions of bell joints in its underground cast iron gas pipes, with many of them leaking. Each year gas companies must excavate thousands of the worst leakers and plug them since the location of the bell joints often is not known and must be found by trial and error. There is a great deal of costly, unnecessary excavation. Similarly, when repairing or rebuilding city streets, workers often do not know what is under them - that is, how many pipes and cables there are, what they carry, and where they are located. Many large test holes have to be dug to map the underground pipes and cables, at a cost of hundreds of millions of

dollars per year for New York City alone, with a much greater cost for the United States.

There presently is no practical way to remotely map the location, diameter, and path of underground pipes and cables from the surface. Ground penetrating radar and seismic methods have been used, but they are unreliable, cannot distinguish individual pipes in a multipipe environment, and do not yield good resolution.

Moreover, there are no practical present method to remotely determine the integrity of underground pipes - that is local cracks or weak spots, excessive stress and strain, corrosion thinning, graphitization of wall material, etc. Because of this, there is no way to find local spots where there is a high probability of failure; and where repairs or replacement efforts should be concentrated.

Magnetic sensing techniques have been proposed by BNL scientists that could Magnetically Image (MAGI) underground pipes to determine location, diameter, path, and integrity. The purpose of the MAGI LDRD is to determine the sensing capability of these new techniques in terms of their discrimination and resolving power, for various types of pipes in both single and multipipe type situations.

Approach: One of the 3 new MAGI techniques proposed, termed PERSUE, has been tested in the AGS magnet laboratory. PERSUE uses a low frequency pulsed background magnetic field that is applied by a coil located at the surface of the ground. A magnetic sensing coil located in the vicinity of the pulse coil measures the small perturbation in the applied background field due to the presence of the underground pipe. By using a bipolar pulse (i.e., square wave) and appropriate nulling methods, the PERSUE

technique can blank out perturbation caused by the earth's field and the effect of extraneous metallic bodies. Thus, only the perturbation from the subsurface pipe is measured.

The magnitude of the perturbation and its relative strength at a number of spatial positions enables an analytic reconstruction of the underground pipe locations in three dimensions, as well as its diameter. The pattern of the spatial variation of the perturbation sequels can also be used to distinguish one pipe from another in a multipipe environment.

Technical Progress and Results: Measurements of the sensitivity of the PERSUE technique have been carried out for a variety of conditions including:

- 1) Iron/steel pipes of various diameter at various depths
- 2) Aluminum pipes of various diameter at various depths
- 3) Bell joints in cast iron pipes of various diameters at various depths
- 4) Determination of pipe location in two pipe environments at different depths and separations.

Two rectangular pulse coils were constructed, each with 4 feet x 8 feet dimensions. Available AGS search coils were used to measure the perturbed flux signals resulting from the "subsurface" pipes. [In the experiments the pulse and search coils were positioned in the air above the pipes to be measured. The absence of an earth cover should not affect the magnetic field].

The results of the above experiments showed great promise. For example, the

location of the center of a bell joint in a cast iron pipe was magnetically determined to within 1/10 the of an inch at a depth of 3 feet (tests at greater depths are planned).

In other tests, iron/steel pipes could be unambiguously distinguished from aluminum pipes by the sign of the magnetic signal, with iron/steel pipes having local field concentration and aluminum local field cancellation.

Pipes could be readily located at depths up to 4 feet, the maximum tested so far, with a strong signal relative to background based on diameter on the results, determination of position and diameter at much greater depths appears practical.

In other tests, two pipes separated by a

relatively short distance, i.e., 18 inches, could be distinguished from a single pipe by the different signals they exhibited.

ACCOMPLISHMENTS:

An AUI patent on MAGI has been applied for by J. Powell, M. Reich, and G. Danby. A joint proposal with Columbia University for the use of MAGI to map underground pipes in New York City has been prepared and submitted to the city. A second proposal for the use of MAGI to locate joints in gas utility piping systems has been submitted to Con Edison.

LDRD FUNDING:

FY 1995

\$ 99,829

Low Dose Gamma Imaging Facility for *In Vivo* Molecular Medicine

Ruimei Ma 95-33

Eugene P. Cronkite

F. Avraham Dilmanian

Ludwig E. Feinendegen

Darrel D. Joel

Ashok Vaswani and

Nora D. Volkow

PROJECT DESCRIPTION:

The subject of this LDRD is to develop a Low Dose Gamma Imaging (LDGI) facility at the Medical Department, BNL, utilizing 1) the existing shielded rooms of the Whole Body Counter (WBC) for reducing the background, and 2) the WBC and a gamma camera equipped with specially designed collimators to provide ultra-high counting sensitivity with acceptable spatial resolution. The facility will be used for certain applications of nuclear medicine imaging in the field of molecular medicine, such as the study of growth factors (GFs), which cannot be carried out using a conventional gamma camera because of the camera's limited sensitivity. Although the image quality of both planar scintigraphy and SPECT imaging in the range of activities commonly used in clinical studies is not affected by the environmental background, scintigraphy at very low doses with very high sensitivity collimators will be affected by such background. The rooms for this purpose are shielded by 122 cm-thick low-activity concrete and 10 cm-thick low-activity (pre-World War II) steel. Measurements of background using a 15 cm diameter x 5 cm length NaI(Tl) detector indicate that in the 50-1000 keV energy range the shielding reduces the background radiation by a factor of 30. Reduction of the background

count for a gamma camera installed in the shielded room depends on the camera's own shielding, the crystal size, and the collimator design.

The collimator design will emphasize high counting sensitivity while maintaining an acceptable spatial resolution. Background reduction, combined with the ultra-high sensitivity collimators of the gamma camera and the WBC should enable us to study the molecular and cellular dynamics of biological systems in humans with absolute minimal risks from radiation and drug exposures using appropriate radiotracers.

Two pilot studies will be carried out using the LDGI facility: 1) assessment of the metabolism of radioiodinated erythropoietin as a representative of GFs, and 2) analysis of lipid synthesis in the liver employing the dual tracer approach with the two fatty acid analogues ^{123}I -o-PPA and ^{131}I -p-PPA. These pilot studies should demonstrate the capability of the LDGI facility, and exemplify its potential for strengthening the new field of research and development of *in vivo* molecular medicine.

TECHNICAL PROGRESS AND RESULTS - Fiscal Year 1995:

Purpose: Our research plan is as follows:

1. Move the Toshiba gamma camera GCA-901A into the shielded room.
2. Design the gamma camera collimators for low dose gamma imaging with very high and ultra high sensitivity (VHS and UHS) for studies using ^{123}I (159 keV photons) and ^{131}I (364.5 keV photons).
3. Design WBC collimators, together with a removable collimator-holding rack.

4. Evaluate the performance of the gamma camera with newly designed collimators, and that of the collimated WBC.
5. Carry out the two pilot research programs indicated above.

The present report includes items 1 and 2 (the camera is scheduled to be moved into the shielded room by the end of November, 1995).

Approach: Four small shielded rooms (9' x 10') were available. The Toshiba GCA-901A gamma camera required a minimum space of two of the shielded rooms. Therefore, the 4" steel wall between the two small shielded room was removed to provide a larger room. The wall removal was carried out by the Central Shops division using an oxygen plasma torch mounted on an articulated jig. Safety procedures included lead paint abatement, fire control measures, and treatment and evacuation of exhaust air gases to the atmosphere. As a result a room of 10' x 18' has become available for the installation of the gamma camera. In addition, a separate room for data acquisition has been established.

Technical Progress and Results: Preliminary collimator design is reported below. Table I compares the efficiency of the two new collimators, VHS(¹²³I) and UHS(¹²³I), that will be built for the low dose gamma imaging using the radioisotope ¹²³I with that of the LEGP (low energy general purpose) collimator provided by Toshiba for nuclides emitting gamma-rays with energy up to 150 keV. All are parallel-hole lead collimators with a hexagonal array of hexagonal holes. Septal penetration for VHS(¹²³I) and UHS(¹²³I) is designed to be less than 5%. Table II compares the efficiency of the VHS(¹³¹I) and UHS(¹³¹I) collimators that will be built for ¹³¹I with that of the MEGP (medium energy general purpose) collimator provided by

Toshiba for nuclides emitting gamma rays with energy up to 300 keV. Septal penetration for these collimators is designed to be less than 10%. The overall spatial resolutions (FWHM in cm) of all collimators listed in Table I and II are presented in Figure 1 as a function of the distance from the collimator face.

The performance of the gamma camera with the new collimator in the shielded room will be evaluated. For certain studies that require very little spatial resolution we plan to use the gamma camera without any collimator. The spatial resolution in this application will be resulted from the $1/r^2$ dependence of the count-density efficiency with the distance between the source and the camera. The camera will be placed as close as possible to the subject's body.

Table I
Comparison of Collimators for ¹²³I

Collimator	LEGP	VHS	UHS
Efficiency	2.1×10^{-4}	2.1×10^{-3}	1.0×10^{-2}
Hole length (cm)	4.0	3.2	3.2
Hole diameter (cm)	0.236	0.60	1.3
Septum thickness(mm)	0.22	0.62	1.1

Table II
Comparison of Collimators for ¹³¹I

Collimator	LEGP	VHS	UHS
Efficiency	3.6×10^{-4}	3.4×10^{-3}	2.0×10^{-2}
Hole length (cm)	4.0	3.5	3.5
Hole diameter (cm)	3.37	9.0	20.0
Septum thickness(mm)	1.08	3.8	6.0

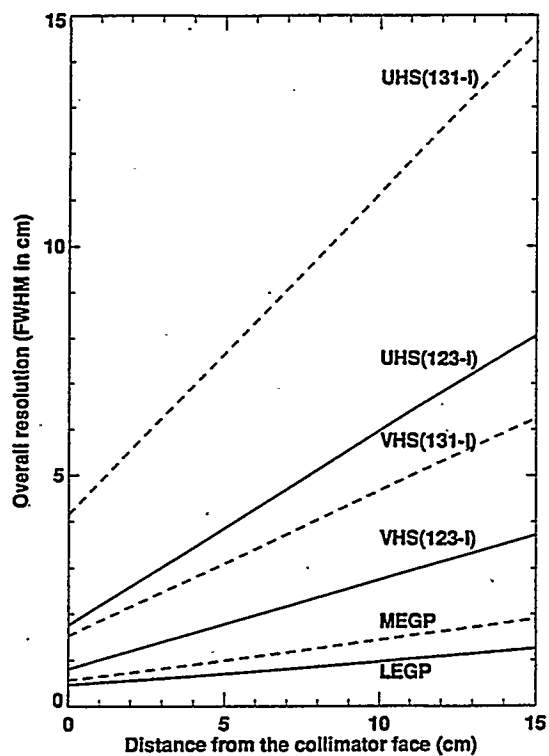


Figure 1

Overall spatial resolution of the gamma camera as the function of the distance from the collimator face.

LDRD FUNDING:

FY 1995	\$ 109,736
FY 1996 est.	\$ 110,000

Note: This project involves human subjects.

Atmospheric Degradation of Halogenated Compounds

Zhengyu Zhang and
R. Bruce Klemm

95-40

PROJECT DESCRIPTION:

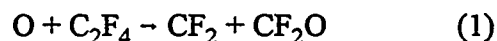
In evaluating the suitability of various CFC alternatives, the potential environmental impact of these compounds, when released to the atmosphere, is manifested in their tropospheric and stratospheric behaviors. As most of these compounds are not naturally occurring species and have not been widely used in industry, their thermochemical and kinetic properties are scarcely known. The objective of this LDRD research project is to determine thermochemical properties of some of the chlorofluorocarbon alternatives and their oxidation intermediates and products by means of studying their photoionization.

TECHNICAL PROGRESS AND RESULTS - Fiscal Year 1995:

Purpose: The main thrust of the project has been to determine ionization energies (IE) and appearance energies (AE) of the species, which are then used, in combination with other available thermochemical data, to derive heats of formation and bond energies.

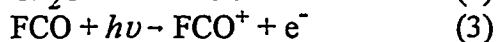
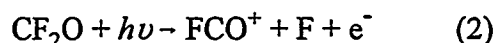
Approach: Experiments have been performed on a discharge flow-photoionization mass spectrometer (DF-PIMS) apparatus at Beamline U-11 of NSLS. The threshold energies are determined from photoionization efficiency (PIE) curves which were obtained by scanning over wavelength ranges of interest at the m/z appropriate for the species under study. While stable compounds were procured from commercial sources, radical species were

generated *in situ* by fast atom-molecule titration reactions. For example, CF_2 radicals were formed in the reaction



where O atoms had been produced by O_2 dissociation in the microwave discharge. Where possible, measurements were carried out using different sources of the species to cross-check results, such as in the case of CF_2O where the IE was determined with both neat CF_2O sample and CF_2O generated *in situ* by reaction (1). Measurements for compounds whose IEs are known usually preceded experiments on the unknown quantities so as to validate the experimental approaches and conditions.

Technical Progress and Results: The photoionization studies were performed for essentially two classes of compounds, hydrofluorocarbons (HFCs) and halon replacements, and/or their respective oxidation intermediates and products. The AE of FCO^+ from CF_2O was obtained from PIE spectra and, while accurate determination of IE(FCO) was precluded by the indistinct threshold in the FCO spectra, IE(FCO) was obtained, instead, from *ab initio* calculations. On completing the following thermodynamic cycle:



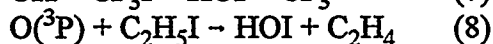
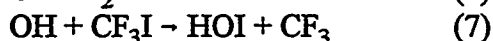
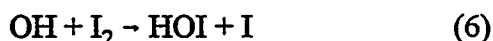
with the AE and IE from this work and the literature value for the third process, we arrived at a value of 3.39 ± 0.14 eV for



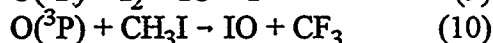
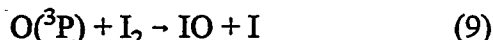
the electron affinity (EA) of F, which is well established; and our result was in good agreement with the accepted value of EA(F) =

3.399 ± 0.003 eV. A significant result of this study was the experimental confirmation of the "higher" heat of formation of CF₂O, which had been reported previously but only in theoretical studies.

Experimental results were obtained on IE(HOI) and IE(IO). HOI was generated in the flow tube reactor *via* three separate reactions:



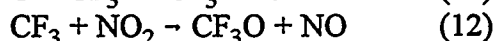
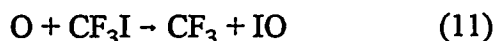
The last reaction is particularly interesting because it had only recently been identified by S. R. Leone and co-workers (Univ. Colorado/Boulder) as having HOI as a major product channel. Our results confirmed, semi-quantitatively, this surprising observation. IO was generated in the flow tube *via* two separate reactions:



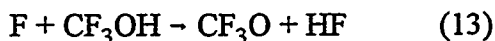
The IE results for both HOI and IO are the first experimental determinations to be reported and thus trend analyses were performed to examine these new values. In both cases, it was possible to understand the magnitude of the observed values in relation to IE trends in a wide variety of other, known compounds.

We will study the dissociative ionization of several perfluorocarbons and HFCs to determine the heat of formation of CF₃, a common functional group in a number of important HFCs. We will also pursue study of the trifluoromethoxy radical, CF₃O, which is an important intermediate in the oxidation of HFC compounds that contain the CF₃ group. We have already attempted to generate the

radical by the reaction sequence:



but failed to detect it. While CF₃O was not necessarily produced in the reaction chain, the failure to detect it may more likely be due to the instability of CF₃O⁺. A further attempt will be made to generate CF₃O *via* reaction (13):



as we expect to have CF₃OH sample for the experiment.

PAPERS/JOURNALS/PUBLICATIONS:

T.J. Buckley, R.D. Johnson, III, R.E. Huie, Z. Zhang, S.-C. Kuo, and R.B. Klemm, "Ionization Energies, Appearance Energies and Thermochemistry of CF₂O and FCO", *J. Phys. Chem.*, 99, 4879 (1995).

P.S. Monks, L.J. Stief, D.C. Tardy, J.F. Liebman, Z. Zhang, S.-C. Kuo, and R.B. Klemm, "A Discharge Flow-Photoionization Mass Spectrometric Study of HOI: Photoionization Efficiency Spectrum and Ionization Energy", *J. Phys. Chem.*, (in press).

Z. Zhang, P.S. Monks, L.J. Stief, J.F. Liebman, R.E. Huie, S.-C. Kuo, and R.B. Klemm, "Experimental Determination of the Ionization Energy of IO(X²Π_{3/2}) and Estimations of Δ_fH⁰(IO⁺) and PA(IO)", *J. Phys. Chem.*, (in press).

LDRD FUNDING:

FY 1995	\$ 94,245
FY 1996 est.	\$ 37,000

Extraction and Destruction of Hazardous and Toxic Chemical Pollutants During Soil/Sludge Remediation Using Innovative Technologies

S. Chalasani, A. J. Francis and M. Giles 95-44

PROJECT DESCRIPTION:

The objective of this research is to develop a new remediation technology for soils/sludges contaminated with various toxic and hazardous organic pollutants using cyclodextrins. Since cyclodextrins are environmentally friendly, non-toxic, non-hazardous and readily form complexes with various organic compounds, their use for environmental remediation was examined. The biodegradation of organic pollutants in the presence of cyclodextrin will be studied as cyclodextrin can potentially enhance the biodegradation of recalcitrant compounds by cometabolism.

TECHNICAL PROGRESS AND RESULTS - Fiscal Year 1995:

Purpose: The remediation of soils contaminated with various toxic and hazardous organic compounds is a major environmental concern. At present, there are numerous contaminated sites across the country requiring clean up and remediation. In the US alone, it is estimated that the cost of remediating most of the Superfund and Resource Conservation and Recovery Act (RCRA) sites is about \$750 billion and this cost is expected to increase in the future. Therefore, it is imperative to develop cost-effective technologies which can address the enormous problem of soil

remediation to protect human health and the environment.

One of the emerging technologies to remediate the contaminated soils is soil washing/flushing technique. With this technique, surfactants (cationic, anionic or neutral) either alone or in combination with acids, bases, or complexing agents are used. However, the surfactant technique suffers from many drawbacks such as i) the chemicals used for remediation are themselves toxic and corrosive making the remediated soil unfit for reuse, ii) forms high viscosity emulsions that are difficult to separate, iii) sorption of surfactant by the soil which means that more extractant is needed for extraction, and iv) inability to recover the surfactant for recycling. Therefore, it is prudent to develop new techniques that can overcome the problems associated with the surfactant method.

Approach: Cyclodextrins are cyclic oligosaccharides comprising of six, seven and eight glucopyranose units, and are called as α -, β -, and γ - cyclodextrins, respectively. Cyclodextrins are obtained by microbial enzymatic degradation of starch and are commercially available. The shape of the cyclodextrin molecule is a half truncated cone with a cavity inside. The outer periphery of the molecule is hydrophilic while the interior of the cavity is apolar and hydrophobic in nature. Because of this unique structural feature, cyclodextrins form soluble inclusion complexes with non-polar organic compounds. Since many of the environmental pollutants that are of major concern to the US EPA and other regulatory agencies are non-polar compounds such as polynuclear aromatics (PNAs), organochlorine pesticides, polychlorinated biphenyls (PCBs), and halogenated hydrocarbons, cyclodextrins can potentially form soluble inclusion complexes with these compounds. Therefore, soils contaminated with non-polar toxic and

hazardous compounds can efficiently be extracted with cyclodextrins. Another advantage of using cyclodextrins is that they are non-toxic, non-hazardous, biodegradable, water soluble and available commercially at a reasonable cost. Because cyclodextrins are environmentally friendly, there is a potential for their use in the in-situ remediation of contaminated soils and ground water, without impacting the environment.

Technical Progress and Results: In this study, soils contaminated with various toxic and hazardous organic compounds (Table 1) were extracted with β -cyclodextrin, and their extraction efficiencies were compared with that of water. For each group of pollutants, seven replicates were prepared 3 for cyclodextrin, 2 for water and 2 for standard controls for determining true concentrations after evaporative losses during sample preparation. For each replicate, about 10g of pre-cleaned soil was spiked with a respective certified analyte mixture. Each sample was extracted with 2 x 20 ml of 4% β -cyclodextrin or deionized water, and shaken at 45°C at 200 rpm for 1 hr. The organics tested essentially contains extractable target compounds listed in the Contract Laboratory Program (CLP) of US EPA's Comprehensive Environmental Response Compensation and Liability Act (CERCLA) or Superfund program. This list includes PNAs, organochlorine pesticides, halogenated hydrocarbons, and phenols.

Cyclodextrin was very effective in extracting several toxic and hazardous organic contaminants from soil. For example, the pesticides such as aldrin, chlordane, dieldrin, endrin, endrin aldehyde, endosulfan-I, heptachlor, and heptachlor epoxide, were extracted with > 90% efficiency. These are highly chlorinated and structurally diverse compounds with significant toxicity and carcinogenicity. Similarly, PNA's such as acenaphthene, acenaphthylene, naphthalene,

and pyrene, which are typical toxic compounds found in many spills due to diesel and heating fuels were extracted with > 80% efficiency. The spills due to petroleum hydrocarbons is a major environmental concern across the country. Also, pentachlorophenol, which is a major contaminant in the wood and paper industry was extracted > 90% efficiency.

However, higher molecular weight PNAs such as benzo(g,h,i)perylene, benzo(a)pyrene were poorly extracted by cyclodextrin. This is probably due to their size and solubility which precludes complex formation. However, using an alcohol-based cosolvent to increase solubility, or using the γ -cyclodextrin which has larger cavity size, is expected to facilitate complex formation and extraction. Some compounds showed similar extraction efficiency in comparison to water and thus is probably due to the effects of extraction temperature and the initial concentration of the compounds used in these experiments. The initial results with the decontamination of soils by cyclodextrin are encouraging because all these compounds tested are i) highly toxic and hazardous; ii) known or suspected human carcinogens; and iii) refractory and persist in the environment for a long time, posing significant health and environmental concerns.

The advantages of using cyclodextrin for remediation of contaminated soils are i) cyclodextrin is environmentally friendly; non-hazardous and non-toxic; ii) no viscous emulsions are formed during extraction; iii) decreases the toxicity of the contaminant by forming the inclusion complex, and iv) does not adsorb to the soil.

PAPERS/JOURNALS/PUBLICATIONS:

Patent: A patent application for the extraction of toxic and hazardous organic compounds

Table 1. Extraction of hazardous organic compounds by β -cyclodextrin.

Compound	% removal		Compound	% removal	
	water	β -CD		water	β -CD
<u>Hazardous Organics</u>					
aniline	93	93	2-methylphenol*	99	93
2-nitroaniline	79	82	2-methyl-4,6-dinitrophenol	92	95
3-nitroaniline	85	87	2-nitrophenol	93	88
4-nitroaniline	80	93	2,4,5-trichlorophenol*	74	92
4-chloroaniline	82	90	2,4,6-trichlorophenol	82	92
n-nitrosodimethylamine	84	90	pentachlorophenol	56	98
n-nitrosodiphenylamine	26	68	<u>Polynuclear Aromatics (PNA's)</u>		
azobenzene*	59	86	acenaphthene	12	97
1,2-dichlorobenzene*	88	90	acenaphthylene	14	97
1,3-dichlorobenzene*	89	90	anthracene	13	39
1,4-dichlorobenzene*	89	89	benzo (a) anthracene	32	9
ethylbenzene	79	89	chrysene	27	20
hexachlorobenzene*	58	93	fluoranthene	19	76
nitrobenzene*	87	98	benzo (k) fluoranthene	51	52
1,2,4-trichlorobenzene*	75	93	fluorene	11	70
1,2,4-trimethylbenzene	57	80	dibenzofuran	17	58
1,3,5-trimethylbenzene	58	74	naphthalene	35	86
benzidine	61	92	2-chloronaphthalene*	65	88
3,3-dichlorobenzidine	26	64	2-methylnaphthalene	23	59
benzoic acid*	100	99	benzo (g,h,i) perylene	27	39
benzyl alcohol	96	96	phenanthrene	13	77
carbazole*	53	78	pyrene	19	89
bis (2-chloroethyl)ether	95	91	benzo (a) pyrene	27	23
bis (2-chloroisopropyl)ether	90	59	<u>Pesticides (Organochlorine)</u>		
4-bromophenylphenylether	8	44	aldrin	39	100
4-chlorophenylphenylether	15	52	alpha-BHC	40	80
hexachlorobutadiene*	73	91	beta-BHC	100	100
hexachloroethane*	88	95	delta-BHC	34	60
hexachlorocyclopentadiene*	69	95	gamma-BHC	38	94
isophorone*	99	98	alpha-chlordane	50	92
bis (2-chloroethoxy)methane	95	85	gamma-chlordane	47	90
bis (2-ethylhexyl)phthalate	26	16	4,4-DDD	37	65
butyl benzylphthalate	51	28	4,4'-DDE	36	18
di-n-butylphthalate	24	45	4,4'-DDT	36	61
di-n-octylphthalate	31	15	dieldrin	38	100
diethyl phthalate	79	87	endosulfan I (alpha)	37	100
dimethyl phthalate	89	92	endosulfan II (beta)	37	65
2,4-dinitrotoluene*	90	91	endosulfan sulfate	36	61
2,6-dinitrotoluene*	85	87	endrin	37	100
m-xylene	79	87	endrin aldehyde	40	99
o-xylene	76	85	endrin ketone	36	84
<u>Phenols</u>			heptachlor	40	99
Phenol	97	96	heptachlorepoxyde isomer b	38	99
2-chlorophenol	90	91	methoxychlor	36	84
4-chloro-3-methylphenol	64	87			
2,4-dichlorophenol	63	86			
2,4-dimethylphenol	84	88			

*These samples were extracted at 25°C.

from soils using cyclodextrin is filed.

FOLLOW ON FUNDING:

A proposal will be submitted to the Office of Health and Environmental Research (OHER), DOE, in response to Natural and Accelerated Bioremediation Research (NABIR) initiative in FY 1996.

LDRD FUNDING

FY 1995	\$ 75,555
FY 1996 est.	\$ 75,000

Study of High Power Density Compact Target Design and Associated Moderators, Beam Ports and Shielding for a 5 Mw Pulsed Spallation Neutron Source

*Hans Ludewig and
Michael Todosow*

95-45

PROJECT DESCRIPTION:

A three-module target/moderator, beam tube configuration has been defined and evaluated for the Pulsed Spallation Neutron Source (PSNS) study. Neutron flux spectra have been calculated for the target structure surrounded by a heavy water reflector, light water moderators, and beryllium/heavy water pre-moderators. Studies carried out are:

- 1) Refine the design choices made in the preliminary design for moderator and pre-moderator,
- 2) Determine the effect of proton pulse length on the neutron pulse length in the moderator,
- 3) Re-configure the target/moderator assembly for an incident proton energy of 1.25 GeV, and
- 4) Determine the effects of thermal-mechanical shock enhancement of stresses in the heavy metal target.

TECHNICAL PROGRESS AND RESULTS - Fiscal Year 1995:

Purpose: The overall purpose of the project is the development of a conceptual

design of a PSNS target-reflector and moderator (TRAM) assembly capable of operating at 5 MW. The TRAM assembly will operate under the following conditions:

Power (MW)	5
Proton Energy (GeV)	1.25 - 3.6
Proton Pulse Length (μ s)	1.2
Target Station Frequency (Hz)	10 and 50

This neutron source is designed to augment the currently operating neutron sources in the United States. In the long term it is the objective of this work that concepts, results, and insights developed during this endeavor be applicable to the conceptual design of a national 5 MW PSNS. BNL has offered to form a team with ORNL to explore the feasibility of such an intense PSNS, and this work will be directly applicable to this co-operative effort.

Approach: The overall strategy for carrying out this piece of work was based on analytical determinations of neutron fluxes, heat deposition, and stresses. The primary effort was in the determination of neutron fluxes, and this was carried out using the LAHET Code System (LCS), developed at the LANL. This code consists of two major modules:

- 1) LAHET, a modified version of the HETC intranuclear cascade code for evaluations above 20 MeV, and
- 2) HMCNP, a modified version of the well known MCNP transport code for calculations from 20 MeV down to thermal energies.

Both modules employ a combinatorial surface/cell specification of the problem geometry which permits modeling of target configurations with minimal approximations.

In addition, HMCNP employs nuclear data from the ENDF/B files in essentially unapproximated point-wise form which avoids the complications associated with generation of group cross sections.

Technical Progress and Results: The technical progress and results of this work are concentrated in the following four areas:

- 1) A study of the reflector/pre-moderator material to maximize the neutron pulse height.

This study was carried out by considering four different materials. These materials were chosen based on their mechanism of slowing down neutrons. Thus, materials were selected which slowed neutrons down essentially by inelastic scattering (PbF_2), to purely elastic scattering (D_2O and H_2O). The results of this study indicate that those pre-moderator/reflectors which rely predominantly on inelastic scattering for slowing neutrons down result in neutron pulses in the moderators which rise faster, die faster and have higher amplitudes than those using elastic scattering.

- 2) A study of the effect of proton pulse length on the neutron pulse in the moderator.

This study was carried out by considering a series of proton pulse lengths and propagating them through a target. The proton pulse shapes were assumed to be Gaussian, and their lengths varied from $1.2(-6)^* \text{ s}$ - $1.0(-3) \text{ s}$. Results of this study indicate that:

- 2.1) The shortest proton pulses result in the highest neutron pulses in H_2O

* $1.2(-6) = 1.2 \times 10^{-6}$

moderators, regardless of reflector/pre-moderator material,

- 2.2) In the case of a liquid hydrogen moderator the neutron pulse height does not decrease monotonically with increasing proton pulse length. There is essentially no decrease in neutron pulse height, up to a proton pulse length of approximately $5.0(-6) \text{ s}$. Following this pulse length the neutron pulse height decreases monotonically, and

- 2.3) In the case of the short proton pulses, the neutron pulse in the heavy metal target and the reflector have died away before the neutron pulse fully develops in the moderator. In the case of the longest proton pulses the neutron pulses in the target overlap the pulse developing in the moderator. This overlapping of pulses in the long pulse case could affect the intensity of the potential background.

- 3) Configure a TRAM assembly operating with a 1.25 GeV proton beam.

This proton beam is consistent with an accelerator system which consists of an accumulator ring rather than a synchrotron ring following the LINAC. The TRAM assembly resulting from this study consisted of:

- 3.1) A two-module heavy metal target separated by a flux trap. The heavy metal consisted of tungsten spheres, packed randomly in rectangular beds, and cooled by heavy water.
- 3.2) A reflector/pre-moderator consisting of beryllium spheres cooled by heavy

water. This reflector also resulted in a limited amount of neutron multiplication due to the (n,2n) reaction in beryllium.

- 3.3) All structures within the TRAM assembly were manufactured of Inconel. This selection was made based on the experience at LANL on the LAMPF.
- 3.4) Two moderator types, one operating at ambient temperature, and the other operating at cryogenic temperature were included. Light water and liquid hydrogen were chosen as the moderating material.
- 4) A preliminary investigation of thermal-mechanical shock enhanced stresses was carried out for the heavy metal target configuration. This study resulted in setting limits on the maximum tungsten sphere diameter, depending on the proton pulse length.

PAPERS/JOURNALS/PUBLICATIONS:

Papers were presented at the International Collaboration on Advanced Neutron Sources - XIII (ICANS - XIII), and submitted to the International Conference on Nuclear Energy (ICONE - IV).

- 1) H. Ludewig, M. Todosow, and J. Powell, "Status of Pulsed Spallation Neutron Source Target Work at Brookhaven National Laboratory", 13th International Collaboration on Advanced Neutron Sources - ICANS XIII, PSI, Villigen, Switzerland. (Oct. 1995).
- 2) H. Ludewig, M. Todosow, and J. Powell, "Characteristics of long-pulse and short-pulse spallation-source targets", to be presented at ICONE- IV

LDRD FUNDING:

FY 1995	\$100,004
---------	-----------

LABORATORY DIRECTED RESEARCH AND DEVELOPMENT

1996 PROPOSED PROGRAM*

***New projects authorized for funding as of October 1, 1995.**

Project Number 96-06

**Positron Emission Magnetic Resonance
Imaging (PEMRI)**

C. S. Springer, Jr.
A. Levy
N. Volkow
F. Hode

"**T**est a new approach involving the complete convolution of data obtained from a PET scan with the data from an MRI scan of the same brain slice of the same human subject."
FY 1996 Funding \$100,000

Project Number 96-11

**In-Vacuum Undulator (IVUN) for the
NSLS X-ray Ring**

P. Stefan
S. Krinsky
D. Lynch
G. Rakowsky

"**A** preliminary study addressing key issues for a prototype in-vacuum undulator for the X13 R&D insertion straight section"
FY 1996 Funding \$100,000

Project Number 96-16

Spin Polarized Coincidence Spectroscopis

P. Johnson
K. Smith, Boston University

"**T**he development of spin polarized core level photoemission and soft x-ray fluorescence spectroscopy on beamline X1B at the NSLS"
FY 1996 \$78,000

Project Number 96-19

**An Evaluation of the WSR-88D Radar
for the Remote Sensing of Cloud**

Properties
M.A. Miller
P. Daum

"**T**o study the cloud sensing capabilities of the WSR- 88D radars (NEXRAD) and to develop algorithms to retrieve cloud structural details over large domains (4500 km²)."
FY 1996 Funding \$80,000

Project Number 96-27

**Tailored Pulse UV/XUV Photon Source
Development**

L. DiMauro
E. Johnson

"**T**o develop strategies of efficient production and control of arbitrary pulse shaping in the UV-XUV range. In addition, the development of a high harmonic source of coherent XUV radiation as a primary and sub-harmonic injector beam for the UP-FEL project."
FY 1996 Funding \$72,000

Project Number 96-32

**Methods for Detecting Activation of the
DNA-Activated Protein Kinase, DNA-PK,
in Human Tissue Culture Cell**

C.W. Anderson

"**T**o identify factors that activate DNA-PK in human tissue culture cells, it is proposed to develop methods to access the activity state of DNA-PK in living cells."
FY 1996 \$103,000

Project Number 96-34

**Enzymatic and Regulatory Interactions
of A Single Protein with Three Different
Sites in Nucleic Acids**

S. Lacks

"*To* demonstrate the principle that an enzymatic protein can also have regulatory functions in which it binds to nucleic acids, to identify the sequences of the regulatory binding sites in DNA and RNA, and to crystallize the DpnM protein."

FY 1996 Funding \$113,000

Project Number 96-37

Low Frequency Dynamics of Novel

Materials

M. Strongin

V. Emery

G. Williams

"*To* carry out a project involving a far infrared beamline at the NSLS for studies of the frequency dependent conductivity of solids."

FY 1996 Funding \$77,000

Project Number 96-38

**BNCT for Leukemia Through Ex-vivo
Purging of Bone Marrow**

J. Coderre

J. Glass

"*To* experimentally determine the feasibility of using boron neutron capture therapy (BNCT) to purge leukemic bone marrow *ex-vivo* prior to autologous bone marrow transplantation."

FY 1996 Funding \$82,000

Project Number 96-40

**Initiation of MRI Studies in Human
Subjects**

N. Volkow

C. Springer

J. Fowler

J-H. Lee

I. Palyka

"*To* develop the methodology for conducting brain fMRI studies in human subjects and to investigate the mechanisms accounting for blood oxygen level dependence (BOLD) signals in fMRI."

FY 1996 Funding \$116,000

Project Number 96-42

**Designer Polymers for Permeable
Ground Water Barrier**

J. Heiser

P. Moskowitz

D. Melamed

"*To* develop and test designer organic polymers for the sorbtion of organic compounds from contaminated ground water plumes."

FY 1996 Funding \$100,000

Project Number 96-46

**BNCT Treatment Planning Software
Proposed Modifications**

E. Selcow

D. Joel

"*To* develop a modification of the BNCT treatment planning software that is tailored to BNL's specific research and development requirements and objectives."

FY 1996 Funding \$100,000

